

**LIGAND TRANSDUCTION MECHANISMS  
OF INWARDLY-RECTIFYING POTASSIUM CHANNELS**

by

Bowen Li

B.Sc., The University of British Columbia, 2011

A THESIS SUBMITTED IN PARTIAL FULFILLMENT OF  
THE REQUIREMENTS FOR THE DEGREE OF

MASTER OF SCIENCE

in

THE FACULTY OF GRADUATE STUDIES

(Pharmacology)

THE UNIVERSITY OF BRITISH COLUMBIA

(Vancouver)

August 2013

© Bowen Li, 2013

## Abstract

Regulation of inwardly-rectifying potassium (Kir) channels by intracellular ligands couples cell membrane excitability to important signaling cascades and metabolic pathways. Particularly, the ATP-sensitive potassium ( $K_{ATP}$ ) channels, highly expressed in diverse excitable tissues, are the keystone components of glucose-stimulated insulin secretion in pancreatic  $\beta$ -cells.  $K_{ATP}$  channels are constituted by a canonical pore-forming transmembrane domain (TMD) and a large cytoplasmic domain (CTD) where ATP binds and inhibits the channel activity. A non-covalent interface domain in Kir channel structures is speculated as a mediator of coupling between the cytoplasmic ('ligand-sensing') and transmembrane ('gating') domains. The work described in this thesis aims to investigate the molecular mechanism that link ligand binding to the channel gating. A significant barrier is that many functionally important channel motifs are highly sensitive to mutagenesis, resulting in a loss-of-function (LOF) phenotype. We have developed a novel 'forced gating' approach by substituting a glutamate in the hydrophobic Kir channel bundle crossing (F168E), generating channels that open upon alkalization, likely due to mutual repulsion of the introduced glutamate side chain. This 'forced gating' approach is implemented in mutagenic scans of the Kir channel domain interface comprising numerous motifs, including the transverse 'slide' helix, the C-linker, the  $\beta$ C- $\beta$ D loop, and the G-loop. Without exception, expression on the 'forced gating' background rescued all loss-of-function interfacial mutants in alkaline pH, and enabled functional characterization of all interfacial mutants on generation of conductive channels and ATP-dependent gating. Our findings highlight a small subset of 'anchor residues' at the Kir6.2 TMD-CTD interface, including D58 and T61 in the 'slide helix', R177 in the C-linker, T294 in the G-loop, and D204 in the  $\beta$ C- $\beta$ D loop, which are required for both formation of conductive channels, and appropriate transmission of ligand binding to the channel gating. Disruption of these residues uncouples the TMD and CTD, causing loss-of-function phenotype combined with profound ligand insensitivity. Additionally, in contrast to a traditional 'allosteric rescue' approach (Kir6.2[C166S]) with an elevated intrinsic channel open probability, the 'forced gating' approach has a more general application due to its efficiency in rescuing all loss-of-function interfacial mutants without inherently perturbing ATP sensitivity in Kir6.2 channel.

## Preface

A version of Chapter III has been published in *J. Biol. Chem.* [Li, B.W.], X.Y. Huang, R.S. Zhang, R.Y. Kim, R.Y. Yang, and H.T. Kurata. (2013) ‘Decomposition of slide helix contributions to ATP-dependent inhibition of Kir6.2 channels’. I conducted most of the experiments. A fellow graduate student X.Y. Huang conducted some of the electrophysiological recordings and is a co-first author on the publication. Most of the manuscript was originally drafted by supervisor Harley Kurata. A version of Chapter III has also been included in Masters’ thesis of X.Y. Huang entitled “Molecular determinants of different gating mechanisms in inwardly-rectifying potassium channels.” in 2012 in Department of pharmacology of University of British Columbia.

## Table of contents

<b>Abstract.....</b>	<b>ii</b>
<b>Preface.....</b>	<b>iii</b>
<b>Table of contents .....</b>	<b>iv</b>
<b>List of figures.....</b>	<b>viii</b>
<b>List of abbreviations .....</b>	<b>x</b>
<b>Acknowledgements .....</b>	<b>xii</b>
<b>Chapter 1: Introduction and background .....</b>	<b>1</b>
1.1    K <sub>ATP</sub> overview.....	1
1.1.1    Broad architecture of K <sub>ATP</sub> channels.....	2
1.1.2    Physiological roles of K <sub>ATP</sub> channels in major organs.....	5
1.1.2.1    Pancreatic $\beta$ cells .....	5
1.1.2.2    Heart.....	6
1.1.2.3    Vascular smooth muscles.....	7
1.1.2.4    Neurons and CNS .....	7
1.1.2.5    Other tissues.....	8
1.1.3    Ligand dependent channel gating in Kir channels.....	9
1.2    Molecular details of K <sub>ATP</sub> channels .....	12
1.2.1    Kir6.2 channel subunit .....	12
1.2.1.1    Overall structure of Kir6.2 channel subunit.....	12
1.2.1.1.1    Transmembrane domain (TMD) .....	12
1.2.1.1.2    Cytoplasmic domain (CTD).....	16

1.2.1.1.3	Slide helix.....	17
1.2.1.1.4	G-loop.....	18
1.2.1.2	ATP binding site of K <sub>ATP</sub> channels.....	19
1.2.2	SUR subunit.....	20
1.2.2.1	Overall structure of SUR subunit.....	20
1.2.2.2	Nucleotide binding and regulation.....	21
1.2.2.3	Interactions of pharmacological agents with SUR subunits .....	22
1.2.3	Protein trafficking and assembly of K <sub>ATP</sub> channels .....	24
1.2.4	Diseases associated with K <sub>ATP</sub> channels .....	24
1.2.4.1	Neonatal diabetes mellitus .....	25
1.2.4.2	Persistent hyperinsulinemic hypoglycaemia of infancy .....	27
<b>Chapter 2:</b>	<b>Materials and methods.....</b>	<b>30</b>
2.1	K <sub>ATP</sub> channel constructs .....	30
2.2	Channel expression and electrophysiology.....	30
2.3	Non-radioactive Rb efflux assay.....	31
2.4	Western blot detection of K <sub>ATP</sub> channel surface expression .....	32
2.5	Cell surface labeling of K <sub>ATP</sub> channel.....	33
2.6	Statistical analysis.....	33
<b>Chapter 3:</b>	<b>Decomposition of slide helix contributions to ATP-dependent inhibition of</b>	
<b>Kir6.2 channels.....</b>		<b>35</b>
3.1	Introduction.....	35
3.2	Results.....	36
3.2.1	Functional scan of the Kir6.2 slide helix .....	36

3.2.2	Slide helix mutants reach the cell surface.....	38
3.2.3	Rationale for a novel functional rescue mechanism .....	39
3.2.4	Functional rescue of slide helix mutants by an <i>engineered</i> “forced gating” mechanism .....	40
3.2.5	Kinetic features of Kir6.2[F168E] channels, and impact of slide helix mutations ...	42
3.2.6	Effects of D58 mutations are independent of intracellular pH .....	43
3.2.7	Stringent requirement for slide helix residue D58.....	44
3.2.8	Residue D58 as an important coupling element between CTD and TMD .....	45
3.2.9	Complexity of contacts between residue D58 and the CTD.....	45
3.3	Discussion.....	49
3.3.1	Non-equivalence of loss-of-function mutations.....	50
3.3.2	Paradoxical effects of D58 mutations .....	50
3.3.3	Stringency and sensitivity of the TMD-CTD interface.....	51
3.4	Conclusion .....	53
3.5	Table and figures.....	54
<b>Chapter 4: Rescue mechanisms of potassium channel loss-of-function highlight essential residues at the Kir6.2 channel domain interface.....</b>		<b>66</b>
4.1	Introduction.....	66
4.2	Results.....	68
4.2.1	Functional scan of the Kir6.2 interfacial domain.....	68
4.2.2	G-loop mutants reach the cell surface.....	70
4.2.2.1	Functional rescue of loss-of-function Kir6.2 interfacial mutants: comparing an engineered ‘forced gating’ approach (F168E) and an allosteric approach (C166S).....	71

4.2.3	ATP sensitivity of Kir6.2 G-loop mutants on [F168E] and [C166S] background ...	73
4.2.4	Kinetic features of Kir6.2 G-loop mutants on [F168E] background .....	77
4.2.5	Distinguishing functional roles of Kir6.2 interfacial residues .....	78
4.3	Discussion: .....	81
4.3.1	Non-equivalence of loss-of-function interfacial mutations .....	82
4.3.2	Ineffectiveness of ‘allosteric approach’ [C166S] .....	82
4.3.3	Comparison of ‘forced gating’ vs ‘allosteric rescue’ approaches .....	83
4.3.4	Functional significance of G-loop on TMD-CTD coupling .....	84
4.3.5	Paradoxical effects of G-loop mutations .....	85
4.4	Conclusion .....	86
4.5	Figures .....	87
<b>Chapter 5: Conclusion .....</b>		<b>95</b>
<b>References .....</b>		<b>102</b>
<b>Appendix .....</b>		<b>123</b>

## List of figures

Figure 3-1 Domain architecture and interface of Kir channels.....	54
Figure 3-2 Systematic scan of channel activity and expression in Kir6.2 slide helix mutants.....	55
Figure 3-3 Cell surface biotinylation of SUR1 expressed in CosM6 cells. ....	56
Figure 3-4 Cell surface expression of loss-of-function slide helix mutant channels.....	57
Figure 3-5 Comparison of rescue approaches for Kir6.2 loss-of-function mutant channels. ....	58
Figure 3-6 ATP sensitivity of Kir6.2 slide helix mutant channels. ....	59
Figure 3-7 Slide helix effects on the unique kinetic features of Kir6.2[F168E] channels.....	60
Figure 3-8 ATP insensitivity of D58 mutants is not pH-dependent. ....	61
Figure 3-9 Stringent aspartate requirement at position D58.....	62
Figure 3-10 Schematic model illustrating ATP binding and gating kinetics of Kir6.2(F168E) channels with slide helix mutations. ....	63
Figure 3-11 Functional assessment of potential D58 interacting partners.....	64
Figure 3-12 Functional assessment of D204 in $\beta$ C- $\beta$ D loop and its potential interaction with R177.....	65
Figure 4-1 Domain interface of Kir channels. ....	87
Figure 4-2 Systemic functional scan in Kir6.2 G-loop, C-linker, and $\beta$ C- $\beta$ D loop mutants. ....	88
Figure 4-3 Surface expression in Kir6.2 G-loop mutants. ....	89
Figure 4-4 Cell surface expression of loss-of-function G-loop mutant channels. ....	90
Figure 4-5 Systemic functional scan in Kir6.2 loss-of-function interfacial mutant channels on two rescue background [F168E] and [C166S].....	91
Figure 4-6 ATP-sensitivity of Kir6.2 G-loop mutant channels on two rescue backgrounds [F168E] and [C166S].....	92



Figure 4-7 Effects of G-loop mutations on the unique kinetic features of Kir6.2[F168E] channels. .....	93
Figure 4-8 Distinguished functional roles of Kir6.2 interfacial mutant channels.....	94
Figure A-1 Functional assessment of multiple potential salt bridges between key interfacial residues in Kir6.2 channels. ....	123

## List of abbreviations

Kir	inwardly-rectifying potassium (channel)
K <sub>ATP</sub>	ATP-sensitive potassium (channel)
TMD	transmembrane domain
CTD	cytoplasmic domain
LOF	loss-of-function
GIRK	G protein-coupled inwardly-rectifying potassium (channel)
SUR	sulfonylurea receptor
ABC	ATP-binding cassette
ATP	adenosine-5'-triphosphate
ADP	adenosine diphosphate
PIP <sub>2</sub>	phosphatidylinositol 4,5-bisphosphate
NDP	nucleotide diphosphate
SUs	sulfonylureas
KCOs	potassium channel openers
VGCC	voltage-gated Ca <sup>2+</sup> channel
Po	open probability
TM1	transmembrane $\alpha$ -helix 1
TM2	transmembrane $\alpha$ -helix 2
GOF	gain-of-function
SNr	substantia nigra
PHHI	persistent hyperinsulinemic hypoglycaemia of infancy
PIPs	phosphatidylinositol polyphosphates

P-loop	pore loop
PNDM	permanent neonatal diabetes mellitus
DEND	developmental delay, epilepsy, and neonatal diabetes
NBD	nucleotide-binding domain
ER	endoplasmic reticulum
WT	wild-type
NDM	neonatal diabetes mellitus
TNDM	transient neonatal diabetes mellitus
DTT	dithiothreitol

## Acknowledgements

Pursuing a Master's degree could not be succeeded without support from my surroundings. I sincerely appreciate all people for instructing, advising, and assisting me in the progress toward my Master's degree.

I would like to thank my supervisor Dr. Harley Kurata for all his guidance and effects in instruction, inspiration, and assistance in completing these projects. I would particularly thank my committee members Chris Ahern (University of British Columbia/University of Iowa), Eric Accili (University of British Columbia), and Filip Van Petegem (University of British Columbia) for their invaluable insights and advice in my project design, progress, and accomplishment.

I would also like to express my appreciation for valuable numerous technical assistance provided by laboratory technicians. Special thanks to Dr. Runying Yang for her technical help on molecular biology, western blots and surface labelling. Western blots and protein surface labeling in Chapter III and Chapter IV were done by Dr. Runying Yang. Special thanks to Yuri Vilin for his technical assistance with electrophysiology recording and patch clamp. I also want to express my special thanks to Dr. Stephan Pless for his guidance on inside out patch recording using *Xenopus* oocytes.

Additionally, I would like to thank undergraduate and graduate students for their technical cooperation. Special thanks to Xinyang Huang, Robin Kim, and Roger Zhang for their help on inside out patch clamp recording and DNA constructs. Some of the inside out patches in Chapter III were collected by graduate student Xinyang Huang, and half of the slide helix mutants were made by undergraduate student Roger Zhang. Several patches examining the loss-of-function mutants described in Chapter IV were carried out by undergraduate student Robin

Kim. My appreciation is also extended to the department secretary Wynne Leung and Jesscia Yu for their advices and assistances with any administrative issues throughout my Master's degree.

Research in the lab is funded by Canadian Institutes of Health Research, Canada Foundation for Innovation, Natural Sciences and Engineering Research Council of Canada, and Heart & Stroke Foundation of Canada.

## Chapter 1: Introduction and background

Inward rectification describes a voltage dependence of current through ion channels in which the inward flow of  $K^+$  ions into the cells is greater than the outward flow of  $K^+$  ions at the same driving force. Kir channels do not exhibit intrinsic voltage-dependence but are predominantly regulated by asymmetric open channel block by intracellular divalent cations (e.g.  $Mg^{2+}$ ) and polyamines (Nichols and Lopatin, 1997; Lu, 2004). Kir channels are expressed in a wide variety of cells such as cardiac myocytes, neurons, blood cells, osteoclasts, endothelial cells, glial cells, epithelial cells, and oocytes (Hibino et al., 2010). With abundant expression in various cells, Kir channels are involved in a number of essential physiological processes and functions. For instance, Kir channels control the heartbeat pace, modulate secretion of hormones into the bloodstream, regulate electrical impulses underlying information transfer in the nervous system, and control airway and vascular smooth muscle tone. Detailed understanding of the molecular mechanisms underlying Kir channel functional activities and how they are modulated by different ligands will expose therapeutic potentials toward related disorders such as epilepsy (Shieh et al., 2000), hypertension, atrial fibrillation, Andersen syndrome (Schulze-Bahr, 2005; Plaster et al., 2001), Bartter syndrome (Schulte et al., 1999), neonatal diabetes (Nichols, 2006; Gloyn et al., 2004), congenital hyperinsulinism (Pinney et al., 2008; Nichols et al., 1996), and primary aldosteronism (Choi et al., 2011).

### 1.1 $K_{ATP}$ overview

There are seven subfamilies of inward rectifiers (Kir1 to Kir7) with a total of at least 15 different subunit genes (Hibino et al., 2010). These subfamilies can be categorized into four functional groups: 1) classical Kir channels (strong rectifier Kir2), 2) G protein-coupled Kir channels (Kir3/GIRK), 3) ATP-sensitive Kir channels (Kir6/ $K_{ATP}$ ), and 4)  $K^+$ -transport channels

(Kir1, Kir4, Kir5, and Kir7) (Nichols and Lopatin, 1997). Due to the strong homology of the basic Kir channel subunit, functional Kir channels can be assembled by four subunits in a tetrameric complex by both homomeric and heteromeric combination. Heteromerization generally occurs among members of the same subfamily (e.g. Kir2.1 can associate with any one of other Kir2.x subfamily members) (Hibino et al., 2010). An exception is that Kir4.1 subunit can assemble with Kir5.1 and form functional hetero-tetramers. Recent crystallographic and structural studies have reinforced the tetramer stoichiometry for Kir channels (Hansen et al., 2011;Whorton and MacKinnon, 2011;Nishida et al., 2007). ATP-sensitive Kir channels ( $K_{ATP}$ ) exhibit distinct stoichiometry from other Kir channels, requiring assembly of four Kir6 subunits (Kir6.1 or 6.2) with four auxiliary regulatory sulfonylurea receptor (SUR1, SUR2A, SUR2B) subunits to form a hetero-octamer. Heteromerization confers diversity to the tissue specific localization and functional variability of Kir channels.

### **1.1.1 Broad architecture of $K_{ATP}$ channels**

This study primarily focuses on the  $K_{ATP}$  channels, which were first identified in cardiac myocytes (Noma, 1983;Trube and Hescheler, 1984). These channels are also expressed in skeletal muscles (Spruce et al., 1987), vascular smooth muscle (Beech et al., 1993), neurons (Ashford et al., 1990b), brains (Ashford et al., 1988), pituitary (Bernardi et al., 1988), and kidney (Hunter and Giebisch, 1988). However, their physiological functions are likely best understood in pancreatic islet  $\beta$ -cells (Ashcroft, 2005;Ashcroft, 2006). As mentioned above,  $K_{ATP}$  channels are hetero-octameric protein complexes made of 4 pore forming Kir6 channel subunits and 4 auxiliary SUR subunits, which are members of the ATP-binding cassette (ABC) protein family (Ashcroft, 1988;Terzic et al., 1995;Tung and Kurachi, 1991). The  $K_{ATP}$  channel complex is regulated by diverse cytoplasmic ligands (most notably adenosine-5'-triphosphate (ATP),

adenosine diphosphate (ADP), and phosphatidylinositol 4,5-bisphosphate (PIP<sub>2</sub>)) and specific pharmacological agents. The distinct subunits of the channel proteins encode separate sensitivity to physiological ligands and drugs. Inhibition by ATP arises from ATP binding to the Kir6 subunits; while channel opening is enhanced by nucleotide diphosphates (NDPs) such as ADP, which along with Mg<sup>2+</sup> ions bind to the SUR subunits (Ashcroft, 1988; Terzic et al., 1995; Tung and Kurachi, 1991). The regulatory SUR units also confer sensitivity to inhibitory actions of sulfonylureas (SUs) (e.g. glibenclamide, tolbutamide) and stimulatory effects of potassium channel openers (KCOs) (e.g. pinacidil, diazoxide). These characteristics allow K<sub>ATP</sub> channels to act as ‘electrical transducers’ and affect membrane excitability in response to cellular metabolism, which is essential in controlling the electrical cascade that triggers insulin secretion. Under high glucose conditions, the increased [ATP]/[ADP] ratio results in closure of K<sub>ATP</sub> channels, favoring depolarization of the membrane potential and Ca<sup>2+</sup> influx through voltage gated L-type Ca<sup>2+</sup> channels (VGCC). In pancreatic  $\beta$ -cells, elevated intracellular Ca<sup>2+</sup> leads to fusion of insulin-containing vesicles with the plasma membrane, and insulin secretion. As metabolic activity (generation of ATP) decreases, the inhibitory effects of ATP are diminished and K<sub>ATP</sub> channels exhibit a higher open probability (P<sub>o</sub>). Assemblies of Kir6 channel and SUR subunits are required for proper trafficking and cell surface expression of functional K<sub>ATP</sub> channels. Expression of either the Kir6 channel or SUR subunit alone fails to produce detectable currents or functional activity (Aguilar-Bryan et al., 1995; Inagaki et al., 1995).

There are two isoforms of Kir6 channels (Kir6.1, Kir6.2) and three isoforms of SUR subunits (SUR1, SUR2A, SUR2B). Kir6.1 is highly expressed in vascular smooth muscle and mitochondria (Inagaki et al., 1996; Inagaki et al., 1995) and Kir6.2 is distributed more widely, including in the pancreatic  $\beta$ -cell, central nervous system, heart, and skeletal muscles (Sakura et



al., 1995). SUR1, predominantly in pancreatic  $\beta$ -cells and neurons, has a high affinity for SUs. In contrast, SUR2A, which shares only 68% identity with SUR1, is highly expressed in cardiac cells, skeletal muscle and ovary, but they can also be identified at a moderate level in pancreatic islets, brain, tongue, testis and adrenal gland. Unlike SUR1, SUR2A has a significantly lower affinity for SUs such as glibenclamide. SUR2B, an alternatively spliced variant of SUR2A differing only in their last 42 amino acids, is mainly located in the vascular smooth muscle and brain. Similar to SUR2A, SUR2B has a relatively lower affinity for SUs. Native  $K_{ATP}$  channels are generated by co-assembly of diverse Kir6 and SUR isoforms, which may account for specific tissue expression, molecular properties, and functional diversity of  $K_{ATP}$  channels (Cheng et al., 2008;Accili et al., 1997;Accili et al., 1997;Flagg et al., 2008;Aguilar-Bryan et al., 1998).

A major step forward in understanding the structure of  $K_{ATP}$  channels came by cloning of the SUR1 (Aguilar-Bryan et al., 1995;Inagaki et al., 1995) and Kir6.2 channel subunit (Inagaki et al., 1995). Each Kir channel subunit consists of two putative transmembrane  $\alpha$ -helices (TM1 and TM2), linked by an extracellular re-entrant pore loop (P-loop) that contains the signature  $K^+$  selectivity sequence (T-X-G-Y-G) (Heginbotham et al., 1994). The ion permeation pore is formed by TM2 helices from each of the four Kir subunits, whereas the bundle of four TM2 helices at the internal face is suggested to form a ligand-sensitive gate (the ‘bundle crossing’). As Kir6 channel structures lack a canonical voltage sensing domain, they are not gated by membrane voltage and in the absence of regulatory ligands (e.g. inhibitory ATP concentrations), Kir6 channels exhibit some constitutive activity.

The other major part of the Kir channels is the cytoplasmic domain (CTD), which is formed by cytoplasmic amino (NH<sub>2</sub>) and carboxy (COOH) terminal domains of the Kir subunits. The CTD forms binding sites for numerous intracellular ligands that modulate the channel

function. The CTD also forms a long permeation pathway, extended much further than in voltage-gated  $K^+$  channels. This provides multiple additional  $K^+$  binding sites, and also important interactions for intracellular  $Mg^{2+}$  and polyamine binding that modulate inward rectification. A unique structural element of Kir channels is an amphipathic transverse ‘slide helix’, which is positioned perpendicular to the pore axis and physically connects the outer TM1 helix and cytosolic  $NH_2$  terminus in the Kir channels. The slide helix sits at the TMD-CTD interface and probably acts as a coupling component between the two domains as well as communicates the ligand binding signals to the gating domain. Appropriate ligand-transduction is critical for the diverse physiological roles Kir channels play in various tissues and organs.

### **1.1.2 Physiological roles of $K_{ATP}$ channels in major organs**

$K_{ATP}$  channels are essential for numerous physiological activities including hormone secretion, regulation of neuronal and muscular excitability, and cytoprotection in heart and brain ischemia, by modulating membrane excitability in response to cellular metabolism and numerous signaling regulators (Ashcroft, 2006). In this section, I provide an overview of a few of the most widely recognized physiological roles of  $K_{ATP}$  channels.

#### **1.1.2.1 Pancreatic $\beta$ cells**

$K_{ATP}$  channels made of Kir6.2 and SUR1 are highly expressed in pancreatic insulin-secreting  $\beta$ -cells (Inagaki et al., 1996; Inagaki et al., 1995), and they are the key components of glucose stimulated insulin secretion (Ashcroft and Kakei, 1989; Ashcroft and Rorsman, 1989). Secretion of insulin is modulated by membrane electrical activity in response to changes in nutrients, hormone, and neurotransmitter levels, with glucose being the most physiologically significant. Pancreatic  $K_{ATP}$  channels are usually active during fasting blood glucose (2–3 mM), thus membrane potential is set close to the potassium reversal potential; therefore insulin

secretion is minimized. An increase in blood glucose (5–7 mM) after a meal increases cellular metabolism, resulting in elevation of ATP/ADP ratio in pancreatic  $\beta$ -cells. The augmented ATP concentration causes the closure of  $K_{ATP}$  channels, leading to membrane depolarization and activation of L-type VGCC. The  $Ca^{2+}$  influx mediates insulin release. Therefore, mutations of pancreatic  $K_{ATP}$  channels are associated with various glucose homeostasis disorders. Gain-of-function (GOF) mutations (loss of ATP sensitivity) suppress insulin release, resulting in diabetic phenotype (Koster et al., 2000; Proks et al., 2004; Proks et al., 2005a). In contrast, loss-of-function mutations in  $K_{ATP}$  channels lead to  $\beta$ -cell membrane hyperexcitability and cause hyperinsulinism (Ashcroft, 2005; Reimann et al., 2003; Thomas et al., 1996).

#### **1.1.2.2 Heart**

Cardiac  $K_{ATP}$  channels, composed largely of Kir6.2 with SUR2A, are highly expressed in the sarcolemmal membrane (Hibino et al., 2010). In the normal functioning heart, cardiac  $K_{ATP}$  channels are predominantly inhibited by high intracellular ATP concentrations, but they become active during myocardial ischemia or hypoxia when ATP concentration is significantly lowered. In this scenario, increased outward  $K^+$  currents shorten the action potential and reduce  $Ca^{2+}$  influx and energy consumption, leading to decreased cardiac contractility and stabilizing atrial and ventricular tachycardia. Opening of cardiac  $K_{ATP}$  channels is suggested to be responsible for ischemic preconditioning in which a brief duration of myocardial ischemia is introduced to prevent the heart from severe myocardial damage produced by a subsequent prolonged ischemia (Murry et al., 1986; Yellon and Downey, 2003). To support the protective role of cardiac  $K_{ATP}$  on ischemic preconditioning, ischemic preconditioning can be mimicked by KCOs and is abolished by SUs (e.g. glibenclamide) in animal studies (Gross and Auchampach, 1992; Mizumura et al., 1995; Schulz et al., 1994). Additionally, Type II diabetes mellitus patients who receive  $K_{ATP}$

channel blocker tolbutamide (Rytter et al., 1985; Soler et al., 1974) also lost the protective effects.

### **1.1.2.3 Vascular smooth muscles**

K<sub>ATP</sub> channels are also found in arterial and vascular smooth muscles. The smooth muscle form is likely composed of either Kir 6.1 or Kir 6.2 with SUR2B subunits (Isomoto et al., 1996; Yamada et al., 1997), with significant insensitivity to ATP inhibition, producing almost constitutively active channels. As a result, arterial and vascular smooth muscle K<sub>ATP</sub> channels are essential for maintaining a negative membrane potential and inducing smooth muscle relaxation and vasodilation. Several KCOs (e.g. pinacidil, nicorandil, and diazoxide) are used clinically as therapeutic treatments against hypertension and angina pectoris (Isomoto et al., 1996; Yamada et al., 1997; Edwards and Weston, 1990). Among them, nicorandil, as a nitric oxide donor, can directly produce vasodilator nitric oxide, which helps further reduce the vascular blood pressure. Additionally, the regulation of vascular smooth muscle contraction by K<sub>ATP</sub> channels also depends on various vasodilators (e.g. prostaglandin and adenosine) and vasoconstrictors (e.g. endothelin, vasopressin, serotonin, and histamine) released from neighboring cells (Quayle et al., 1997).

### **1.1.2.4 Neurons and CNS**

K<sub>ATP</sub> channels composed of either Kir6.2 or Kir6.1 with SUR1 are expressed in the glial cells and neurons in different brain regions (Ashford et al., 1990a; Roper and Ashcroft, 1995; Stanford and Lacey, 1996; Ohno-Shosaku and Yamamoto, 1992). K<sub>ATP</sub> channels expressed in the hippocampus and substantia nigra (SNr) are involved in modulation of hormone and neurotransmitter release in response to glucose changes (Ashford et al., 1990a). They close upon elevated glucose and ATP levels, resulting in membrane excitation and neurotransmitters release.

Therefore, neuronal  $K_{ATP}$  channels play physiologically fundamental roles on hypothalamic regulation of sleep-wake cycles, locomotor activity, energy expenditure, and appetite. Additionally, during ischemia or hypoxia, the increased  $K_{ATP}$  channel activity results in membrane hyperpolarization, helping reverse neuronal hyperexcitability mediated by excessive glutamate release (Dirnagl et al., 1999). The high fat ketogenic diet, with adequate proteins but low carbohydrates, is primarily used clinically to treat epilepsy in children, since the oxidative metabolism of high fat diet (ketone bodies) is suggested to reduce the ATP production from glycolysis, enabling the activation of  $K_{ATP}$  channels and thus controlling the seizure activity (Yellen, 2008). However, overactivity of  $K_{ATP}$  channels can also lead to epilepsy in patients with severe gain of function mutations (Huang et al., 2008).

#### **1.1.2.5 Other tissues**

$K_{ATP}$  channels can also be found in other tissues such as skeletal muscle, nonvascular smooth muscle, endocrine cells, renal cells, vascular endothelial cells, and follicular cells of the ovary (Ashcroft, 2006; Edwards and Weston, 1993; Quast, 1996). Activation of  $K_{ATP}$  channels in skeletal muscle is suggested to offer protective effects on myotonia congenita (characterized by delayed relaxation of the muscles after voluntary contraction) and periodic paralysis (characterized by muscle hyperexcitability, together with uncontrolled shaking followed by paralysis). Membrane hyperpolarization induced by  $K_{ATP}$  channel opening decreases skeletal muscle spontaneous twitches (Grafe et al., 1990; Spuler et al., 1989). Moreover, increased uterine myometrial smooth muscle contraction during the late stage of pregnancy may increase the risk of premature labor; thus some KCOs are used clinically to relax uterine smooth muscle via activation of  $K_{ATP}$  channels. Additionally,  $K_{ATP}$  channels expressed in the proximal tubule, thick

ascending limb of Henle's loop, and cortical collecting duct play crucial roles on  $K^+$  homeostasis and reabsorption of electrolytes (Quast, 1996).

### **1.1.3 Ligand dependent channel gating in Kir channels**

Seven subfamilies of Kir channels have multiple members with high sequence conservation and strong similarities in the domain architecture, yet a remarkable diversity in function and ligand sensitivity. The TMD encloses the ion permeation pathway with high  $K^+$  ion selectivity, and the ion conduction pore is extended to the CTD where multiple ligands bind and modulate channel function and gating. However, the molecular mechanism underlying the transduction/communication of ligand-binding domain (CTD) to channel gating domain (TMD) are largely unknown in most Kir channels

Kir channels are physiologically modulated by a variety of regulatory molecules specific to each subfamily, such as  $G\beta\gamma$  subunits (Kir3/GIRK channels), ATP (Kir6 channels), and pH (Kir1 and Kir4 channels). Structural studies indicate that binding of intracellular ligands to the cytoplasmic domain result in rotating and twisting of the cytoplasmic domain relative to the transmembrane pore (Clarke et al., 2010). This conformational rearrangement of CTD results in a propagation of the gating signal to the channel pore in the TMD, associated with rotation and bending of the inner helix TM2 and widening of the bundle crossing constriction. Previous structural, biochemical and functional studies suggest that both the selectivity filter and bundle crossing regions in Kir channels might functionally act as intrinsic gates regulating the ion permeation (Khurana et al., 2011; Yi et al., 2001b), and the conformational changes in the bundle crossing region are functionally coupled to the ATP-binding site in the CTD of  $K_{ATP}$  channels (Phillips and Nichols, 2003; Phillips et al., 2003; Loussouarn et al., 2000; Khurana et al., 2011). All eukaryotic Kir channels contain a transverse 'slide helix' at the TMD-CTD interface, which

is commonly suggested to structurally link cytoplasmic ligand-regulatory domain to the gating domains in the TMD. The slide helix has significant clinical relevance and gain-of-function mutations in the slide helix in Kir6.2 channels (Q52R and V59M/G) have been identified in neonatal diabetic patients whose pancreatic insulin secretion is greatly defective (Proks et al., 2004; Proks et al., 2005a), emphasizing its functional significance on modulation of ligand-dependent  $K_{ATP}$  channel function. The slide helix is a highly conserved motif identified in all eukaryotic Kir channels; thus understanding the functional role of slide helix on ligand-dependent gating in Kir6.2 channels may provide general information on the gating mechanisms for all other eukaryotic Kir channel families (Chapter III).

Recent crystal structures of Kir2 and Kir3 cytoplasmic domain suggest that the ion permeation pathway in the CTD can be occluded by a highly flexible pore-facing G-loop, which forms a girdle surrounding the central pore and restricts the ion flow in the absence of PIP2 (Pegan et al., 2005). Binding of PIP2 results in conformational changes of the G-loop, possibly by removing the occlusion and allowing cytoplasmic ion pore opening (Whorton and MacKinnon, 2011). The intrinsically flexible G-loop is also involved in binding of multiple ligands (e.g.  $G\beta\gamma$ ,  $Na^+$ , and PIP2) and is proposed to undergo a large structural rearrangement during channel gating in Kir3 channels. Several loss-of-function mutations in the G-loop in Kir2.1 (G300V, V302M and E303K) (Pegan et al., 2005; Tristani-Firouzi et al., 2002) and Kir6.2 (T294M and R301A/C/H/G/P) (Shimomura et al., 2009; Lin et al., 2003) have been identified in patients with Anderson syndrome and persistent hyperinsulinemic hypoglycaemia of infancy (PHHI) respectively. These findings, along with the observed structural variability and sequence conservation, suggest a potential universal role of G-loop on modulating ion permeation and pore gating across different subfamilies of Kir channels.

In addition to diverse intracellular regulators specific to each subfamily, all eukaryotic Kir channels share one common modulator, the membrane anchored highly negatively charged “signaling” phosphatidylinositol polyphosphates (PIPs), especially PIP2. Binding of PIP2 to the cytoplasmic region likely induces an overall conformation change of the CTD, resulting in an upward movement of CTD and widening of the bundle crossing region and/or the G-loop near the apex of the CTD (Hansen et al., 2011;Whorton and MacKinnon, 2011). All eukaryotic Kir channels share common structural elements involved in PIP2 binding, which increases the channel open probability and stabilizes the open state of Kir channels (Sadjja et al., 2001;Rohacs et al., 1999;Rohacs et al., 2003;Lu et al., 2002;Hilgemann and Ball, 1996;Fan and Makielski, 1997;Huang et al., 1998;Kim and Bang, 1999). Recent crystallographic studies have demonstrated that the negatively charged head-group of PIP2 interacts with positively charged residues clustered in the COOH-terminal extension (‘C-linker’) of the pore-lining TM2 helix (H175, R176, R177 in Kir6.2 and K185, K187, K188, R189 in Kir2.1 channels) (Schulze et al., 2003). These essential ‘PIP2 binding partners’ are highly conserved among eukaryotic Kir channel families, suggesting a similar molecular mechanism of PIP2-induced channel gating of other inward rectifiers.

All above highlights that despite the diversity in the regulatory molecules, the strong similarities of domain architecture, the high sequence conservation, and the unique interfacial features suggest that different Kir channels might share a similar gating mechanism and a better understating of ligand-dependent gating in Kir6.2 channels may have a general application for all the other Kirs. This thesis will explore the functional relevance of multiple unique motifs located at the TMD-CTD interface in Kir6.2 channels on ligand-dependent channel gating. Before



discussing our findings on the ligand communication/transduction mechanism, I will first review the molecular structure of  $K_{ATP}$  channels in detail.

## **1.2 Molecular details of $K_{ATP}$ channels**

### **1.2.1 Kir6.2 channel subunit**

#### **1.2.1.1 Overall structure of Kir6.2 channel subunit**

##### **1.2.1.1.1 Transmembrane domain (TMD)**

The TMD of Kir6 channels is composed of two TM helices from each subunit, named outer helix (TM1) and inner helix (TM2), which are linked by a roughly 30 amino acid pore loop (P-loop) consisting of the turret, the descending pore helix, and the ascending selectivity filter. The TM2 helices are slightly tilted with respect to the plasma membrane and they are also slightly kinked, forming an “inverted tepee” in a closed channel conformation. The internal bases of the four TM2 helices come together and make up a narrow bottom region of the ion conduction pore (bundle crossing region). The entire length of the ion conduction pore is  $\sim 64\text{\AA}$  with variable widths along the way. The central cavity is a roughly  $10\text{-}\text{\AA}$  spherical water-filled space about halfway through the membrane. It contains water in the closed state and gets enlarged in the open state and holds more water molecules. Due to the wide diameter of the internal pore and the central cavity,  $K^+$  ions can move throughout these parts with their hydrated water shell. Conversely, the selectivity filter becomes too narrow for hydrated  $K^+$  ions to pass through and  $K^+$  ions must shed their hydrating water to enter the selectivity filter.

The overall structure of selectivity filter is well conserved in all  $K^+$ -selective channels (Nishida et al., 2007). The selectivity filter (length  $\sim 12\text{ \AA}$ ), defined as the narrowest part of the ion conductance pathway in the open conformation of Kir channels, is the rate limiting step for  $K^+$  ions passing across the channel pore. The selectivity filter contains the signature  $K^+$

selectivity amino acid sequence (T-X-G-Y-G) (Heginbotham et al., 1994). The side chains of valine and tyrosine residues from the signature sequence project outward away from the inner face of the pore, making specific contacts with amino acid residues from the tilted P-loop. The hydrogen bonding between the hydroxyls of tyrosine with nearby residues on the pore helix, along with van der Waals interactions, provide strong stability when the pore opens outward to allow  $K^+$  pass through. The second glycine residue on the  $K^+$  selectivity sequence offers a rotational flexibility for the selectivity filter, which permits the polar main chain carbonyl oxygen atoms of the signature sequence to project into the pore and mimic a hydration shell that can interact with naked  $K^+$  ions (Morais-Cabral et al., 2001; Zhou et al., 2001). This interaction with dehydrated  $K^+$  ions allows them to easily pass through the ion conduction pathway and creates high selectivity since the position of these carbonyl oxygen atoms is well oriented for  $K^+$  ions, but either too far or too close for other ions (Zhou and MacKinnon, 2004). Thus this high ion selectivity permits the permeation of only  $K^+$  ions (radius  $\sim 1.33 \text{ \AA}$ ) but not the smaller  $Na^+$  ions (radius  $\sim 0.95 \text{ \AA}$ ). However, due to the similarity of ion size and permeability characteristics between  $Rb^+$  (radius  $\sim 1.48 \text{ \AA}$ ) and  $K^+$  ions, Kir channels also allow  $Rb^+$  permeation through the ion conducting pore. The electrostatic mutual repulsion between two  $K^+$  ions in the close proximity in the selectivity filter overcomes the strong electrostatic interactions between  $K^+$  ions and pore lining residues, allowing for rapid ion conductance through the channel pore (Doyle et al., 1998).

Notably, a highly conserved glycine residue (G175) located in the middle of the TM2 helix in GIRK channels is suggested to form a crucial kink, especially during  $G\beta\gamma$ -induced activation of GIRK channels (Jin et al., 2002). Structural studies demonstrated that substitution of certain residues in the TM2 helix below residue G175 with proline would increase the

flexibility of TM2 helix, producing constitutively open GIRK channels. Therefore, this glycine residue was suggested to provide flexibility and act as a hinge in the TM2 helix, allowing TM2 helix to swing away from the ion conduction pathway upon G $\beta\gamma$ -induced channel activation (Jin et al., 2002). Substitution of this essential glycine (G175P) abolished most of the basal channel activity, further supporting the hinge hypothesis. This glycine residue is highly conserved among most Kir channels, and in Kir6.2 channels, mutation of the equivalent glycine hinge residue to an arginine (G156R) has been identified in patients with congenital hyperinsulinism. In Kir4 and Kir5 channels where this glycine residue is absent, another lower glycine residue (equivalent to G143 in KirBac) located beneath the originally hypothetical glycine kink on TM2 helix, is identified as an alternative hinge of the channel (Shang and Tucker, 2008). However, the functional role of this lower glycine residue on ion permeation is less clear.

Additionally, the bundle crossing region where the TM2 helices converge near the cytoplasmic end of the TMD has been emphasized in various functional and structural studies for its functional significance on regulation of Kir channel gating, particularly in Kir6 and Kir3 subfamilies. The bundle crossing region is commonly referred as a 'lower' intrinsic gate governing the K<sup>+</sup> ion conduction across the pore by adopting either closed or open conformations (Antcliff et al., 2005; Xiao et al., 2003; Clarke et al., 2010; Proks et al., 2003; Phillips and Nichols, 2003). Based on the structural studies of KcsA and KirBac channels, in the closed conformation, the bundle crossing region seems to be a narrow constriction that restricts the flow through of hydrated K<sup>+</sup> ions (Perozo et al., 1999). TM1 and TM2 helices rotate relative to the central axis of the Kir channels upon channel opening, leading to the widening of the ion conducting pore at the bundle crossing region. The diameter of bundle crossing region varies from 3.5 Å to 12 Å during channel opening, and a ring of hydrophobic residues (such as phenylalanine and valine) at the

bundle crossing are essential for Kir channel gating. For instance, a hydrophobic phenylalanine residue F168, identified at the cytosolic end of TM2 near the bundle crossing region in Kir6.2 channels, is implied to form a narrow constriction along the ion permeation pathway and play fundamental roles on regulation of channel gating. Substitution of this residue to glutamate (F168E) in Kir6.2 channels conducted very little current around pH 7.0, but caused large channel activation upon intracellular alkalization (Khurana et al., 2011;Khurana et al., 2011). Conversely, substitution of the corresponding phenylalanine residue in Kir3 channels with small residues such as alanine or serine produced constitutively active channels (Claydon et al., 2003;Sadja et al., 2001). The opposite effects induced by mutations at this phenylalanine position highlight its functional significance on modulation of channel gating among various Kir channels. Mutations at residue V188 on TM2 near the bundle crossing region in Kir3.2 result in constitutively active channels due to disruption of inter-subunit interaction as well as stabilization of channel opening (Minor, Jr. et al., 1999;Yi et al., 2001a). All above emphasizes a clear involvement of TM2 in coupling the gating sensors to the channel gates and suggests that the bundle crossing may act as an intrinsic gate pinching off the permeation pathway to close the channel (Jin et al., 2002;Enkvetchakul et al., 2000;Loussouarn et al., 2001).

In addition to the critical roles of TM2 helix in channel gating, TM1 helix is also functionally relevant on ligand-dependent channel gating in Kir channels. Structural analysis highlights that hydrogen bond formation between key residues on the two TM helices near the bundle crossing region is crucial for Kir channel gating. For instance, in Kir1.1 channels, residue K80 on TM1 forms a hydrogen bond with residue A177 on TM2 near the bundle crossing region (Rapedius et al., 2007). Mutations of either residue disrupt the hydrogen bond, resulting in a reduced pH sensitivity and faster reactivation rate by PIP<sub>2</sub> in Kir1.1 channels (Rapedius et al.,

2007). Similarly, mutation of the corresponding residue on TM1 in Kir3.2 channels (N94H) also interrupts the hydrogen bonding, leading to a constitutively open channel (Yi et al., 2001b). Additionally, a tryptophan residue (W68) at the cytosolic end of TM1 helix in Kir6.2 channels is demonstrated to interact hydrophobically with residues T171 (and/or I167 and K170) on the COOH-terminal end of TM2 helix near the bundle crossing region, and their interaction favors channel closure (Mannikko et al., 2011). Mutations at either residue disrupt the interaction, facilitating channel opening with an intrinsic high  $P_o$  (Mannikko et al., 2011).

#### **1.2.1.1.2 Cytoplasmic domain (CTD)**

A number of crystallographic studies have investigated the detailed structure of the cytoplasmic domain of Kir channels (Pegan et al., 2005; Nishida and MacKinnon, 2002; Inanobe et al., 2007). The CTD is composed of both cytoplasmic  $\text{NH}_2$ - and  $\text{COOH}$ - terminal domains from each Kir subunit, and forms the binding sites for diverse intracellular regulatory ligands, such as ATP,  $\text{G}\beta\gamma$  subunits,  $\text{Na}^+$  ions, protons ( $\text{H}^+$ ), or PIP2 (Logothetis et al., 1987; Lu et al., 2002; Batulan et al., 2010). The CTD extends the ion permeation pathway (7-15 Å in diameter) by  $> 30$  Å than TMD alone, which is physiologically relevant for binding of intracellular open-pore blockers (e.g.  $\text{Mg}^{2+}$  ions and polyamines such as putrescine, spermidine, and spermine) to the negatively charged acidic residues (aspartate or glutamate) on the internal face of the cytoplasmic conducting pore (Nishida and MacKinnon, 2002; Kuo et al., 2003; Lopatin et al., 1994). Unlike strongly rectifying Kir2 channels, Kir6 channels are weak inward rectifiers exhibiting much weaker sensitivity for polyamine block due to lack of the classical ‘rectification controller’ aspartate residue (D172) in the pore lining TM2 helix (Kurata et al., 2004; Wible et al., 1994; Lu and MacKinnon, 1994). Instead, Kir6.2 channel subunit has an asparagine residue (N160) at the corresponding position; therefore,  $\text{K}_{\text{ATP}}$  channels permit large outward  $\text{K}^+$  currents

at depolarized potentials in the presence of polyamines, and the physiological roles of  $K_{ATP}$  channels strongly depend on ligand-dependent regulation (predominantly ATP).

Additionally, each  $NH_2$  terminus has a single  $\beta$ -strand ( $\beta A$ ), which forms  $\beta$ -sheets with another two  $\beta$ -strands ( $\beta L$  and  $\beta M$ ) in the  $COOH$ -terminus of adjacent Kir subunits (Hibino et al., 2010). This inter-subunit interaction is essential for the overall stability of the CTD and plays crucial roles on regulation of channel activity (Tucker et al., 1998). For example, association between  $NH_2$ -terminus of Kir3.1 subunits with  $COOH$ -terminus of Kir3.4 subunits greatly enhances the binding of  $G\beta\gamma$  subunits and thus the  $G\beta\gamma$ -induced channel activation (Huang et al., 1997).

#### **1.2.1.1.3 Slide helix**

The TMD forms an interface with the CTD via a transverse ‘slide helix’, which is a ~21 residue segment running parallel to the cytoplasmic face of the membrane and connecting the outer TM1 helix to the  $NH_2$ -terminus of the CTD (see Figs 3-1 and 4-1 highlighted in black). The slide helix is a unique structural element in Kir channels because it is absent in KcsA (Doyle et al., 1998), calcium-gated  $K^+$  channels (Jiang et al., 2002), or voltage-gated  $K^+$  channels (Jiang et al., 2003; Long et al., 2005). The transverse ‘slide helix’ is hypothesized to couple the ligand-induced reorientation of CTD to the bundle crossing region in the TMD in Kir channels. The crystal structure of the KirBac1.1 channel supports the role of slide helix as a ‘ligand transducing mediator’, as the slide helix is observed to stretch and swing the outer TM1 helix away from the central axis during channel activation (Kuo et al., 2003). The negatively charged  $COOH$ -terminal of the slide helix also interacts with a highly conserved arginine residue (R148) on the lower TM2 helix in KirBac1.1 channels (equivalent to K170 in Kir6.2 channels), which may help transfer the movement/reorientation of CTD to the pore lining TM2 helix and eventually the

bundle crossing (Kuo et al., 2003). Loss-of-function mutations in Kir6.2 slide helix are associated with neonatal diabetes (Proks et al., 2004; Proks et al., 2005a), but the underlying molecular mechanism of disease-causing mutants is largely unknown. In Chapter III of this thesis, a functional screening of the entire slide helix mutations in Kir6.2 will be described and the functional relevance of each slide helix residue on coupling ligand binding in CTD to channel gating in the TMD will be discussed.

#### **1.2.1.1.4 G-loop**

The ion permeation pore of CTD adjoining to the TMD also contains a flexible pore-facing ‘G-loop’ located between the  $\beta$ C and  $\beta$ D strands at the apex of CTD, and it structurally connects the  $\beta$ H and  $\beta$ I strands (Fig 4-1, in green) (Hibino et al., 2010). Crystal structures of the CTD in Kir2.1 and Kir3.1 channels reveal that the cytoplasmic ion permeation pathways are occluded by ‘G-loop’ in the absence of PIP2 (Pegan et al., 2005). The crystal structure of a KirBac3.1-Kir3.1 chimera further highlights that G-loop has at least two different conformations: dilated and constricted, suggesting that the ‘G-loop’ may act as another intrinsic gate that regulates opening and closure of the cytoplasmic ion permeation pore (Nishida et al., 2007). In the constricted conformation, the channel pore becomes too narrow for dehydrated  $K^+$  ions to pass through, whereas in the dilated conformation, the pore is wide enough to allow hydrated  $K^+$  ions to pass through. The ‘G-loop’ has high sequence conservation but considerable variation in structure among different published Kir structures. Gain-of-function mutations in the G-loop in Kir6.2 channels are associated with disorders such as permanent neonatal diabetes mellitus (PNDM) (T293N) (Shimomura et al., 2009) and neonatal diabetes coupled with developmental delay and epilepsy (DEND) (I296L) (Proks et al., 2005b). Conversely, loss-of-function G-loop mutations have been identified in patients with PHHI (T294M in Kir6.2 channels) (Shimomura

et al., 2009), and Andersen's syndrome (G300V, V302M and E303K in Kir2.1 channels) (Pegan et al., 2005;Tristani-Firouzi et al., 2002). In Chapter IV of this thesis, a functional scan of multiple unique motifs at the TMD-CTD interface including the G-loop in Kir6.2 will be carried out to investigate the critical roles of G-loop on TMD-CTD coupling as well as communicating ligand binding signals to gating domains.

#### **1.2.1.2 ATP binding site of $K_{ATP}$ channels**

Kir channels are modulated by a wide variety of intracellular regulatory molecules specific to each subfamily. The most physiologically crucial modulator affecting the  $K_{ATP}$  channels is intracellular ATP, which binds to the CTD of Kir6 channels and inhibits channel opening (Antcliff et al., 2005;John et al., 2003;Li et al., 2000;Proks et al., 1999;Reimann et al., 1999). The putative ATP binding pocket is well established from previous studies, which is located at the interface of the NH<sub>2</sub>- and COOH- terminus of adjacent Kir6.2 subunits in the CTD (Antcliff et al., 2005;Trapp et al., 2003). Five basic or uncharged residues, including R50 in the NH<sub>2</sub> terminus and I182, K185, R201, and G334 in the COOH terminus are shown to be directly involved in ATP binding (Antcliff et al., 2005;Cukras et al., 2002;Reimann et al., 1999;Tucker et al., 1998;Tsuboi et al., 2004). The stoichiometry of ATP binding suggests that each Kir6 subunit has one high affinity ATP binding site, and as a result, a functional  $K_{ATP}$  channel has four ATP binding pockets. Binding of one ATP molecule to a single Kir6.2 subunit is sufficient to promote Kir6.2 channel closure (Craig et al., 2008).

PIP<sub>2</sub>, which binds an overlapping but non-identical site as ATP, competes with ATP and reduces the apparent ATP inhibitory effects of  $K_{ATP}$  channels (Baukrowitz et al., 1998;Shyng and Nichols, 1998). Firstly, experimental assays suggest a biochemically competitive binding (also described as 'negative heterotropic' interaction) between ATP and PIP<sub>2</sub>; thus binding of PIP<sub>2</sub>



likely reduces the ATP binding affinity (Shyng et al., 2000;MacGregor et al., 2002). Secondly, binding of PIP<sub>2</sub> to the cytoplasmic region likely affects ATP inhibition allosterically by inducing an overall local conformational rearrangement of CTD, resulting in alteration of ATP binding pocket and reduced ATP-induced channel inhibition (Baukrowitz et al., 1998;Shyng and Nichols, 1998). Lastly, binding of PIP<sub>2</sub> elevates the intrinsic P<sub>o</sub> and stabilizes the open state of K<sub>ATP</sub> channels, which may also account for the decreased ATP sensitivity (Nichols, 2006;Gloyn et al., 2004;Enkvetchakul and Nichols, 2003).

## **1.2.2 SUR subunit**

### **1.2.2.1 Overall structure of SUR subunit**

In addition to the pore-forming Kir6 channel subunits, functional K<sub>ATP</sub> channels also require auxiliary SUR subunits, which are ATP-binding cassette (ABC) transporter proteins with a molecular mass around 177 kDa (Aguilar-Bryan et al., 1995;Inagaki et al., 1995). SUR is a regulatory subunit containing the structural determinants for channel stimulation by Mg-nucleotides and K<sup>+</sup> channel openers (KCOs), as well as channel inhibition by sulfonylureas (SUs). Similar to most ABC transporter proteins, SUR is typically made of two nucleotide-binding domains (NBD1 and NBD2) in the cytoplasmic domain and two transmembrane domains (TMD1 and TMD2), each comprising six TM  $\alpha$  helical segments (TM6 to TM17) (Bienengraeber et al., 2000;Matsuo et al., 2000). In addition to the typical four domain protein core (TMD1, TMD2, NBD1, NBD2), SUR subunits have an additional transmembrane domain (TMD0) made up of five  $\alpha$ -helical segments (TM1 to TM5) in the NH<sub>2</sub>-terminus. NBD1 is located on the intracellular loop connecting TMD1 and TMD2, and NBD2 is located on the cytoplasmic COOH terminus following TMD2. Walker A and Walker B motifs (G-X-X-X-X-G-K-T/S) are identified in both NBDs, and mutations in the Walker A motif in NBD1 disrupt

nucleotide binding to both NBDs and impair the stimulatory effects of NDPs, emphasizing the functional importance of the Walker motifs (Gribble et al., 1997; Babenko et al., 2000; Shyng and Nichols, 1997). The cytoplasmic loop (L0) connecting TMD0 with TMD1, along with TMD0, are suggested to be the interaction site coupling the SUR subunit with the Kir6 subunit, and this coupling is functional essential on transduction of ligand-induced conformational changes in the SUR subunits to the Kir6 channel pore, and thus modulating  $K_{ATP}$  channel gating (Babenko and Bryan, 2003; Babenko and Bryan, 2002; Aittoniemi et al., 2009).

#### **1.2.2.2 Nucleotide binding and regulation**

Although ATP primarily binds to the Kir6 channel subunit, ATP also shows a high binding affinity to the SUR1 in the absence of  $Mg^{2+}$  and inhibit channel opening (Ueda et al., 1997). Mutations in NBD1 (e.g. K719R/M and D854N) severely disrupt the high-affinity  $Mg^{2+}$ -independent ATP binding. Conversely, in the presence of  $Mg^{2+}$ , ATP is rapidly hydrolyzed to ADP, and Mg-ADP antagonizes the high affinity binding of ATP and stimulates  $K_{ATP}$  channel activity (Hollenstein et al., 2007). Crystallographic and biochemical studies on multiple prokaryotic ABC proteins suggest that the two NBDs on SUR1 subunits form heterodimers and function cooperatively in the presence of nucleotides (Bienengraeber et al., 2000; Matsuo et al., 2000; Zingman et al., 2002; Ueda et al., 1999). Dimerization of the two NBDs forms catalytic sites for ATP hydrolysis, which are composed of the Walker A motif from one NBD and the ABC signature sequence motif from the other NBD. Mutations (G1479R in the NBD2 and V187D in the TMD0 of SUR1) (Nichols et al., 1996; Otonkoski et al., 1999; Sharma et al., 2000) that prevent the dimerization of NBDs are shown to decrease Mg-ADP-mediated channel activation. As a result,  $Mg^{2+}$ -dependent ATP hydrolysis at the SUR subunits can overcome the inhibitory action of ATP on Kir6 channel subunit.

In addition to ATP, the SUR1 subunit in pancreatic  $K_{ATP}$  channels also confers sensitivity to NDPs, particularly ADP, which bind to the NBDs of SUR1 and exert their stimulatory effects in the presence of  $Mg^{2+}$  (Gribble et al., 1997). Mutations within the NBDs can prevent ADP binding, resulting in a significant reduction in Mg-ADP-induced channel stimulation without modifying ATP inhibition or the intrinsic gating of  $K_{ATP}$  channels (Gribble et al., 1997; Shyng et al., 1996). NBDs on SUR1 subunits have been shown to go from a closed channel-associated state to an open channel-associated state upon nucleotide binding in the presence of  $Mg^{2+}$  (Yamada et al., 2004). Therefore, activation of  $K_{ATP}$  channels can result from either the rapid hydrolysis of Mg-ATP or from high affinity Mg-ADP binding on SUR subunits, which, in both cases, subsequently stabilize the post-hydrolytic conformation of the NBDs.  $K_{ATP}$  channels are suggested to have a stimulatory NDP-binding site (e.g. ADP from ATP-hydrolysis) distinct from the ATP binding site on the Kir6.2 subunit (Terzic et al., 1994; Tung and Kurachi, 1991).

### **1.2.2.3 Interactions of pharmacological agents with SUR subunits**

A number of pharmacological therapeutic compounds bind to the SURs and regulate the functional activity of  $K_{ATP}$  channels. Sulfonylureas (SUs) such as chlorpropamide, tolbutamide, acetohexamide, glipzide, and glibenclamide bind to SURs and inhibit the channel activity (Edwards and Weston, 1993; Doyle and Egan, 2003; Wickenden, 2002); therefore they are used clinically as therapeutic treatments of type II diabetes mellitus to stimulate insulin secretion (Doyle and Egan, 2003; Schmid-Antomarchi et al., 1987b; Schmid-Antomarchi et al., 1987a). A single serine residue (S1237) identified at the cytoplasmic loop linking the TM15-TM16 of SUR1 subunit is essential for the high affinity binding of SUs (Ashfield et al., 1999). Residues located on the intracellular loops connecting TM5-TM6 are also suggested to be important for SUs binding with a relatively lower affinity (Ashfield et al., 1999; Mikhailov et al., 2001).

Similar to ATP, SUs stabilize the closed state of the channels (Gillis et al., 1989;Barrett-Jolley and Davies, 1997). Biochemical studies suggest that binding of Mg-ADP on SURs seems to competitively disrupt the binding of SUs and vice versa. As a result, Mg-nucleotide stimulation reduces the inhibitory effects of SUs on  $K_{ATP}$  channels (Gribble et al., 1997). Moreover, SUs such as tolbutamide have been shown to directly interact with Kir6.2 channel subunit with a significantly lower potency and affinity (Gribble et al., 1997).

In contrast,  $K^+$  channel openers (KCOs), including pinacidil, nicorandil, minoxidil, and diazoxide (Ashcroft, 1988;Terzic et al., 1995;Tung and Kurachi, 1991), bind to SURs and stimulate channel activity. Several key residues identified on the intracellular loop connecting TM13-TM14, on the segment surrounding TM16 and TM17, and on a short fragment of NBD2 are crucial for KCOs binding (Ueda et al., 1999;Babenko et al., 2000). Electrophysiological studies imply that KCOs and Mg-nucleotides synergistically enhance  $K_{ATP}$  channel activation (Yamada and Kurachi, 2004). Binding of Mg-nucleotides enhance the channel sensitivity to KCOs (Ueda et al., 1999), while KCOs stimulate the ATP hydrolysis at the NBDs, resulting in an elevated Mg-ADP stimulated channel activation (Bienengraeber et al., 2000;Matsuo et al., 2000). As a result, the reduced ATP inhibitory effects induced upon KCObinding are mediated partially by enhanced Mg-ADP binding. KCOs have diverse therapeutic potentials on management of numerous diseases including hypertension, angina pectoris, chronic myocardial ischemia, congestive heart failure, bronchial asthma, urinary incontinence, congenital hyperinsulinemia, and certain skeletal muscle myopathies. For example, diazoxide is clinically used to treat PHHI and selective KCOs are used for uterine smooth muscle relaxation during late pregnancy to prevent premature labor (Edwards and Weston, 1990).

### **1.2.3 Protein trafficking and assembly of K<sub>ATP</sub> channels**

Assembly of Kir6.2 channel subunits with SUR1 subunits in the endoplasmic reticulum (ER) is required for proper trafficking and cell surface expression of functional K<sub>ATP</sub> channel. However, truncated Kir6.2 channels with the deletion of either the last 26 residues (Kir6.2ΔC26) or 36 (Kir6.2ΔC36) amino acids in the COOH-terminus can form functional K<sub>ATP</sub> channels that are appropriately trafficked and expressed on the cell membrane surface independently without SURs (Tucker et al., 1997). This allows the intrinsic properties of Kir6.2 to be assessed in the absence of SUR1. The truncated region contains an amino acid sequence R-K-R, which serves as an ER-retention signal. The same ER-retention sequence is also identified in the cytoplasmic loop between TMD1 and NBD1 in SUR1 subunit (Zerangue et al., 1999). Therefore, it is hypothesized that both ER-retention motifs are masked upon association of Kir6.2 and SUR1 subunits, ensuring the appropriate trafficking and membrane surface expression of fully functional K<sub>ATP</sub> channels. In addition to the independent surface expression, Kir6.2ΔC26 and Kir6.2ΔC36 channels remain intrinsically sensitive to ATP inhibition with a remarkably attenuated Po (~0.09), as compared to wild-type (WT) Kir6.2 channels with a much higher Po (~0.69).

### **1.2.4 Diseases associated with K<sub>ATP</sub> channels**

K<sub>ATP</sub> channels couple cellular metabolism to membrane potential and electrical excitability by sensing changes in ATP concentrations and modulating K<sup>+</sup> fluxes. Mutations that alter the sensitivity of K<sub>ATP</sub> channels to intracellular ATP/ADP ratios or modify the intrinsic channel characters will result in impaired regulation of K<sub>ATP</sub> channels, leading to severely deleterious physiological consequences.

#### 1.2.4.1 Neonatal diabetes mellitus

GOF mutations of  $K_{ATP}$  can trigger neonatal diabetes mellitus where constitutively active  $K_{ATP}$  results in membrane hyperpolarization, suppression of  $Ca^{2+}$  influx and decreased insulin secretion in pancreatic  $\beta$ -cells (Ashcroft, 2005). Neonatal diabetes mellitus (NDM), defined as insulin-requiring hyperglycemia that occurs within the first 3 months of life, is a rare disorder with an estimated incidence of 1 in 400,000 neonates (Polak and Shield, 2004). Approximately half of NDM cases resolve completely within 18 months (transient neonatal diabetes mellitus (TNDM)), while the other half have historically been treated with lifelong insulin injections (permanent neonatal diabetes mellitus (PNDM)). Heterozygous GOF mutations in *KCNJ11* encoding Kir6.2 subunits are associated with insulin secretory insufficiency and account for ~50% of PNDM (Edghill et al., 2004; Sagen et al., 2004), and some of them are also accompanied with neurological disorders such as development delay, muscle weakness, and epilepsy (DEND syndrome) (Hattersley and Ashcroft, 2005). Most  $K_{ATP}$ -linked neonatal diabetes-associated mutations result in significantly decreased sensitivity of  $K_{ATP}$  channels to ATP inhibition. Most PNDM patients are now treated with SUs, which bind to SUR subunits and inhibit the  $K_{ATP}$  channel activity. In more severe cases, insulin injections are required. Mutations of  $K_{ATP}$  channels exhibit strong genotype-phenotype relationship as the severity of disease is correlated with the extent of reduction on ATP sensitivity (Ashcroft, 2005). Mutations causing a smaller decrease in ATP sensitivity likely result in neonatal diabetes alone, whereas mutations producing a larger impact in ATP sensitivity are associated with multiple neurological complications together with neonatal diabetes.

In general, neonatal diabetes-associated mutations either impair the ATP binding pocket directly or disrupt the ATP sensitivity without directly perturbing the ATP binding. Neonatal

diabetes-associated mutations at residues located within or close to the putative ATP binding pocket in the CTD of Kir6.2 channels (such as R201H/C, R50P, I192, and F333) likely induce conformational changes of ATP binding site and reduce ATP binding affinity (Proks et al., 2004;Proks et al., 2005a;Gloyn et al., 2005;Gloyn et al., 2004). These mutations generally do not affect the intrinsic channel gating in the absence of ATP. Conversely, other diabetes-linked mutations are located in positions involved in channel gating such as the ‘slide helix’ (Q52R and V59M/G), the cytoplasmic interface, or the ‘G-loop’ (T293N, T294M and I296L); therefore they most likely perturb the inhibitory effects of ATP allosterically (Proks et al., 2004;Proks et al., 2005a). In Chapter III and IV of the thesis, I will dissect the functional relevance of residues in the ‘slide helix’, the ‘G-loop’, and other conserved interfacial motifs in Kir6.2 channels on ATP sensitivity. Screening of the entire TMD-CTD interface may suggest a model in which ligand-dependent channel gating is achieved via an intact TMD-CTD coupling. Interestingly, most mutations impairing the putative ATP binding site directly are associated with neonatal diabetes only (e.g. R50P and R201H); whereas mutations disturbing ATP-dependent channel gating and disrupting ATP inhibition allosterically are likely associated with additional neurological complications (e.g. I296L).

Additionally, GOF mutations in SUR1 can also lead to neonatal diabetes via an enhancement of Mg-ADP-induced stimulatory effects and a reduction on the overall ATP sensitivity. Most of them are concentrated in TMD0 (F132L), cytoplasmic loop connecting TMD0 to TMD1, and NBD2 (R1380L) in SUR1 subunits (Aittoniemi et al., 2009;Proks et al., 2006;Proks et al., 2007). The TMD0 and the intracellular loop connecting TMD0 to TMD1 are involved in functional coupling with neighboring pore-forming Kir6.2 channel subunits (Babenko and Bryan, 2003;Fang et al., 2006); therefore, GOF mutations near these regions affect

the Kir6.2-SUR1 interaction and decrease ATP inhibitory effects. Additionally, GOF mutations clustered near NBD2 in SUR1 subunits impair ATP inhibition by either enhancing  $Mg^{2+}$ -ADP stimulation or strengthening the MgATPase activity in NBD2, which in turn indirectly reinforces the  $Mg^{2+}$ -ADP stimulation via shortening pre-hydrolytic Mg-ATP-bound state and prolonging the Mg-ADP-bound state of SUR1 (de Wet et al., 2008; de et al., 2007).

Most PNDM patients are treated with oral administration of SUs such as tolbutamide or glibenclamide. Additionally, SUs help improve the muscle weakness and mental developmental delay, so several SUs are used clinically to ameliorate the extra-pancreatic symptoms (Shimomura et al., 2007; Slingerland et al., 2006). Unfortunately, in PNDM patients with neurological complications, SUs are sometimes not very effective due to high intrinsic  $P_o$  of Kir6.2 mutations.

#### **1.2.4.2 Persistent hyperinsulinemic hypoglycaemia of infancy**

LOF mutations in *KCNJ11* encoding Kir6.2 (Ashcroft, 2005; Reimann et al., 2003; Thomas et al., 1996) have been shown to produce sustained membrane depolarization and continuous  $Ca^{2+}$  influx, leading to excessive insulin secretion, irrespective of blood glucose level. As a result, LOF mutations in Kir6.2 channels are associated with inherited persistent hyperinsulinemic hypoglycaemia of infancy (PHHI). However, the most common cause of PHHI is LOF mutations of *ABCC8* encoding the SUR1 subunit (Huopio et al., 2000; Thomas et al., 1995). Most of the LOF mutations in SUR1 either lead to reduced surface expression of  $K_{ATP}$  channels due to abnormal gene expression, protein assembly or membrane trafficking (Ashcroft, 2005; Dunne et al., 2004; Yan et al., 2004; Taschenberger et al., 2002; Partridge et al., 2001), or produce channels with impaired responses to Mg-ADP stimulation so the channels are preferentially closed (Ashcroft, 2005; Dunne et al., 2004; Yan et al., 2004). For instance, one of



the most common PHHI mutations (SUR1 [ $\Delta$ F1388]) leads to trafficking deficiency and reduced surface expression; therefore most  $K_{ATP}$  channel mutants are retained in the ER (Cartier et al., 2001). Most mutations associated with perturbed Mg-ADP stimulation cluster within the NBDs of SUR1 where they impair adenosine nucleotide binding or hydrolysis directly. Some of them are located elsewhere of SUR1 and affect the nucleotide binding/hydrolysis allosterically (Abdulhadi-Atwan et al., 2008). In general, due to largely reduced surface expression of functional  $K_{ATP}$  channels, most PHHI patients do not respond to KCOs and require subtotal pancreatectomy to further reduce excessive insulin secretion (Hibino et al., 2010). Therefore, future research on patients' genotype and  $K_{ATP}$  channel function will aid in the proper selection of therapeutic treatments, adjustment of therapy dosages, and development of more rational approaches to treat PNDM and PHHI.

With a clear recognition of the functional significance of appropriate ligand-modulated channel gating of  $K_{ATP}$  channels to their various physiological roles, the rest of the thesis will focus on investigating the molecular mechanism that links ligand binding to the channel gate in ATP-sensitive Kir6.2 channels. The rest of the thesis is divided into 2 chapters exploring the functional relevance of multiple conserved motifs at the TMD-CTD interface of Kir6.2 channels on transduction/communication of ATP binding in the cytoplasmic domain to the channel gating domain in the TMD, followed by a concluding chapter.

Chapter III: *Decomposition of slide helix contributions to ATP dependent inhibition of Kir6.2 channels.* A conserved 'slide helix' forms an interface between the cytoplasmic (ligand-binding) domain and transmembrane pore, and many mutations in this region cause loss-of-function. Using a novel 'forced gating' approach (Kir6.2[F168E]) to rescue electrically silent channels, we have decomposed the contribution of each slide helix residue to ATP-dependent

gating. We demonstrate that effective inhibition by ATP relies on an essential aspartate residue D58, which enables functional channel expression and control of Kir6.2 gating by intracellular ATP. The D58 anchor position exhibits an extremely stringent requirement for aspartate, as even a highly conservative mutation to glutamate is insufficient to restore normal channel function. Additionally, we scanned nearby positively charged residues in the CTD that potentially interact with this essential ‘aspartate anchor’ and highlighted that R177 in the C-linker is also essential for ATP-dependent gating.

Chapter IV: *Rescue mechanisms of potassium channel loss of function highlight essential residues at the Kir6.2 channel domain interface.* In addition to the transverse ‘slide helix’, the interface between the TMD and CTD in Kir6.2 channels comprises of various other conserved motifs, most notably the COOH-terminal extension (‘C-linker’) of the pore-lining TM2 helix, the cytoplasmic fore-facing ‘G-loop’, and the  $\beta$ C- $\beta$ D loop. We have expanded our mutagenic scan to characterize functional roles of the other motifs in the interfacial region on  $K_{ATP}$  channel function and ligand sensitivity. Since most interfacial mutants result in channel loss-of-function, both the ‘forced gating’ approach (Kir6.2[F168E]) and a traditional ‘allosteric rescue’ approach (Kir6.2[C166S]) were implemented to rescue electrically silent mutants. Their rescue efficiency and secondary effects on ATP sensitivity were compared. Recognition of a subset of residues at the Kir6.2 TMD-CTD interface with dichotomous responses to the rescue mechanisms mechanistically suggest their essential roles on both formation of conductive channels and appropriate communication of ligand binding to gating domains. Disruption of these residues uncouples the TMD and CTD, causing loss of function combined with profound ligand insensitivity and gating defects.

## **Chapter 2: Materials and methods**

### **2.1 K<sub>ATP</sub> channel constructs**

All mutant channel constructs were derived from the mouse Kir6.2 gene expressed in the pcDNA3.1(−) plasmid (Invitrogen, Carlsbad, CA). All mutant channel constructs had a GFP tag fused to the Kir6.2 COOH-terminus by a 6X-glycine linker. Site specific point mutations of individual residue at the TMD-CTD interfacial region (including the slide helix, the G-loop, the C-linker, and the βC-βD loop) with alanine were introduced by overlapping PCR-based methods. Then the fragments containing the mutations were subcloned into pcDNA3.1(−), and verified by restriction endonuclease digestion and Sanger sequencing (Genewiz). SUR1 (hamster) and FLAG-SUR1 (gift from Show-Ling Shyng, OHSU, Portland, Oregon) were also expressed in pcDNA3.1(−).

### **2.2 Channel expression and electrophysiology**

COSm6 cells were cultured in a 50 ml polystyrene tissue culture flask (Becton Dickinson Labware) in DMEM (Invitrogen) supplemented with 10% FBS and 1% penicillin-streptomycin. Cells were incubated in a 5% CO<sub>2</sub> incubator at 37 °C. The COSm6 cells were cotransfected with Kir6.2 mutant channel constructs (1.0 μg) and hamster SUR1 (1.2 μg) with either Fugene6 (Roche) or jetPRIME (Polyplus transfection SA). The cells were incubated in the presence of transfection mixture for 24 hrs, and then the transfected cells were split onto sterile glass cover slips, followed by electrophysiological recording 2-3 days later.

Inside-out patch clamp experiments were performed using the RSC-200 rapid solution exchanger (BioLogic) to enable solution jumps with a multi-barreled solution delivery turret at room temperature, and the solutions were delivered by pressure-driven flow (syringe pump) (Kurata et al., 2011). For continuous recordings, data were typically filtered at 1 kHz, sampled at

5 kHz, and stored directly on a computer hard drive using Clampex software (Axon Inc.). For voltage-step recordings, data were filtered at 2 kHz and sampled at 10 kHz. Glass pipettes were pulled to a resistance of 1-2 M $\Omega$ . In most experiments, symmetrical recording solutions (the standard pipette and bath) were used, with the following composition: 140 mM KCl, 1 mM K-EGTA, 1 mM K-EDTA, and 4 mM K<sub>2</sub>HPO<sub>4</sub>. ATP (FLUKA chemicals, Sigma-Aldrich) was stored as 100 mM stocks (dissolved in standard bath solution, with pH adjusted to 7.3). For experiments using different ATP concentrations, all other components were maintained with the only adjustment on the ATP concentrations. Pipette solution was adjusted to pH 7.3 using KOH. The pH of each patching solution was verified to the desired level (7.3 or 8.0) using 1 mM KOH and 1 mM HCl each experimental day, with particular attention to the addition of solutes that can affect solution pH (in this case, particularly ATP). Chemicals were purchased from Sigma-Aldrich or Fisher. Through the text, data are presented as mean  $\pm$  s.e.m.

### **2.3 Non-radioactive Rb efflux assay**

COSm6 cells in 24-well plate were transiently cotransfected with SUR1 and various Kir6.2 mutants with Fugene6 (Roche) or jetPRIME (Polyplus transfection SA), and efflux assays were performed 2 days after transfection. Cells were loaded for 1 hour with Rb<sup>+</sup> loading media (in mM: RbCl, 5.4; NaCl, 150; CaCl<sub>2</sub>, 2; NaH<sub>2</sub>PO<sub>4</sub>, 0.8; MgCl<sub>2</sub>, 1; glucose, 5; HEPES, 25; pH7.4). Then they were washed rapidly with PBS twice, and incubated in 600  $\mu$ l glucose free activating buffer (in mM: 118 NaCl, 118; CaCl<sub>2</sub>, 2.5; KH<sub>2</sub>PO<sub>4</sub>, 1.2; KCl, 4.7; NaHCO<sub>3</sub>, 25; MgSO<sub>4</sub>, 1.2; HEPES, 10; pH 7.4) supplemented with metabolic inhibitors (2.5  $\mu$ g/mL oligomycin, 1 mM 2-deoxy-D-glucose) when indicated. Aliquots of the assay buffer (150 $\mu$ l) were removed at multiple time points (5, 10, 20, 40 minutes). After completion of the assay, the cells were lysed with 1% SDS lysis buffer, and the Rb<sup>+</sup> concentration in the supernatant was

determined by flame atomic absorption spectroscopy using the Aurora Biomed ICR8000 instrument.  $\text{Rb}^+$  efflux was calculated as a fraction of total loaded  $\text{Rb}^+$  (determined as the sum of extruded  $\text{Rb}^+$  and  $\text{Rb}^+$  left in lysed cells at the end of the assay). For clarity of figure presentation, data was normalized to efflux from WT Kir6.2 transfected cells (normalized  $\text{Rb}^+$  efflux =  $(\text{Efflux}_{\text{Mutant}} - \text{Efflux}_{\text{Untransfected}}) / (\text{Efflux}_{\text{WT Kir6.2}} - \text{Efflux}_{\text{Untransfected}})$ ). However, raw efflux data was used for statistical tests. For simplicity, only data from the 40 minute time point has been presented (as mean  $\pm$  s.e.m.).

## **2.4 Western blot detection of $\text{K}_{\text{ATP}}$ channel surface expression**

COSm6 cells in 6-well plates were transfected with mouse Kir6.2 channel cDNA (1.0  $\mu\text{g}$  per well) and either FLAG-tagged hamster SUR1 (1.2  $\mu\text{g}$  per well), or WT hamster SUR1 (1.2  $\mu\text{g}$  per well), as indicated in respective figures. After 3 days of incubation, transfected cells were washed with 4°C PBS (in mM: 137 NaCl, 2.7 KCl, 10  $\text{Na}_2\text{HPO}_4$ , 2  $\text{KH}_2\text{PO}_4$ ) and lysed in 250  $\mu\text{l}$  lysis buffer (150mM NaCl, 20mM HEPES, 10mM EDTA, 1% NP-40, one protease inhibitor tablet per 10ml, pH7.3) for 30 min at 4°C. Western blotting was carried out on collected total cell lysates, using 7.5% SDS-PAGE, followed by transfer to nitrocellulose membrane. SUR1 protein was detected by labeling with mouse anti-FLAG primary antibody (for FLAG-SUR1, Sigma-Aldrich), or a monoclonal SUR1 antibody (UC Davis/NIH NeuroMab facility, clone N289/16, for WT SUR1), and HRP-conjugated goat anti-mouse secondary antibody (ABM, Vancouver, Canada). Blots were visualized by ECL methods (Femto ECL detection kit, Pierce) using a FluorChem SP gel imager (Alpha Innotech).

## 2.5 Cell surface labeling of K<sub>ATP</sub> channel

COSm6 cells in 6-well plates were cotransfected with Kir6.2 channel cDNA (1.0 µg) and SUR1 (1.2 µg in the pECE vector) with jetPRIME (Polyplus transfection SA). After 3 days of incubation, transfected cells were washed two times with 4°C PBS (in mM: 137 NaCl, 2.7 KCl, 10 Na<sub>2</sub>HPO<sub>4</sub>, 2 KH<sub>2</sub>PO<sub>4</sub>). Then the transfected cells were incubated with 50µM Sulfo-NHS-SS-biotin (Pierce) for 30 mins and were washed three more times with TBS (in mM: 10 Tris-Hcl, 120 NaCl). Then the cells were solubilized in 200 µl lysis buffer (in mM: 150 NaCl, 20 HEPES, 110 K-Acetate, 1 MgCl<sub>2</sub>, 1 pefabloc, 0.5% Na-DOC, 0.1% Tween, 1% Triton X-100, 0.5% Na-DOC, 1 µg/ml pepstatin, one protease inhibitor tablet per 10ml, pH7.3) (Pierce) by rotation at 4 °C for 15 mins. Then the biotinylated channel proteins were affinity-purified using streptavidin beads (Pierce). The beads were washed two times with 500 µl lysis buffer before use, and the mixture of biotinylated proteins and beads was allowed to incubate overnight at 4 °C with rotation. The beads were washed three times with 1ml lysis buffer. Proteins were eluted in 100 µl of SDS sample buffer, followed by treatment with 1 mM dithiothreitol (DTT) for 30 mins at 50°C to reduce disulfide bonds. Proteins were separated by 7.5% SDS-PAGE, followed by transfer to nitrocellulose membrane. SUR1 protein was detected by labeling with mouse anti-FLAG primary antibody (for FLAG-SUR1, Sigma-Aldrich), or a monoclonal SUR1 antibody (UC Davis/NIH NeuroMab facility, clone N289/16, for WT SUR1), and HRP-conjugated goat anti-mouse secondary antibody (ABM, Vancouver, Canada). Blots were visualized by ECL methods (Femto ECL detection kit, Pierce) using a FluorChem SP gel imager (Alpha Innotech).

## 2.6 Statistical analysis

Data are presented as (mean ± s.e.m.) and analyzed using pCLAMP software (Axon Instrument) and Microsoft Excel programs. All patch data reported were based on four or more

patches obtained from different COSm6 cells. All experiments required multiple comparisons of mutants with WT Kir6.2 or Kir6.2[F168E] channels. We used a one-way ANOVA multiple comparison test, followed by Dunnett's post-hoc test to compare mutants with WT Kir6.2 or Kir6.2[F168E] background channels, as indicated in appropriate figure legends. Dunnett's post-hoc test is a multiple comparison to compare a number of experimental treatments against a single control group

## **Chapter 3: Decomposition of slide helix contributions to ATP-dependent inhibition of Kir6.2 channels**

### **3.1 Introduction**

In addition to voltage-dependent block by  $Mg^{2+}$  and polyamines, some Kir channels (in the Kir3 and Kir6 families) are regulated by ligand-dependent gating that controls conformational changes around the helix bundle-crossing (in the TMD), and potentially a second auxiliary gate in the cytoplasmic G-loop (Pegan et al., 2006;Khurana et al., 2011;Hansen et al., 2011;Whorton and MacKinnon, 2011;Bavro et al., 2012). These ligand-dependent gating mechanisms act physiologically to influence or trigger cellular depolarization. One very well-known example is regulation of heart rate by the sino-atrial node  $I_{K,ACh}$  current (mediated by GIRKs) (Logothetis et al., 1987). A second example is regulation of glucose stimulated insulin secretion by  $K_{ATP}$  channels – the pancreatic  $K_{ATP}$  isoform comprises Kir6.2 and SUR1 subunits, and is the model for ligand-dependent regulation used in the present study (Aguilar-Bryan et al., 1995;Inagaki et al., 1995). In this physiological system, glucose metabolism elevates intracellular ATP, leading to inhibition of  $K_{ATP}$  channels and membrane depolarization, triggering  $Ca^{2+}$  influx essential for insulin secretion.

Kir channels comprise a canonical tetrameric pore-forming module similar to other  $K^+$ -selective channels (Nishida et al., 2007;Whorton and MacKinnon, 2011). In place of the voltage-sensing domain that typifies the voltage-gated  $K^+$  channel family, the Kir channel pore module is coupled to a CTD that extends the ion permeation pathway and serves as a ligand binding site for regulatory molecules like  $G\beta\gamma$  subunits (in Kir3 channels) or ATP (in Kir6 channels) (Nishida et al., 2007;Whorton and MacKinnon, 2011). In addition, all Kir channels require binding of  $PIP_2$



for channel activity, and recent crystallographic studies have demonstrated that the binding site for this essential phospholipid is formed predominantly by positively charged side-chains in the COOH-terminal extension ('C-linker') of the pore-lining TM2 helix (Hansen et al., 2011;Whorton and MacKinnon, 2011).

This modular architecture necessitates a mechanism for transduction of ligand-binding to the channel gate. The observation of a transverse 'slide helix' in Kir channel structures has provoked considerable speculation regarding its role as a mediator of coupling between the CTD ('ligand-sensing') and TMD ('gating') domains (Logothetis et al., 1987;Lu et al., 2002;Batulan et al., 2010), with obvious analogies drawn to the S4-S5 linker as a coupling element for voltage sensor movement and channel gating in voltage-gated channels (Logothetis et al., 1987;Lu et al., 2002;Batulan et al., 2010). Guided by recently reported structures of eukaryotic Kir channels, we have taken a systematic structure-based approach to investigate the role of the slide helix, and identify components that are essential for functional channel expression and ATP inhibition of Kir6.2 channels. Importantly, our experiments tackle a frequently encountered problem in structure-function studies of ion channels: mutations in particularly interesting channel motifs often lead to loss-of-function, impeding further analysis. We describe an effective targeted approach to rescue of loss-of-function mutants, enabling characterization of mutants that have been overlooked due to their loss-of-function phenotype.

## **3.2 Results**

### **3.2.1 Functional scan of the Kir6.2 slide helix**

The modular structure of Kir channels comprises a canonical pore-forming TMD, and a CTD (Fig. 3-1A). The TMD forms an interface with the CTD via the NH<sub>2</sub>-terminal transverse 'slide helix', and the COOH-terminal extension ('C-linker') of the pore-lining TM2 helix (Fig. 3-

1A) (Hansen et al., 2011;Whorton and MacKinnon, 2011), which also makes significant contacts with PIP<sub>2</sub>. We have designated helix Sa and helix Sb, based on a ‘kink’ apparent in recent eukaryotic Kir crystal structures (Hansen et al., 2011;Whorton and MacKinnon, 2011) (Fig. 3-1A). It is noteworthy that helix Sb is very highly conserved among the eukaryotic Kir channels while helix Sa is more divergent (Fig. 3-1B). However the functional significance of the slide helix ‘kink’ is not known.

We tested whether slide helix mutants could form functional channels by scanning their activity (co-expressed with SUR1) using a non-radioactive Rb<sup>+</sup> efflux assay (Fig. 3-2A). Under conditions of metabolic inhibition (2-deoxy-D-glucose + oligomycin, to activate K<sub>ATP</sub> channels, Fig. 3-2A, black bars), robust Rb<sup>+</sup> efflux was observed through 7 of 10 helix Sa mutants, while 6 of 10 helix Sb mutants exhibited significant or complete loss of function. Overall, these data are consistent with Rb<sup>+</sup> efflux experiments conducted in the absence of metabolic inhibition (Fig. 3-2A, white bars). Channel mutants with complete loss-of-function (e.g. F55A, D58A, F60A, T61A, D65A) exhibit little activity in either condition, while other mutants (with less extreme loss of function, e.g. L56A, T62A, L66A) exhibit some residual activity that is apparent in metabolic inhibition conditions.

These findings highlight a significant challenge that must be overcome to systematically scan the functional role/impact of residues in the interfacial slide helix on ligand-dependent gating. That is, a large fraction of mutations in this region prevent expression of functional channels. Due to the significant loss-of-function of numerous slide helix mutants, we aimed to determine the underlying defect(s), and explore mechanisms to rescue and characterize channel function.

### 3.2.2 Slide helix mutants reach the cell surface

We first investigated whether loss-of-function of slide helix mutants resulted from a trafficking deficiency, using western blot analysis and cell surface biotinylation of SUR1. As described elsewhere, maturation and glycosylation of SUR1 (dependent on SUR1 interaction with Kir6.2) generates a high molecular weight band (mature, labeled 'Mat' in Fig. 3-2B), while immature 'core' glycosylated SUR1 comprises a lower molecular weight band (immature, labeled 'Imm' in Fig. 3-2B) (Zerangue et al., 1999; Schwappach et al., 2000; Yan et al., 2007). Total protein expression level varied somewhat between specific mutant channels, most likely due to differences in transfection efficiency (all western blots were performed on transiently transfected cells expressing Kir6.2 mutants and SUR1). However, all Kir6.2 slide helix mutants examined appeared to confer maturation of SUR1 (Fig. 3-2B) based on the appearance of a higher molecular weight band. Furthermore, all Kir6.2 slide helix mutants generated increased mature:immature SUR1 ratios, relative to cells transfected with SUR1 alone (Fig. 3-2C).

The glycosylation event(s) resulting in the higher molecular weight band do not directly demonstrate cell surface expression. Using cell surface biotinylation and purification on streptavidin beads (Fig. 3-3), we observe that the upper band is selectively enriched in the biotinylated 'surface fraction' (middle lanes), and depleted in the column flow-through ('unbound fraction', right lanes), confirming that the upper band on SDS-PAGE corresponds to cell surface protein (Fig. 3-3). We also included a negative control using a trafficking deficient SUR1 mutant (R1419H), previously reported to disrupt cell surface  $K_{ATP}$  expression (Ribalet et al., 2006; Shyng et al., 2000; Enkvetchakul et al., 2001). Channels made up of Kir6.2 and SUR1[R1419H] did not exhibit an upper band, and generated very little surface biotinylated

signal, indicating that the lower molecular weight band does not appear significantly at the cell surface (Fig. 3-3).

We also used surface biotinylation to confirm that loss-of-function slide helix mutants (identified in Fig. 3-2) were reaching the cell surface (Fig. 3-4A,B). All loss-of-function slide helix mutants exhibit a pattern comparable to channels comprising WT Kir6.2 + SUR1, in which a significant upper band was observed on SDS-PAGE, and the upper band was selectively enriched in the surface labeled fraction. As a negative control, we also included the Kir6.2[H259R] mutant, previously reported to disrupt cell surface  $K_{ATP}$  expression (Ribalet et al., 2006; Shyng et al., 2000; Enkvetchakul et al., 2001). Much like SUR1[R1419H], Kir6.2[H259R] channels exhibited no upper band on SDS-PAGE, and very little signal in the surface labeled protein fraction (Fig. 3-4B).

Taken together, these findings demonstrate that loss-of-function in the slide helix mutants arises from a failure to form conductive channels, rather than a failure to traffic to the cell surface. For the remainder of the study, we focus on a novel ‘forced gating’ approach to rescue function in electrically silent mutants, allowing a systematic scan of the functional contributions of slide helix residues to ATP dependent gating of Kir6.2.

### **3.2.3 Rationale for a novel functional rescue mechanism**

Due to the loss-of-function phenotype of numerous slide helix mutants, we sought to further investigate the functional role of this motif. A previously reported approach to recover function in Kir6.2 loss-of-function channels was to express mutants on C166 mutant backgrounds with high intrinsic open probability (e.g. C166A, or C166S channels) (Ribalet et al., 2006; Shyng et al., 2000; Enkvetchakul et al., 2001). However, in the context of studying mechanisms of ATP inhibition, this approach has the disadvantage of dramatically shifting ATP

sensitivity well into the mM range (Antcliff et al., 2005; Proks et al., 1999). In our experiments, C166S shifted the Kir6.2 ATP IC<sub>50</sub> from  $32 \pm 4 \mu\text{M}$  (Fig. 3-5A,D) to  $> 5 \text{ mM}$  (Fig. 3-5C,D). We suspected that this relatively ATP-insensitive background (due to the C166S mutation) would likely confound comparisons of ATP sensitivity between slide helix mutants.

We have developed an alternative approach to rescue channel function using a recently described ‘forced gating’ mechanism (Khurana et al., 2011). In this strategy, substitution of a glutamate in the hydrophobic Kir channel bundle crossing (F168E mutation in Kir6.2), generates channels that open upon alkalization, likely due to mutual repulsion of the acidic glutamate side chains at the bundle crossing gate. A similar mechanism of mutual repulsion has been described for activating mutations in KirBac channels (Bavro et al., 2012; Paynter et al., 2010). Despite perturbation of the helix bundle crossing, Kir6.2[F168E] channels remain well-inhibited by ATP, with ~80% current inhibition in 1 mM ATP (Figs. 3-5B,D, 3-6A,B), and an IC<sub>50</sub> for ATP (at pH8.0) of  $61 \pm 15 \mu\text{M}$ . This differs modestly from the ATP sensitivity of WT Kir6.2 ( $32 \pm 4 \mu\text{M}$ ), especially when compared to alternative rescue methods such as the C166S background. However, an important difference from WT Kir6.2 channels is that Kir6.2[F168E] exhibits a ‘plateau’ conductance at high ATP concentrations (Fig. 3-5D).

### **3.2.4 Functional rescue of slide helix mutants by an *engineered* “forced gating” mechanism**

Remarkably, when expressed on the background of the Kir6.2[F168E] mutant, all slide helix mutants generated large macroscopic currents in excised membrane patches (Fig. 3-6), including all deleterious slide helix mutants identified in Figure 3-2A. This suggests that the F168E background mutation effectively rescues loss-of-function slide helix mutants, consistent with our demonstration of intact surface expression of these mutants (Figs. 3-2B, 3-4). Thus, we

employed this novel and highly effective rescue approach for systematic comparison of mutations at all slide helix positions.

We determined the  $IC_{50}$  for ATP inhibition of each slide helix mutant (on the Kir6.2[F168E] background, at pH 8.0 because currents are considerably larger) (Fig. 3-6B). It is noteworthy that activity and ATP sensitivity of Kir6.2[F168E] channels are pH sensitive (Khurana et al., 2011), so it was essential to meticulously adjust pH in all solutions to ensure effects did not arise from slight variations in pH. Exemplar sweeps measuring ATP sensitivity in various slide helix mutants are depicted (Fig. 3-6A), in which patches were formed and excised in pH 7.3, switched to pH 8.0 to demonstrate the F168E-mediated pH-dependence, and stepped through several ATP concentrations at pH 8.0. Effects of pH and ATP were all rapid, stable, and fully reversible.

ATP sensitivity of most slide helix mutants closely resembled the Kir6.2[F168E] background channel (Kir6.2[F168E][L56A] is provided as an example in Fig. 3-6A). However, numerous slide helix mutations had statistically significant effects on ATP sensitivity relative to the Kir6.2[F168E] background channel (Fig. 3-6B). Many of these positions have been identified in early biophysical studies of Kir6.2, or in patients diagnosed with neonatal diabetes, so we focused on two prominent clusters with the most dramatic effects. The first set (I49A, R50A) has been previously described and lies close to the well-described ATP binding site, likely contributing to binding the ATP  $\gamma$ -phosphate (Antcliff et al., 2005; Proks et al., 1999). Positions I49 and R50 are tolerant to mutation (Fig. 3-2A), and so both residues have been functionally characterized in earlier studies (Antcliff et al., 2005; Proks et al., 1999). More interesting was the cluster of mutants (D58A, F60A) in the ‘kink’ region of the slide helix (at the helix Sa and Sb junction, Fig. 3-1A). These positions are not predicted to contribute to the putative ATP binding

site, and are unlikely to make any direct contacts with ATP (Antcliff et al., 2005; Proks et al., 1999). Moreover, they are relatively intolerant of mutations (Fig. 3-2A), although an F60Y mutation has been identified previously in a neonatal diabetes patient, and appears to play an important role for ATP inhibition (there is strong conservation for aromatic residues at this position, Fig. 3-1B, though we have not investigated their functional role any further in this study) (Mannikko et al., 2010). The D58 position had the largest effect on ATP sensitivity in our scan, a novel effect previously impossible to explore due to the complete loss-of-function that accompanies this mutation. D58A mutant had profoundly reduced ATP sensitivity, with very little inhibition observed even in 10 mM ATP (Fig. 3-6A, right panel). It is noteworthy that effects of the D58A mutation significantly outweigh effects of Kir6.2 mutations at positions identified in neonatal diabetic patients (R50, Q52, G53, R54, V59, F60, T61) (Nishida and MacKinnon, 2002; Lopatin et al., 1994; Kuo et al., 2003). Also noteworthy is that these data discriminate different contributions of functionally ‘essential’ residues to the channel gating mechanism. That is, not all loss-of-function mutations impact the ATP sensing mechanism in equivalent ways. By rescuing non-functional mutant channels, these experiments distinguish previously unrecognized components of the ATP-dependent gating mechanism.

### **3.2.5 Kinetic features of Kir6.2[F168E] channels, and impact of slide helix mutations**

Notably, in addition to rescuing loss-of-function mutants, the Kir6.2[F168E] mutation imparts a weakly voltage-dependent gating phenotype that is absent in WT Kir6.2 channels (Kurata et al., 2010). Membrane hyperpolarization causes time-dependent opening of Kir6.2[F168E] channels, and these kinetic features persist clearly in inside-out patches after washout of endogenous polyamines (Fig. 3-7A). Therefore, this voltage-dependence appears to be an intrinsic property of Kir6.2[F168E] mutant channels (rather than a consequence of block

by residual polyamines) (Lu, 2004). These properties are similar to a previously reported polyamine-independent voltage-dependence in Kir6.2[L157E] channels, but with opposite polarity (Kurata et al., 2010). The voltage-dependent kinetic features of Kir6.2[F168E] offered a unique additional assay to compare the effects of slide helix mutants on channel function.

Most slide helix mutants had little or no effect on gating kinetics, with hyperpolarization-dependent channel opening remaining similar to Kir6.2[F168E] channels (Fig. 3-7A). Only two slide helix mutations near the helix Sa-Sb ‘kink’ (D58A, T61A) markedly altered the kinetics of voltage-dependent channel opening (Fig. 3-7A,B). The D58 position stood out in this comparison of slide helix positions, as kinetics in Kir6.2[F168E][D58A] mutant channels were too rapid to resolve (Fig. 3-7A,B). We estimate that in well-formed inside-out patches we can confidently resolve time constants of  $\sim 0.5$  ms, and so  $2 \text{ ms}^{-1}$  is indicated as a lower limit for  $1/\tau_{\text{step}}$  of D58A channels. It is noteworthy that the ATP binding site mutations (I49A, R50A) did not alter the gating kinetics (Fig. 3-7A,B), suggesting that D58A changes ATP sensitivity by a distinct mechanism that does not involve disruption of the ATP binding site.

### **3.2.6 Effects of D58 mutations are independent of intracellular pH**

A well understood property of  $K_{\text{ATP}}$  channels is that ATP sensitivity is a variable channel parameter that changes with channel open probability. Manipulations that increase  $P_o$  (e.g. mutations or increased membrane PIP2 content) typically weaken ATP sensitivity (Mannikko et al., 2010; John et al., 2005; Shimomura et al., 2006; Koster et al., 2005; Koster et al., 2008). The F168E background channel has a unique property of pH-dependent  $P_o$ , enabling rapid and reversible changes of channel  $P_o$  by changing intracellular pH (Khurana et al., 2011). We exploited this to ensure that the loss of ATP sensitivity in D58 mutants did not result from a significant enhancement of channel  $P_o$  relative to the F168E background channel. We tested



inhibition of Kir6.2[D58A][F168E] by 10 mM ATP over a wide pH range, from pH 7.3 (where few channels are open) to pH 8.8 (often yielding 10-20 fold larger currents than pH 7.3), and found that channels remained highly insensitive to ATP over this broad range of channel activity (Fig. 3-8A,B). These experiments indicate that the loss of ATP sensitivity in Kir6.2 D58A mutant channels does not arise from saturation of channel open probability.

### **3.2.7 Stringent requirement for slide helix residue D58**

While multiple Kir6.2 slide helix mutations abolish functional expression (Mannikko et al., 2010; John et al., 2005; Shimomura et al., 2006; Koster et al., 2005; Koster et al., 2008), systematic comparisons enabled by our rescue approach highlight a distinct role for D58 among these functionally essential residues. In particular, D58 appears to make essential contributions both to formation of conductive channels, and to appropriate transduction of ATP binding to the channel gate. We further investigated residue D58 by introducing numerous mutations at this position. Notably, D58 exhibits an extremely stringent amino acid tolerance, as even the most conservative mutations examined (D58E and D58N) were unable to generate functional channels by Rb<sup>+</sup> efflux (Fig. 3-9A). To confirm that D58 mutants were not affecting Rb<sup>+</sup> permeability, we also tested whether Rb<sup>+</sup> efflux of different D58 mutants could be rescued with the F168E background (Fig. 3-9A). We also repeatedly tested the conservative D58E and D58N mutations (on a WT background) with patch clamp experiments, but failed to detect any functional expression (data not shown). Based on the presence of an upper band on SDS-PAGE (with caveats as discussed previously with Figs. 3-2, 3-4), D58 mutants appeared to reach the plasma membrane (Fig. 3-9B), and this was also directly confirmed for D58A channels by surface biotinylation (Fig. 3-4). Furthermore, all D58 mutants characterized by patch clamp were

functionally rescued by F168E (demonstrating robust surface expression), and exhibited extremely severe disruption of ATP sensitivity and gating kinetics (Fig. 3-9A inset, C, D).

### **3.2.8 Residue D58 as an important coupling element between CTD and TMD**

We propose that ATP sensitivity of Kir6.2 channels requires both an appropriate ATP binding site and an intact interface between the CTD and TMD (Fig. 3-10A). Our findings indicate that this interface depends significantly on D58, a residue we refer to as the ‘aspartate anchor’. A model to explain our findings is that when the D58 TMD-CTD anchor is in place, gating kinetics are slow, possibly because conformational changes of the TMD and CTD are coupled (Pegan et al., 2006;Khurana et al., 2011;Hansen et al., 2011;Whorton and MacKinnon, 2011;Bavro et al., 2012), resulting in an energetic barrier to opening. Mutations in the vicinity of the ATP binding site (i.e. I49A or R50A) attenuate ATP sensitivity but preserve slow gating kinetics similar to the F168E background channel (Fig. 3-10B), because this D58 ‘coupling element’ is still intact. This interpretation is generally consistent with previous reports describing Kir6.2 I49 and R50 mutants, which alter ATP sensitivity but do not affect gating properties of the channel in ATP free conditions (Mannikko et al., 2010;John et al., 2005;Shimomura et al., 2006;Koster et al., 2005;Koster et al., 2008). In contrast, disruption of the TMD-CTD interface by mutation of D58 abolishes both ATP inhibition and slow gating kinetics (Fig. 3-10C). We describe the effects of these mutants as uncoupling the TMD and CTD, such that conformational changes of the TMD domain are no longer linked to the CTD (Fig. 3-10C).

### **3.2.9 Complexity of contacts between residue D58 and the CTD**

Kir6.2 position D58 stands out as a functionally important element that lies at the interface of the CTD and TMD of Kir channels. We have also investigated residues within the complimentary CTD in the vicinity of D58. Inspection of recent eukaryotic Kir channel

structures reveals that the D58 side chain is positioned especially close to residue R206, a highly conserved residue among Kir channels (Fig. 3-11A). However, the organization of the TMD-CTD interfacial region varies considerably between different published structures, and contacts may change in different channel states. In addition to R206, D58 is located in a dense region of positively charged side chains that might also form important interactions (namely, R206 and K207 in the CTD, and H175, R176, R177 in the 'C-linker' extension of the TM2 helix) (Fig. 3-11A). We investigated this interfacial region by mutating these positive charges and examining their functional effects. We first neutralized each cluster of positive charge (R206A/R207A double mutant, and H175A/R176A/R177A triple mutant). Both of these compound mutants ablate channel function in  $\text{Rb}^+$  efflux assays (Fig. 3-11B), consistent with previous reports that the R206A and R177A mutations abolish Kir6.2 function (Shyng et al., 2000). This was also consistent with  $\text{Rb}^+$  efflux assays for individual mutants: R177A and R206A had no detectable activity, H175A and R176A exhibited ~20% efflux relative to WT Kir6.2, and K207A exhibited efflux comparable to WT Kir6.2 (Fig. 3-11B).

We exploited the F168E background to rescue activity and characterize non-functional CTD mutants. Surprisingly, despite the predicted close proximity of D58 and R206, neutralization of R206 (and/or K207) does not reproduce features of D58 mutants. Notably, Kir6.2[F168E][R206A][K207A] channels exhibit only slightly perturbed ATP sensitivity (Fig. 3-11C,D). We also examined positions R206 and K207 individually with more disruptive mutations. Of these, only a highly disruptive charge reversal mutation at R206D significantly altered ATP inhibition, to a degree comparable to D58 mutations (Fig. 3-11D). However, severe mutations at position 207 (e.g. K207D) did not alter ATP sensitivity. All R206 mutations exhibited accelerated gating kinetics relative to F168E alone, but they were nevertheless slower

than the D58 mutants (Figs. 3-9A inset, 3-10E). Kinetics in K207 mutant channels were indistinguishable from the F168E background (Fig. 3-11E). These findings suggest that a salt bridge between D58 and R206, apparent in recent crystal structures, does not contribute significantly to the mechanism of ATP inhibition.

In contrast, the Kir6.2[H175A][R176A][R177A] triple mutant (on the F168E background) exhibited dramatically reduced ATP inhibition (Fig. 3-11C,D). This finding indicates that this charge cluster in the C-linker plays a more important functional role in ATP inhibition compared to R206. We also analyzed these effects with individual point mutations on the F168E background. Based on these assays, we attributed the loss of ATP sensitivity of the triple mutant almost entirely to the R177A mutation, as both H175A and R176A channels were well-inhibited by ATP (Fig. 3-11D). Kir6.2[F168E][H175A][R176A][R177A] channels exhibited accelerated gating kinetics, although again not as rapid as the D58 mutants (Fig. 3-11E). Both R176A and R177A individual mutations (on the F168E background) exhibited accelerated gating kinetics, while H175A had minimal effects (Fig. 3-11E).

Inspection of recent GIRK channel structure, the R177 equivalent side chain closely approaches another nearby aspartate residue D204 in the  $\beta$ C- $\beta$ D loop in the CTD, suggesting an additional interaction in this interfacial region by which R177 mutations could exert their effects. This aspartate residue D204 seems to be functionally relevant on modulating Kir channel gating as it is highly conserved among all ligand-dependent Kir channels, such as Kir6 and Kir3 subfamilies, which are dominantly regulated by ATP and G $\beta$  $\gamma$  subunits, respectively. In contrast, it is replaced by asparagine at equivalent position in less ligand-sensitive Kir channels, such as Kir2.1 channels. We introduced various mutations at this aspartate residue D204 (expressed on F168E background), and highlighted that the severe mutation Kir6.2[F168E][D204N] and a

highly disruptive charge reversal mutation Kir6.2[F168E][D204R] significantly abolished the ATP sensitivity (Fig. 3-12A, B), consistent with our hypothesis that residue D204 is important on ligand sensitivity in Kir6 channels. All D204 mutations exhibited accelerated gating kinetics relative to F168E alone (Fig. 3-12C), but they were nevertheless slower than the D58 mutants (Figs. 3-9A inset, 3-10E). We then attempted site-specific disulfide bond formation by engineering double cysteine pairs at residues R177 and D204 to further investigate any functional relevant salt bridge interactions. Once again, the F168E background was exploited to rescue activity and characterize non-functional CTD mutants. Notably, Kir6.2[F168E][D204C][R177C] mutant exhibited a relatively strong ATP inhibition comparably to WT Kir6.2 channels, with moderately accelerated channel gating kinetics, although again not as rapid as the D58 mutants (Fig. 3-12A,B,C). These findings suggest that this unique aspartate D204 in the  $\beta$ C- $\beta$ D loop might also play a functionally important role in ATP inhibition, and R177 might dynamically interacts with multiple charged residues, with D58 and D204 being the most possible ones. Their functional interactions allow the transmission of ligand-induced conformational changes in the CTD to the bundle crossing gate.

Overall, these findings indicate that the effects of mutating the essential D58 position cannot be replicated by a single structurally-rationalized CTD/C-linker residue, suggesting that D58 interactions with the CTD may be more complex than a salt bridge interaction with a single residue (see Discussion). Nevertheless, within the cluster of positively charged residues at the domain interface, R177 (and its potential binding partner D204) stand out as important determinants of ATP sensitivity.

### 3.3 Discussion

Inwardly-rectifying potassium channels translate metabolic and signaling pathways into changes in membrane voltage. This function relies on transduction of ligand binding from the cytoplasmic domain, to changes in the stability of the channel gate in the transmembrane domain. Despite diversity in the signaling molecules that regulate various Kir channels (Hibino et al., 2010), conservation of domain architecture and primary sequence suggests that aspects of channel gating will be similar among different Kirs. Thus, our findings will hopefully provide insights that translate to ligand-dependent gating mechanisms in other Kir channels, such as G $\beta$  $\gamma$  regulation of GIRK channels.

In this study, we developed a novel ‘forced gating’ approach to systematically evaluate the functional importance of each Kir6.2 slide helix residue, and other residues in the TMD-CTD interface. In considering this ‘forced gating’ approach, we highlight several important features of F168E relative to WT Kir6.2 (Khurana et al., 2011). Firstly, the F168E mutation imparts pH sensitivity, and enables forced opening of channels (allowing rescue of loss-of-function mutants). Secondly, Kir6.2[F168E] channels exhibit an intrinsic voltage-dependence, by a mechanism that remains unclear. Most importantly, the Kir6.2[F168E] ATP IC<sub>50</sub> is quite close to WT Kir6.2 (Fig. 3-5D), unlike previously described rescue mechanisms employing C166 mutations (with an IC<sub>50</sub> of 5-10 mM) (Antcliff et al., 2005; Proks et al., 1999). In this regard, it is clear that a robust mechanism for ATP inhibition persists in Kir6.2[F168E] channels. Consistent with this conservation of the ATP inhibition mechanism in Kir6.2[F168E] channels, mutations of numerous residues known to affect ATP sensitivity in WT channels (eg. I49, R50, Q52, G53, V59, F60, T62) (Nichols, 2006; Gloyn et al., 2004) also diminish ATP sensitivity on the F168E background.

### **3.3.1 Non-equivalence of loss-of-function mutations**

Our findings highlight positions that are highly intolerant of mutation, and would be impossible to characterize without a functional rescue approach. From the perspective of a genetic disease mechanism, loss-of-function  $K_{ATP}$  mutants are expected to cause similar phenotypes (McTaggart et al., 2010). However, when considering detailed mechanisms of channel function, these data highlight previously untestable features, because they distinguish functional differences between loss-of-function mutations – particularly in terms of contributions to ligand-dependent gating. For instance, while residue D58 is essential and intimately involved in TMD-CTD transduction of ATP binding, other positions (despite being ‘essential’ for functional expression), appear to be less involved in interdomain communication (eg. F55, T61, and D65 mutants all retain significant ATP sensitivity, Fig. 3-6B). Also, we were surprised to observe large effects on ATP sensitivity clustered to a very small subset of slide helix residues. Mutations that perturb ATP sensitivity have been identified at numerous slide helix positions, in patients with neonatal diabetes (Nichols, 2006; Gloyn et al., 2004). However, our rescue and functional screen highlight that many of these disease-causing mutations (although clearly severe from a physiological perspective), are not especially severe perturbations of interdomain communication relative to mutations of D58.

### **3.3.2 Paradoxical effects of D58 mutations**

It is noteworthy that D58 mutations exhibit complete loss-of-function ( $P_o$  of zero), despite being essentially insensitive to ATP. This might be considered paradoxical, because ATP insensitivity is normally associated with channel gain-of-function (high  $P_o$ ) (Nichols, 2006; Gloyn et al., 2004; Enkvetchakul and Nichols, 2003). However, in the case of position D58, we suspect that this apparent paradox relates to its essential function at the domain interface, for

*both* ATP sensitivity and functional expression. Consistent with this essential role for D58 in channel function expression, a previous study has demonstrated interactions between slide helix residues and the CTD in Kir2.1, and their disruption by certain Andersen syndrome (loss of Kir2.1 function) mutations (Proks et al., 2004; Proks et al., 2005a). These findings highlight a generally important role for TMD-CTD interactions in functional channel expression (including an essential role for Kir2.1 residue D71, equivalent to Kir6.2 D58). However, these experiments could not distinguish relative contributions of different slide helix residues to the channel gating mechanism, because no functional recordings were possible from loss-of-function mutant channels. Our study overcomes this experimental difficulty, and identifies a subset of residues at the Kir channel domain interface that are essential for both channel activity and appropriate transduction of ligand-dependent gating.

### **3.3.3 Stringency and sensitivity of the TMD-CTD interface**

The demonstration of the essential role for the D58 position adds important functional context to recently reported structures of Kir2.2 and Kir3.2 (Pegan et al., 2006; Khurana et al., 2011; Hansen et al., 2011; Whorton and MacKinnon, 2011; Bavro et al., 2012). These structures suggest that the D58 equivalent residue closely approaches a nearby arginine in the  $\beta$ C- $\beta$ D loop (Kir6.2 residue R206), possibly forming a salt bridge. However, our functional results indicate that this is likely not the only important interaction in this vicinity, since neutralization of R206 (and/or its neighbour K207) has little effect on ATP sensitivity, except for the severe charge reversing R206D mutation. In addition, neutralization of R177 had the most significant effect on ATP sensitivity of the charged CTD residues tested, although no crystal structures to date have suggested a salt bridge between D58 and R177. Additionally, our experiment demonstrates that R177 might exert its effect via dynamic interactions with multiple charged residues in CTD since



the double cysteine mutant Kir6.2[F168E][D204C][R177C] generated a relatively strong ATP inhibition comparably to WT Kir6.2 channels. These interactions may be functionally relevant for ligand-dependent channel gating in Kir6.2 channels. Lastly, residue D58 lies at a slide helix ‘kink’ that was not apparent in prokaryotic Kir channel structures, but has emerged in the most recent Kir2.2 and Kir3.2 structures. The functional significance of this kink is not yet known, nor have we been able to assess whether D58 mutations disrupt the kink. Overall, our approach highlights a subset of mutation intolerant residues (particularly D58 and R177) as previously unrecognized contributors to ATP-dependent inhibition. However, their specific interactions with nearby charged residues remain undefined.

As described above, recent Kir structures suggest numerous close contacts of charged side chains, raising many possibilities for functionally relevant salt bridge interactions. However, we must clarify that these hypothetical contacts have been difficult to convincingly demonstrate experimentally. Multiple approaches, including targeted metal bridges, and complimentary charge reversal mutations (eg. [D58R][R206D], and [D58R][R177D]), have been attempted in our lab. However, none of these manipulations regenerate WT channel function (data not shown). We suspect this may be due in large part to the extreme stringency of position D58 - recall that even a highly conservative D58E mutation could not recapitulate WT channel function (Fig. 3-9). Thus it is perhaps not surprising that other manipulations of this region also severely perturb channel function and ATP sensitivity. At present, our approach enables characterization of functional contributions of individual residues in the TMD-CTD interface. However, further investigation of potential state-dependent contacts between residues in this region will be required to identify dynamic changes that underlie inter-domain communication of ATP binding.

### 3.4 Conclusion

A ‘forced gating’ approach has yielded novel insights into the ATP-dependent gating mechanism of Kir6.2, by identifying unique functional contributions of residues that are highly sensitive to mutation. Our findings reveal that a highly conserved slide helix aspartate plays a central role in the transmission of ligand binding to the channel gate. Additionally, residues R177 and D204 in the TMD-CTD interface are highlighted as essential residues for ATP-dependent gating. Lastly, the F168E ‘forced gating’ rescue mechanism has worked very efficiently, enabling rescue of every loss-of-function mutation that we have tested. We anticipate that this will be a useful tool to probe other channel motifs that are particularly sensitive to mutation, such as the cytoplasmic ‘G-loop’.

### 3.5 Table and figures

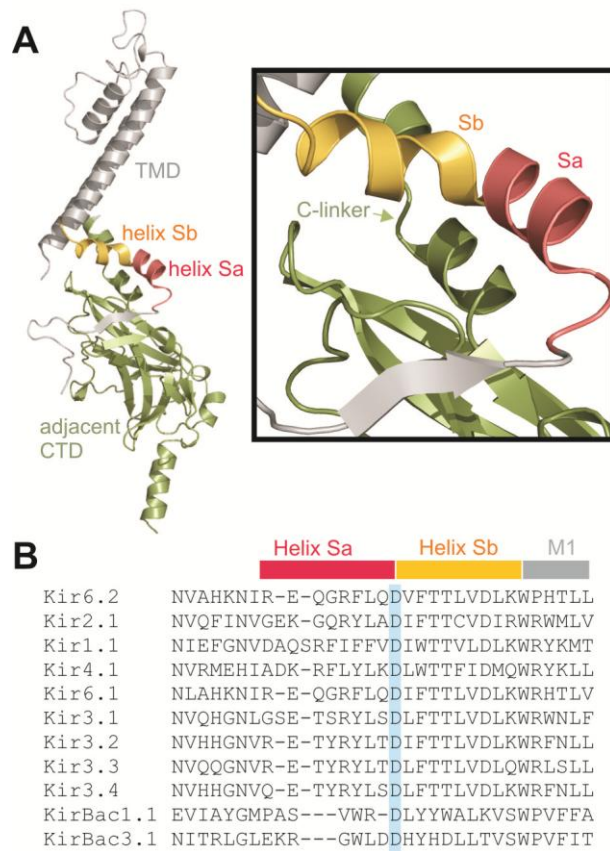


**Figure 3-1 Domain architecture and interface of Kir channels.**

(A) Kir channel structure (Kir2.2+PIP2, pdb: 3SPI) highlighting the interface between the N-terminal half of one subunit (silver, with the interfacial 'slide' helix highlighted in red and yellow), and the C-terminal half of an adjacent subunit (green). The magnified image illustrates the close approach of the interfacial slide helix with the C-terminal extension ('C-linker') of the M2 helix, and the cytoplasmic  $\beta$ C- $\beta$ D loop. (B) Alignment of multiple Kir channel slide helix segments. The highlighted position corresponds to residue D58 at the 'kink' between helices Sa and Sb.

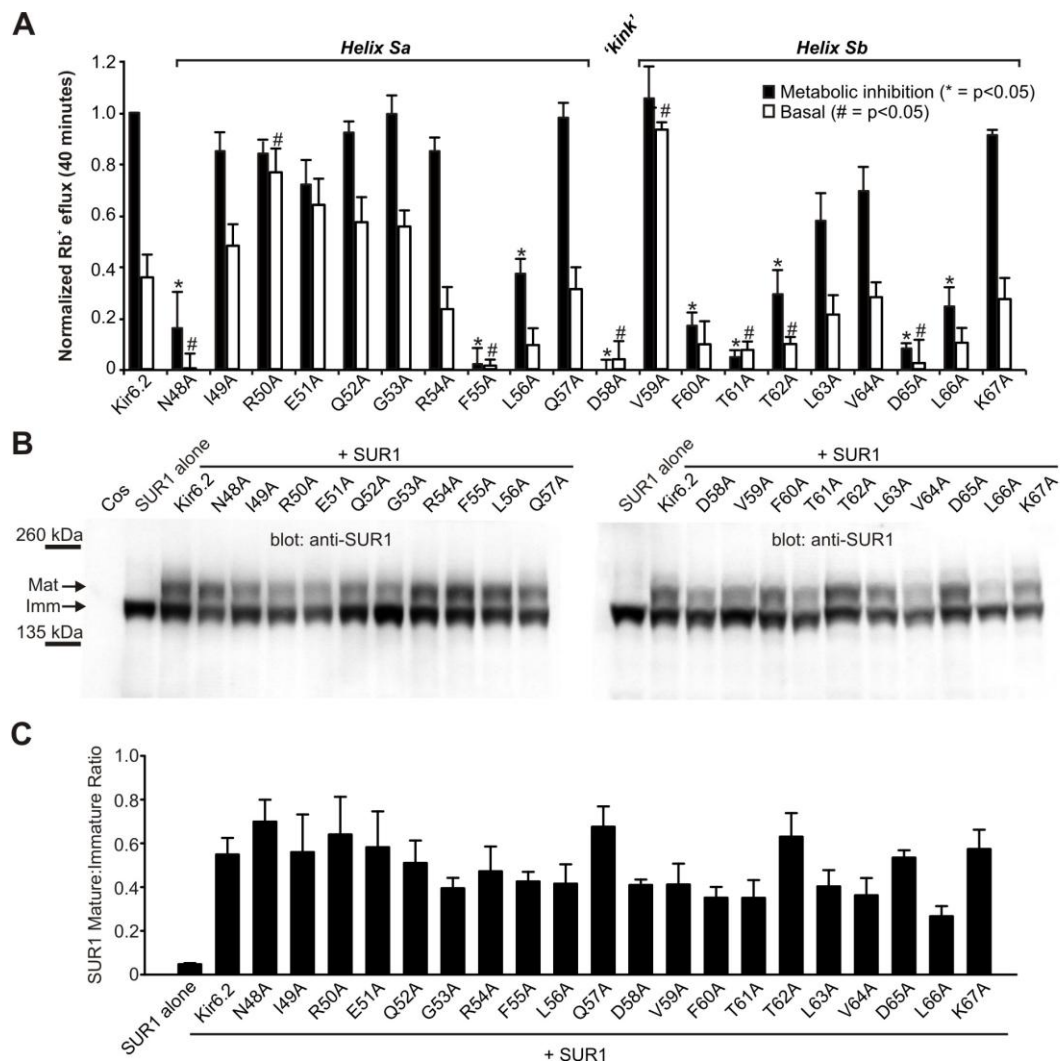


**Figure 3-2 Systematic scan of channel activity and expression in Kir6.2 slide helix mutants.**

(A) A non-radioactive rubidium efflux assay was used to determine channel activity of Kir6.2 mutants (co-expressed with SUR1, in CosM6 cells). Rb<sup>+</sup> efflux from pre-loaded cells was measured by atomic absorption spectrometry to determine the percentage of loaded Rb<sup>+</sup> released during a 40 minute incubation. For presentation, data has been normalized to Rb<sup>+</sup> efflux from cells expressing WT Kir6.2 + SUR1 (n=6 per construct), in the presence of metabolic inhibitors. One-way ANOVA followed by post-hoc Dunnett's test between WT Kir6.2 and each mutant was carried out in each condition (\* indicates p<0.05 relative to WT Kir6.2 for comparisons in metabolic inhibition; # indicates p<0.05 relative to WT Kir6.2 for comparisons in the absence of metabolic inhibitors). Note that statistical tests were carried out using the raw data (% efflux) – normalized data is presented for clarity of comparisons. (B) Western blots to probe trafficking of the K<sub>ATP</sub> channel complex. Total cell lysates from CosM6 cells transfected with SUR1 alone or with WT Kir6.2 were probed with a monoclonal anti-SUR1 antibody (NeuroMAb), along with untransfected cells (Cos). Co-transfection of SUR1 and all Kir6.2 mutants generate a higher molecular weight band (mature glycosylated, 'Mat'). (C) The ratio of mature:immature SUR1 was calculated by densitometry, after coexpression with each slide helix mutant (n=3-6 per condition). All slide helix mutants had significantly higher Mature:Immature ratio of SUR1 protein, relative to expression of SUR1 alone (p<0.05, one-way ANOVA, followed by Dunnett's test).

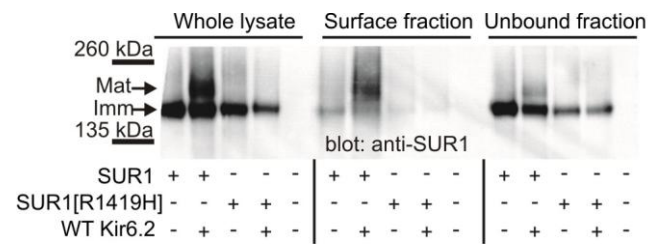


**Figure 3-3 Cell surface biotinylation of SUR1 expressed in CosM6 cells.**

Proteins present on the surface of cells transfected with combinations of WT Kir6.2, SUR1, or SUR1[R1419H], as indicated, were surface labelled with sulfo-NHS-SS-biotin and lysed. Surface labeled protein was isolated using streptavidin coated beads, followed by elution with DTT. Protein samples from the lysate, purified surface labeled fraction, or the flow-through following purification were separated by SDS-PAGE and detected with a monoclonal anti-SUR1 antibody (NeuroMAb). Similar data were observed in five separate experiments.

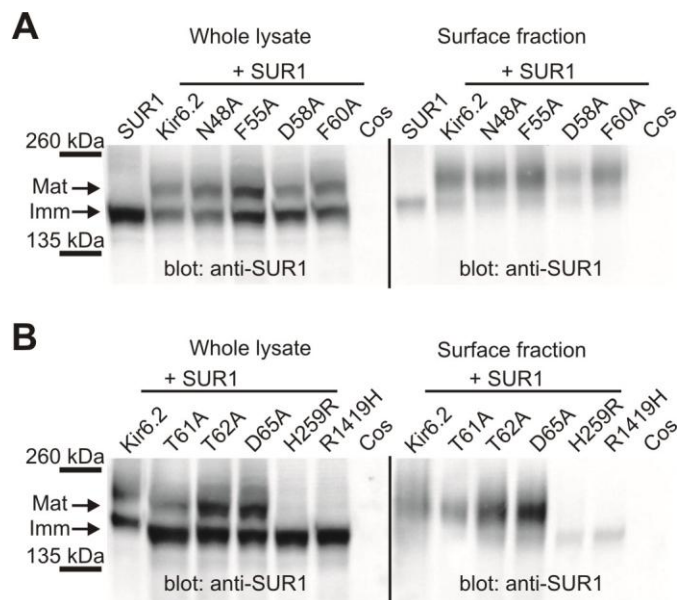


**Figure 3-4 Cell surface expression of loss-of-function slide helix mutant channels.**

(A,B) CosM6 cells were transfected with various Kir6.2 slide helix mutants that result in loss-of-function in  $Rb^{+}$  efflux assays (Fig. 2). In addition, the Kir6.2[H259R] (co-expressed with WT SUR1) and SUR1[R1419H] (co-expressed with WT Kir6.2) mutations, both previously reported to disrupt trafficking of KATP channels, were tested. Labeling of surface exposed protein was done using sulfo-NHS-SS-biotin, followed by isolation of biotinylated protein using streptavidin coated beads. Proteins in the cell lysate, or the purified surface fraction were separated by SDS-PAGE and detected with a monoclonal anti-SUR1 antibody (NeuroMAb). Similar data were obtained in three separate experiments.

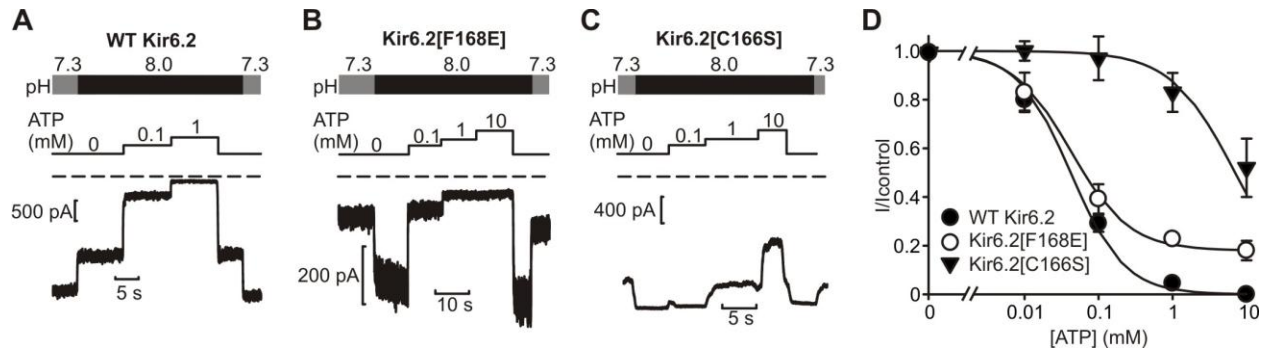


**Figure 3-5 Comparison of rescue approaches for Kir6.2 loss-of-function mutant channels.**

(A-C) Continuous inside-out patch clamp recordings at -50 mV for CosM6 cells expressing (A) WT Kir6.2 (n=12), (B) Kir6.2[F168E] (n=10), and (C) Kir6.2[C166S] (n=4) (all co-expressed with SUR1). Internal pH and ATP concentrations were switched as indicated, with a rapid solution exchange device. (D) Dose-response curves for ATP inhibition. Kir6.2[F168E] channels are inhibited with similar sensitivity to WT channels, but exhibit a small plateau conductance at high ATP concentrations. Kir6.2[C166S] channels are significantly less ATP-sensitive relative to WT Kir6.2. The ATP dose-response curves were empirically quantified by fitting the data with a Hill equation:  $I_{rel} = A + \frac{1-A}{1 + \left(\frac{[ATP]}{IC_{50}}\right)^{-H}}$ , where  $I_{rel}$  is the current relative to that in the absence of ATP,  $A$  is the relative current remained in the presence of ATP,  $IC_{50}$  is the half-maximal inhibitory [ATP], and  $H$  is the Hill coefficient 1.3.

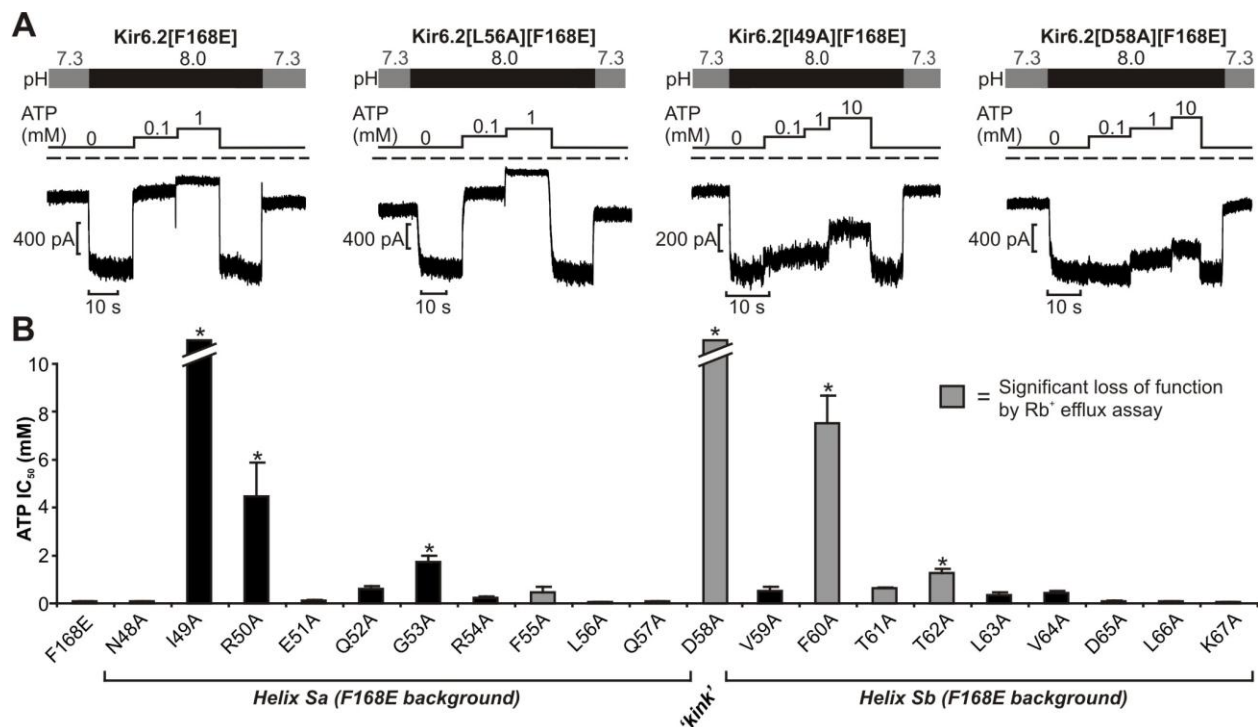


**Figure 3-6 ATP sensitivity of Kir6.2 slide helix mutant channels.**

(A) Continuous inside-out patch clamp recordings at -50mV for CosM6 cells expressing Kir6.2[F168E] and exemplar Kir6.2[F168E] slide helix mutants (all co-expressed with SUR1). Internal pH and ATP concentrations were switched as indicated, with a rapid solution exchange device. (B) IC<sub>50</sub> for ATP inhibition of slide helix mutants on the Kir6.2[F168E] background. ATP inhibition was recorded at internal pH 8.0 (n=6-10 per construct). The broken bars for I49A and D58A on indicate IC<sub>50</sub> concentrations considerably higher than the largest ATP concentration (10 mM) tested. Grey filled bars highlight mutants that exhibited loss-of-function in Rb<sup>+</sup> efflux assays (Fig. 2). One-way ANOVA followed by a post-hoc Dunnett's test for comparisons to the Kir6.2[F168E] control was used, with \* indicating p<0.05 relative to Kir6.2[F168E].



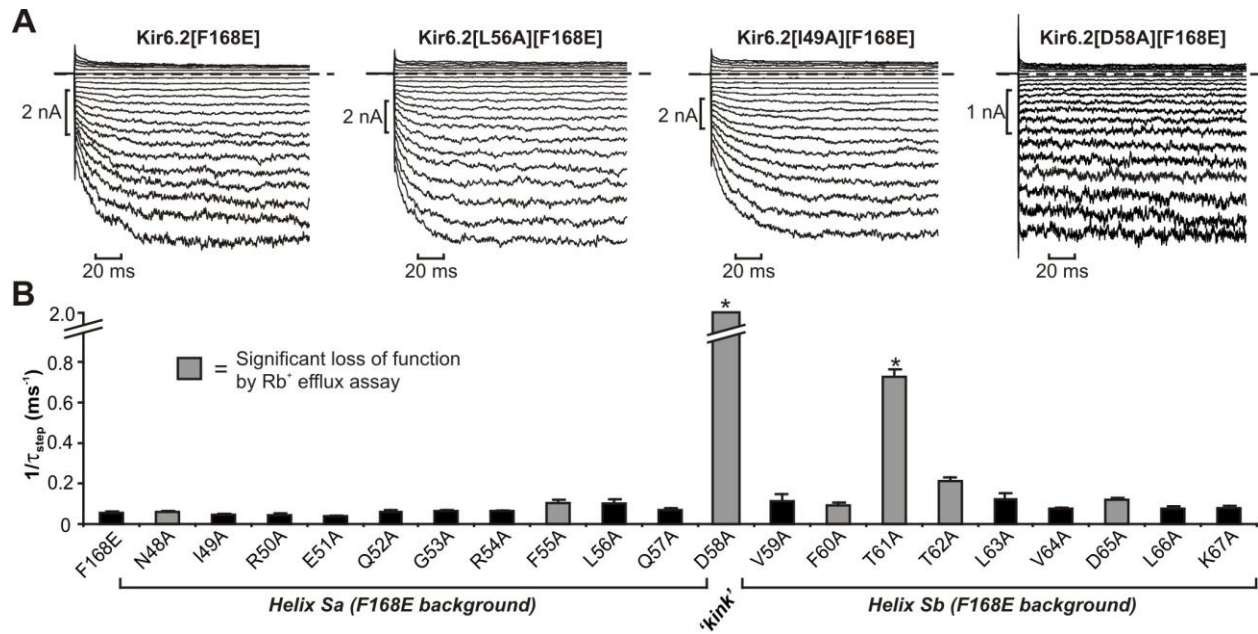


**Figure 3-7** Slide helix effects on the unique kinetic features of Kir6.2[F168E] channels.

(A) Inside-out patch recordings from CosM6 cells expressing Kir6.2[F168E] and various exemplar Kir6.2[F168E] slide helix mutants (all co-expressed with SUR1). Patches were pulsed between -150 mV and +50 mV (0 mV holding potential), in 10 mV steps. (B) Activating components of current after voltage steps to -150 mV were fit with a single exponential equation to extract the time constant  $\tau_{\text{step}}$  at pH 8.0 ( $n=6-10$  per construct). The broken bar for D58A indicates that channel opening was too rapid to confidently resolve. Grey filled bars indicate mutants that exhibited loss-of-function in Rb<sup>+</sup> efflux assays, and required the F168E rescue approach to detect ionic currents. One-way ANOVA followed by a post-hoc Dunnett's test for comparisons to the Kir6.2[F168E] control was used, with \* indicating  $p < 0.05$  relative to Kir6.2[F168E].

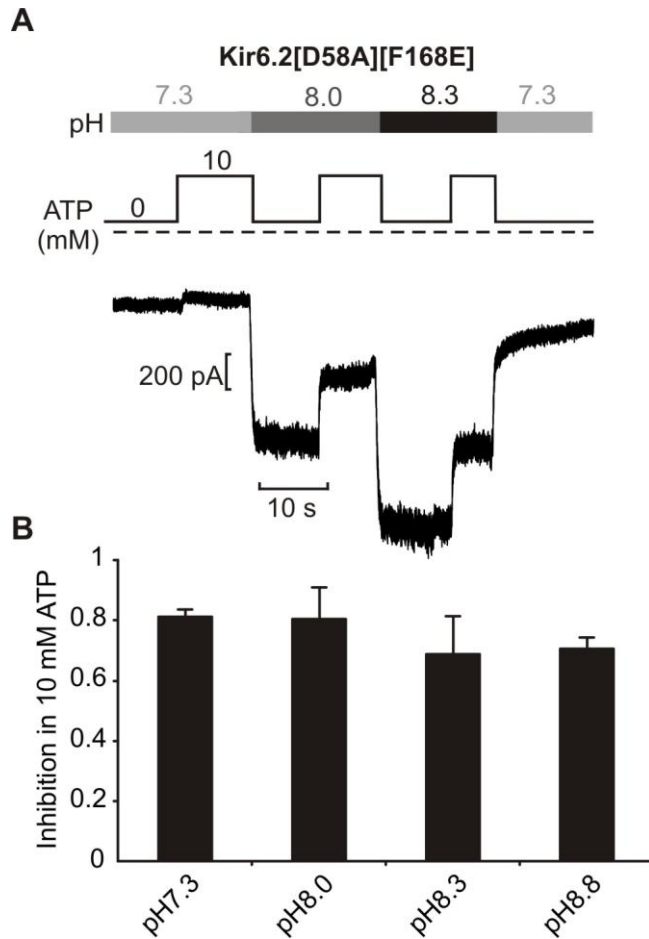


**Figure 3-8 ATP insensitivity of D58 mutants is not pH-dependent.**

(A) Continuous inside-out patch clamp recordings at -50mV for CosM6 cells expressing Kir6.2[D58A][F168E] (co-expressed with SUR1). Internal pH and ATP concentrations were switched as indicated, with a rapid solution exchange device. (B) ATP inhibition in 10 mM was determined with internal pH between 7.3 and 8.8. No statistically significant difference of ATP inhibition was observed at different pH, despite dramatic changes in current magnitude. Kir6.2[D58A][F168E] channels remained extremely insensitive to ATP over the entire pH range tested. No statistically significant differences were detected.

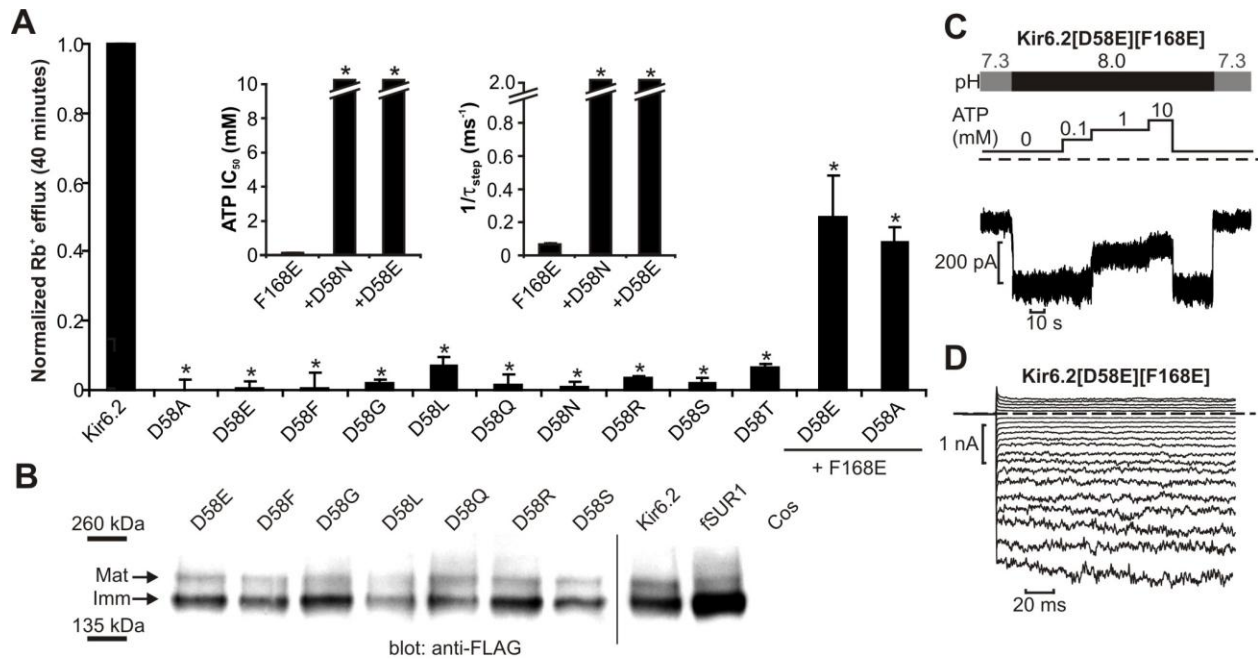


**Figure 3-9 Stringent aspartate requirement at position D58.**

Numerous amino acid substitutions at position D58 were tested for (A) functionality by Rb<sup>+</sup> efflux assays, and (B) cell surface expression by western blot (see Fig. 2). (C,D) Inside-out patch recordings of Kir6.2[F168E][D58E] channels, measuring ATP sensitivity and gating kinetics in response to a series of voltage steps. The conservative D58E mutation renders channels ATP insensitive, and abolishes voltage-dependent gating kinetics. Panel (A) inset depicts mean data for ATP IC<sub>50</sub>, and gating kinetics (1/τ<sub>step</sub>) for conservative substitutions at position D58. In each panel, ANOVA followed by a Dunnett's post-hoc test were used for comparisons to WT Kir6.2, or Kir6.2[F168E] channels (panel A inset), with \* indicating p<0.05 relative to control.

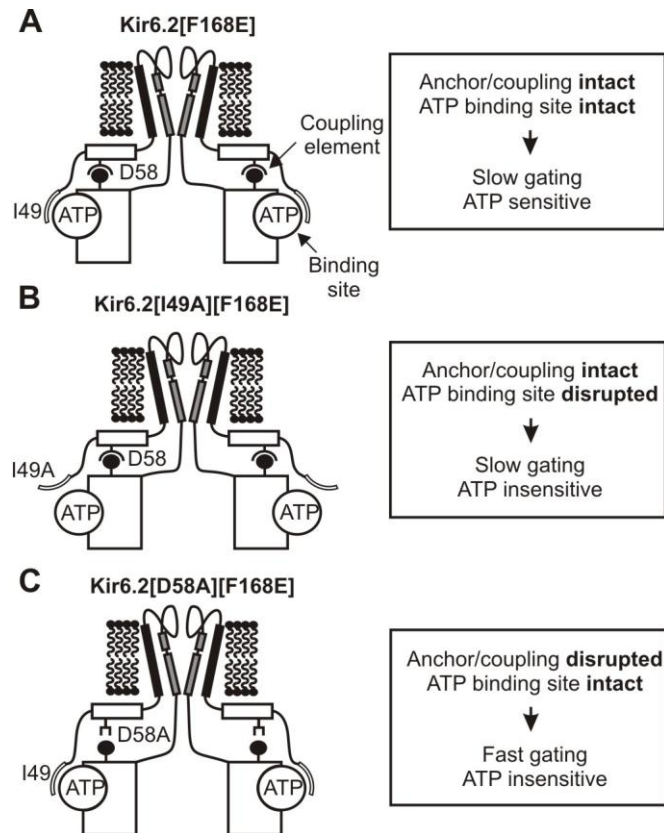


**Figure 3-10 Schematic model illustrating ATP binding and gating kinetics of Kir6.2(F168E) channels with slide helix mutations.**

(A) Kir6.2[F168E] channels have an intact ATP binding site and coupling mechanism between cytoplasmic (CTD) and transmembrane (TMD) domains, enabling ATP-dependent inhibition and slow voltage-dependent kinetics. (B) I49A or R50A mutations disrupt the ATP binding site without affecting the coupling mechanism between CTD and TMD domains, resulting in loss of ATP insensitivity, but persistence of slow voltage-dependent kinetics. (C) The D58A mutation disrupts the 'aspartate anchor' coupling element between CTD and TMD. This prevents transduction of ATP binding to the channel gate (resulting in ATP insensitivity), together with fast voltage-dependent gating.

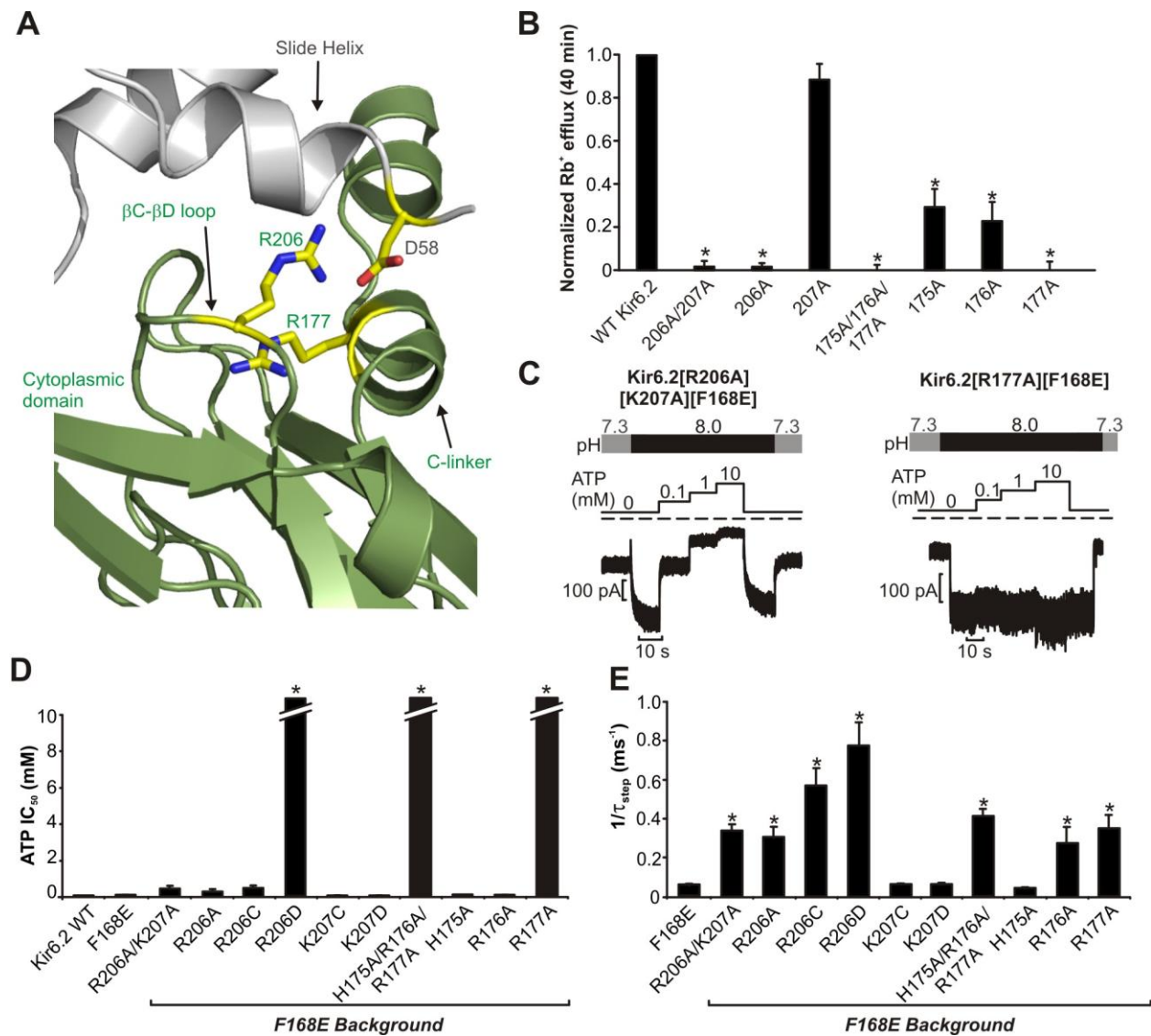


**Figure 3-11 Functional assessment of potential D58 interacting partners.**

(A) Structural model of the TMD-CTD interacting surface in Kir6.2 channels. (B) Multiple potential interface residues were assessed in combination or individually by Rb<sup>+</sup> efflux. (C) Continuous inside-out patch clamp recordings at -50mV for CosM6 cells expressing Kir6.2[F168E] with mutations of cytoplasmic domain residues (all co-expressed with SUR1). (D) IC<sub>50</sub> for ATP inhibition of mutant channels was determined, using the F168E mutation to rescue loss-of-function mutations. The R177A mutation completely abolishes ATP inhibition. (E) Gating kinetics of multiple interface residues expressed on the Kir6.2[F168E] background.

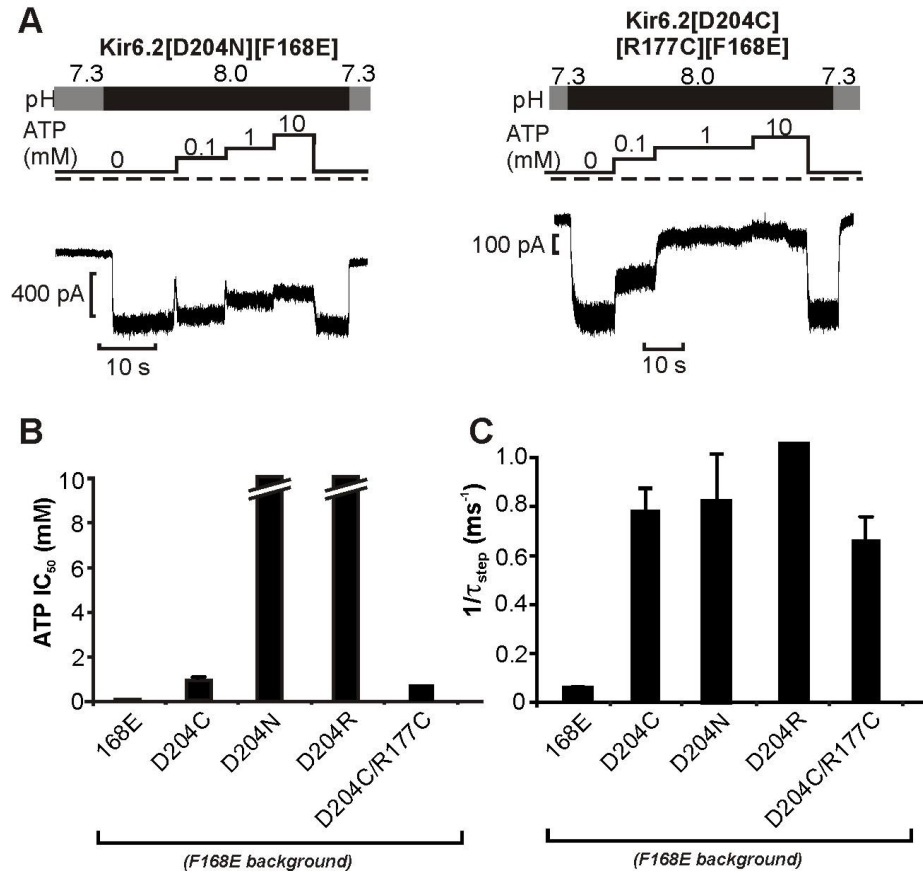


**Figure 3-12 Functional assessment of D204 in  $\beta$ C- $\beta$ D loop and its potential interaction with R177**

(A) Continuous inside-out patch clamp recordings at -50mV for CosM6 cells expressing Kir6.2[F168E] with mutations of cytoplasmic domain residues (all co-expressed with SUR1). (B)  $IC_{50}$  for ATP inhibition of mutant channels was determined, using the F168E mutation to rescue loss-of-function mutations. The D204N and D204R mutations completely abolish ATP inhibition. (E) Gating kinetics of multiple interface residues expressed on the Kir6.2[F168E] background.

## **Chapter 4: Rescue mechanisms of potassium channel loss-of-function**

### **highlight essential residues at the Kir6.2 channel domain interface**

#### **4.1 Introduction**

Inwardly-rectifying potassium (Kir) channels are regulated by diverse intracellular ligands that couple channel activity to cellular signalling and metabolism (Wickman et al., 1994; Logothetis et al., 1987; Stanfield et al., 2002). Appropriate regulation of Kir channel activity is essential for their functions in a variety of physiological processes. For example, regulation of the pancreatic  $K_{ATP}$  channels by the ATP/ADP ratio couples cellular metabolism to membrane excitability, comprising a keystone element in glucose-dependent insulin secretion. A central question in studies of Kir channel gating is how ligand interaction with the cytoplasmic domain of the channel is communicated to the channel gating apparatus. Inspection of the general architecture of Kir channel structure reveals a non-covalent interface between the ‘ligand-sensing’ COOH-terminal domain (CTD) and the canonical pore-forming ‘gating domain’ formed by the TM1 and TM2 transmembrane helices. This interface is likely involved in transduction of ligand binding, and intact coupling between the CTD and TMD of Kir6.2 channels has been emphasized in previous studies to be critical for propagation of gating effects induced by intracellular ligands in both prokaryotic and eukaryotic Kir channel structures (Clarke et al., 2010). For instance, a family of KirBac3.1 channel structures has been interpreted to reflect a sequence of conformational changes upon ligand binding in the CTD, leading to rearrangements at the subunit-subunit interface, rotation of the slide helix near the bundle crossing region, altered distribution of ion at the selectivity filter, and changes in the diameter of ion conduction pore near the cytoplasmic end (Clarke et al., 2010). The TMD-CTD interface is

also the location for binding of the essential modulator phospholipid PIP2 in eukaryotic Kir channels. In structures of Kir2.2, co-crystallization with PIP2 causes engagement of the CTD with the TMD, allowing the close interactions of the two domains and widening the bundle crossing region and potentially another narrow constriction formed by G-loop near the apex of CTD (Hansen et al., 2011). The association of the CTD and TMD does not appear to be as dependent on PIP2 in structures of Kir3.2; however, both Kir2.2 and Kir3.2 structures contain very similar PIP2 binding motifs.

The TMD-CTD interface of K<sub>ATP</sub> channels comprises numerous conserved motifs, including the NH<sub>2</sub>-terminal transverse 'slide helix', the 'C-linker', the G-loop and the  $\beta$ C- $\beta$ D loop in the CTD (Fig. 4-1). All four motifs are clustered in a close proximity with numerous potential interactions that may be involved in formation of conductive channels, and transduction of ligand binding between the CTD and TMD. The primary sequences of all four motifs are well conserved among different eukaryotic Kir channels (Fig. 4-1).

Crystallographic studies have highlighted three relatively constricted regions lying along the ion permeation pathway, which may function as intrinsic gates regulating K<sup>+</sup> ion permeation. The selectivity filter, the bundle crossing region, and a flexible pore-facing G-loop resided in the CTD have all been suggested to play functional roles on ligand-dependent channel gating. Mutations in the G-loop significantly disrupt channel gating in numerous Kir channels, and mutations in this region in Kir6.2 channels are associated with disorders such as neonatal diabetes (E292G, T293N, I296L) (Shimomura et al., 2009; Proks et al., 2005b; Girard et al., 2006) and PHHI (R301A and T294M) (Shimomura et al., 2009; Lin et al., 2003). Additionally, mutations in the G-loop in Kir2.1 channels have been identified in patients with Andersen's syndrome (G300V, V302M and E303K) (Pegan et al., 2005; Tristani-Firouzi et al., 2002).



Numerous residues in the C-linker have also been highlighted as crucial to ligand-regulation of Kir channel function. Recent crystallographic studies of Kir3.2 have identified residues (corresponding to **K170, R176, and R177 in Kir6.2 channels**) in the C-linker in direct interactions with PIP2 (Hansen et al., 2011; Whorton and MacKinnon, 2011; Shyng et al., 2000), which is an essential membrane phospholipid required for activity of all eukaryotic Kir channels. Additionally, residues R176 and R177 have been highlighted as potentially important for functional coupling between Kir6.2 and SUR1 subunits (John et al., 2001).

In Chapter III, we carried out a systematic scan of the transverse ‘slide helix’ and identified an aspartate ‘anchor’ residue D58, which is essential for functional channel expression and ATP inhibition of Kir6.2 channels. Additionally, we highlighted R177 in the C-linker and D204 in the  $\beta$ C- $\beta$ D loop as other essential residues for ATP-dependent gating. In this chapter, we have expanded our systematic structure-based mutagenic scan beyond the slide helix to include other motifs located in the TMD-CTD interface region. As mentioned earlier, this interfacial region is especially sensitive to perturbation by mutation, and so the ‘forced gating’ approach described in Chapter III has proven to be especially valuable to rescue these loss-of-function interfacial mutants. Importantly, our results highlight a subset of ‘anchor residues’ required for both formation of conductive channels, and appropriate communication of ligand binding to gating domains. Disruption of these residues uncouples the TMD and CTD, causing a loss-of-function phenotype combined with profound ligand insensitivity and gating defects.

## **4.2 Results**

### **4.2.1 Functional scan of the Kir6.2 interfacial domain**

The overall architecture of Kir6.2 channels comprises a pore-forming TMD and a large ligand-binding CTD. The TMD-CTD interface is formed by multiple conserved channel motifs,

including the NH<sub>2</sub>-terminal ‘slide helix’ (Fig. 4-1, black), the C-terminal extension (‘C-linker’) of the pore-lining TM2 helix (Fig. 4-1, blue), the ‘G-loop’ (Fig. 4-1, green) and the  $\beta$ C- $\beta$ D loop (Fig. 4-1, red). The TMD-CTD interface appears to be important for both formation of conductive channels and appropriate communication of ligand binding. However, based on previous scanning mutagenesis of the slide helix (Chapter III), we have recognized that these functions (communication of ligand binding vs. generation of conductive channels) are not always overlapping. That is, by using a novel rescue mechanism to restore function in Kir6.2 loss-of-function mutant channels, we identified several residues that paradoxically cause loss-of-function together with severe loss of ATP sensitivity. However, other slide helix interfacial residues appeared to play essential roles in generating functional conductive channels (i.e. mutations caused loss-of-function function), but had little or no apparent effect on ligand sensitivity. The ability to systematically scan loss-of-function mutants in these conserved domains, enabled distinction of specific amino acids with essential roles in communication of ligand binding. In this study, we have expanded our mutagenic scan to characterize all motifs that form the TMD-CTD interfacial region (Hibino et al., 2010).

*The interfacial domain is highly sensitive to mutation*

We first investigated whether mutations at three conserved interfacial motifs, including the ‘G-loop’, the ‘C-linker’, and the  $\beta$ C- $\beta$ D loop (Fig. 4-2D), could form functional channels, by testing functional effects of alanine substitution at all positions. We used a non-radioactive Rb<sup>+</sup> efflux assay to test whether these mutants (co-expressed with SUR1) were able to form conductive channels. In the presence of metabolic inhibitors (2-deoxy-D-glucose + oligomycin, to activate K<sub>ATP</sub> channels), considerable reduction of Rb<sup>+</sup> efflux (moderate or severe loss of function) was observed in 8 of 13 G-loop mutants (Fig. 4-2A), whereas the C-linker and  $\beta$ C- $\beta$ D

loop were generally more tolerant of mutations. However, one C-linker mutant (R177A) (Fig. 4-2B) and two  $\beta$ C- $\beta$ D mutants (D204A and R206A) (Fig. 4-2C) stood out as exhibiting virtually complete loss of overall functional activity. To ensure the validity of these observations, we also followed up with inside out excised patch clamp recordings of cells transfected with severe loss-of-function G-loop mutants such as G289A, V291A, and T294A to establish that their functional activities are truly not detectable. Indeed, we were unable to record functional currents from any of these mutants. Taken together, these data indicate that the TMD-CTD interface (comprising the slide helix, G-loop, C-linker, and  $\beta$ C- $\beta$ D loop) is highly sensitive to perturbation by mutagenesis.

#### **4.2.2 G-loop mutants reach the cell surface**

We were confident that the G-loop channel mutants were well-expressed, due to the observation of robust fluorescence using GFP-tagged constructs. However, the localization of these mutant channels was not known. Therefore, we tested whether the decreased functional activity of G-loop mutants could be due to a trafficking deficiency, using western blot analysis and cell surface biotinylation of SUR1. As previously described, maturation and glycosylation of SUR1 generates a high molecular weight band (mature, labeled 'Mat' in Fig. 4-3A,B), while immature 'core' glycosylated SUR1 comprises a lower molecular weight band (immature, labeled 'Imm' in Fig. 4-3A,B) (Zerangue et al., 1999; Schwappach et al., 2000; Yan et al., 2007).  $K_{ATP}$  maturation and generation of the high molecular weight band requires appropriate assembly of Kir6.2 and SUR1, and reflects cell surface expression of the channel complex, so we used anti-SUR1 western blots as a surrogate measurement for maturation of Kir6.2/SUR1 channels (with various Kir6.2 G-loop mutants). Notably, all Kir6.2 G-loop mutants in our study generated

a higher molecular weight mature SUR1 band, indicating appropriate cell surface maturation of all G-loop mutant channels (Fig. 4-3A,B).

We also used cell surface biotinylation to confirm that all loss-of-function G-loop mutants (E288A, G289A, V290A, V291A, T294A, G295A, I296A, T297A, T298A, Q299A, and R301A) were reaching the cell surface (Fig. 4-4). As previously described, the upper band of channels comprising WT Kir6.2 + SUR1 is selectively enriched in the biotinylated (cell surface) fraction (Fig. 4-4). All loss-of-function G-loop mutants exhibit a pattern comparable to WT Kir6.2 channels (co-expressed with SUR1), in which a significant upper band was observed on SDS-PAGE, and the upper band was selectively enriched in the surface labeled fraction (Fig. 4-4). We also included a negative control using the Kir6.2[H259R] mutant, previously reported to disrupt cell surface  $K_{ATP}$  expression (Marthinet et al., 2005). Consistent with this, Kir6.2[H259R] channels produced very little signal from a higher molecular band on SDS-PAGE, and generated very little surface biotinylated signal (Fig. 4-4).

Taken together, these findings demonstrate that loss-of-function characteristics in G-loop mutants are not due to trafficking deficiency to the cell surface. Rather, the loss-of-function in G-loop mutants arises from a functional defect in these channels.

#### **4.2.2.1 Functional rescue of loss-of-function Kir6.2 interfacial mutants: comparing an engineered ‘forced gating’ approach (F168E) and an allosteric approach (C166S)**

Since a large proportion of interfacial mutants result in channel loss-of-function, we explored various approaches to rescue/recover their functional activity and investigate the role of these unique motifs. Firstly, our previous studies have described a ‘forced gating’ mechanism (Khurana et al., 2011) that was demonstrated to functionally rescue all loss-of-function Kir6.2 slide helix mutants (described in Chapter III). Here, we have applied the same mechanism to

recover loss-of-function Kir6.2 interfacial mutants. With this approach, substitution of a glutamate in the hydrophobic Kir channel bundle crossing (F168E mutation in Kir6.2), generates pH-dependent channels that open upon intracellular alkalization, likely due to mutual repulsion of the acidic glutamate side chains at the bundle crossing gate. Using the F168E background mutation, we observed robust  $\text{Rb}^+$  efflux (under metabolic inhibition conditions) through all G-loop mutants (Fig. 4-5A), all C-linker mutants (Fig. 4-5B), and all  $\beta\text{C}$ – $\beta\text{D}$  mutants (Fig. 4-5D). Since we have already reported a detailed study of the application of the ‘forced gating’ approach to slide helix mutants (Chapter III), we have only highlighted slide helix mutants that cause severe loss-of-function (Fig. 4-5C), and indeed (as reported previously), these mutants are rescued by the [F168E] background mutation. These findings reinforce the remarkable effectiveness of the [F168E] rescue mechanism. That is, so long as channels reach the cell membrane, expression on the ‘forced gating’ [F168E] background has proven sufficient to rescue all loss-of-function Kir6.2 mutants, and enable further functional characterization.

Another previously reported approach to rescue loss-of-function Kir6.2 mutants has been to express mutants on C166 mutant backgrounds with high intrinsic open probability (e.g. C166A, or C166S channels) (Ribalet et al., 2006; Shyng et al., 2000; Enkvetchakul et al., 2001). Residue C166 is located at the cytoplasmic end of TM2 in Kir6.2 channels and mutation of this cysteine (C166S) can markedly elevate channel  $P_o$ . The logic behind applying C166 mutations as a rescue mechanism is that channels with intrinsically low open state stability might exhibit enhanced activity due to allosteric effects of the C166 mutations. Thus, we refer to the C166S background as an ‘allosteric rescue’ approach, in contrast to the F168E background mutation, that we envision as a targeted modulation that forces conformational changes of the bundle crossing gate.

In parallel to experiments with the F168E background, we tested the ability of the ‘allosteric rescue’ approach (C166S background) to recover function in Kir6.2 interfacial mutants (Fig. 4-5, plotted alongside the F168E rescue data for comparison). The ‘allosteric rescue’ approach was generally effective at rescuing channel function in loss-of-function mutants. However, several mutants exhibited disparate responses to these rescue approaches. In these cases, while the F168E background mutation was sufficient to rescue function, the same mutations expressed on the C166S background were non-functional (Fig. 4-5 colored bars). In particular, five interfacial mutants (highlighted with colored bars in Fig. 4-5) stood out as exhibiting virtually no functional activity with the C166S background: T294 in the G-loop (green bar), R177 in the C-linker (blue bar), D58 and T61 in the slide helix (yellow bars), and D204 in the  $\beta$ C– $\beta$ D loop (red bar). We also applied inside out excised patch clamp recordings to further establish that functional activities are truly not detectable from these mutants (despite expression on the C166S background). Out of twenty patches, Kir6.2[C166S][T294A] exhibited extremely limited activity and non-detectable currents (data not shown).

These findings demonstrate that the F168E background mutation is a more universally applicable rescue approach than the C166S mutation, as it has proven sufficient to rescue function in all electrically silent channels that reach the cell membrane.

#### **4.2.3 ATP sensitivity of Kir6.2 G-loop mutants on [F168E] and [C166S] background**

Our previous studies have highlighted that despite the localization of the F168E mutation at a functionally important site in the Kir6.2 channel bundle crossing gate, it does not substantially perturb ATP sensitivity of these channels. This contrasts starkly with the profound loss of ATP sensitivity observed in C166S mutant channels (or other potential ‘allosteric rescue’ mechanisms based on high open state stability background mutations). We applied the ‘forced

gating' rescue approach to measure the  $IC_{50}$  of ATP-inhibition for each G-loop mutant (on the Kir6.2[F168E] background, at pH 8.0) (Fig. 4-6C black bars). Exemplar sweeps measuring ATP-sensitivity in several G-loop mutants are depicted (Fig. 4-6A). Similar to experiments in Chapter III, patches were formed and excised in pH 7.3, stepped to pH 8.0 to illustrate the [F168E]-mediated pH-dependence, and then stepped sequentially through various ATP concentrations at pH 8.0.

G-loop mutations clustered into two distinct groups. The first group exhibited strong ATP inhibition, similar to the Kir6.2[F168E] background channel (Kir6.2[F168E][T297A] is provided as an example in Fig. 4-6A), in which 100 $\mu$ M ATP was able to inhibit ~ 80-90% of current. A second group of mutations dramatically weakened ATP sensitivity relative to Kir6.2[F168E] (Fig. 4-6C black bars). Specifically, five G-loop mutants (G289A, V290A, T294A, G295A, and R301A) exhibited profoundly reduced ATP sensitivity, with very little current inhibition observed even in 10 mM ATP (see Kir6.2[F168E][G289A] in Fig. 4-6A,C). These positions are unlikely to make any direct contacts with ATP, so we suspect their effects are mediated by an effect on the channel gating apparatus, rather than directly interfering with ATP binding (Antcliff et al., 2005; Proks et al., 1999). Mutations at these five G-loop residues shifted the ATP  $IC_{50}$  to > 10 mM, as compared to Kir6.2[F168E], with an ATP  $IC_{50}$  ~60  $\mu$ M (at pH8.0).

As mentioned, the alternative C166S rescue mutation has been demonstrated to shift channel ATP sensitivity well into the mM range (Trapp et al., 1998). We had previously used the F168E background exclusively, because we suspected that this relatively ATP-insensitive background (due to the C166S mutation) would confound comparisons of ATP sensitivity between G-loop mutants. Here, we have tested this hypothesis directly, by measuring the  $IC_{50}$  for ATP-inhibition for each G-loop mutant on the Kir6.2[C166S] background (at pH 8.0, to allow

for a direct comparison with our recordings in F168E channels, Fig. 4-6C grey bars). Exemplar sweeps measuring ATP-sensitivity in G-loop mutants are depicted (Fig. 4-6B).

Most G-loop mutants on Kir6.2[C166S] closely resembled the strong insensitivity to ATP inhibition imparted by Kir6.2[C166S] background channel (Kir6.2[C166S][T297A] and Kir6.2[C166S][G289A] are provided as examples in Fig. 4-6B), with very little current inhibition even in 10 mM ATP. The ATP  $IC_{50}$  of most G-loop mutants (E288A, G289A, V291A, E292A, T293A, G295A, T297A, T298A, and R301A) expressed on Kir6.2[C166S] background exceeded 10 mM (Fig. 4-6C grey bars). We draw attention in particular to G-loop mutants including E288A, V291A, E292A, T293A, T297A, T298A, and Q299A, which maintained a strong sensitivity to ATP inhibition on the ‘forced gating’ rescue background Kir6.2[F168E] (Fig. 4-6C black bars), but exhibited a profoundly diminished sensitivity to ATP inhibition on Kir6.2[C166S] background (Fig. 4-6C grey bars). To illustrate this stark difference between the two rescue mechanisms, we have presented exemplar sweeps measuring ATP sensitivity in T297A on both rescue backgrounds (Fig. 4-6A, B). Kir6.2[F168E][T297A] exhibited strong sensitivity to ATP inhibition with an  $IC_{50} \sim 60\mu M$  (Fig. 4-6A), whereas Kir6.2[C166S][T297A] showed severe insensitivity to ATP inhibition with  $IC_{50}$  exceeding 10mM (Fig. 4-6B). This highlights that the C166S approach likely perturbs ATP sensitivity much more than the F168E approach, making it difficult to use this approach to draw significant comparisons between mutations expressed on the C166S background.

In general, these trends hold true between mutations expressed on the F168E and C166S backgrounds. However, some exceptions have arisen. The G-loop mutant V290A on the ‘forced gating’ background (Kir6.2[F168E][V290A]) showed a pronounced insensitivity to ATP inhibition, but exhibited strong sensitivity to ATP inhibition on the ‘allosteric rescue’



background Kir6.2[C166S] with  $IC_{50}$  of  $\sim 70 \mu M$  (Fig. 4-6C). This is the only example that we have encountered in which a mutation on the C166S background exhibited stronger ATP sensitivity than on the F168E background. The mechanistic basis of this observation has not been investigated, and it is difficult to speculate on an underlying cause.

A final important point related to comparisons of these two rescue mechanisms is that since the C166S ‘allosteric rescue’ approach is not sufficient to rescue currents in all mutants, functional information is not available for mutants expressed on the C166S background. Specifically, the ATP  $IC_{50}$  of Kir6.2[C166S][T294A] could not be measured due to its undetectable functional activity, mirroring our observation of loss-of-function of these mutants in  $Rb^+$  efflux assays (Fig. 4-5A). Therefore, this position falls into a small subset of amino acids that is efficiently rescued by the F168E background, but fails to be rescued by the C166S allosteric rescue approach.

Overall, these findings highlight several important distinctions between the ‘forced gating’ and ‘allosteric rescue’ mechanisms. Firstly, the ‘allosteric rescue’ mechanism generally distorts the apparent ATP sensitivity due to the high  $P_o$  imparted by the C166S mutation, whereas the ‘forced gating’ approach seems to provide a more reliable estimate of ATP sensitivity after rescue (due to the relative benign effects of the background F168E mutation on ATP sensitivity). As a result, the ‘forced gating’ rescue approach Kir6.2[F168E] seems to be more informative since it enables systematic comparison of all G-loop mutants without inherently perturbing ATP sensitivity. These findings emphasize the potential general utility of this ‘forced gating’ method to study and compare gating behavior and ligand sensitivity in loss-of-function channel mutants.

More importantly, although the ‘allosteric rescue’ mechanism is often able to rescue functional activity, there are positions that cause loss-of-function that is unrecoverable by the C166S mutation (eg. T294), whereas the ‘forced gating’ mechanism has been able to rescue every loss-of-function mutation tested to date (so long as the mutant does not cause a trafficking deficiency). One possible explanation for this is that the C166S mutation is only sufficient to rescue channels that are adequately coupled between the transmembrane and cytoplasmic domains. In this way, recognition of residues with dichotomous responses to the rescue mechanisms may have mechanistic implications for a subset of absolutely essential interface residues. We explore this possibility in the following sections.

#### **4.2.4 Kinetic features of Kir6.2 G-loop mutants on [F168E] background**

In addition to rescuing loss-of-function mutants by alkalization-mediated forced channel opening, the Kir6.2[F168E] mutation imparts a weakly voltage-dependent gating phenotype, which is absent in WT Kir6.2 channels (Kurata et al., 2010). Membrane hyperpolarization causes time-dependent opening of Kir6.2[F168E] channels (Fig. 4-7A), and we have used the voltage-dependent kinetic features of Kir6.2[F168E] to further compare the effects of G-loop mutants on channel function. Several G-loop mutants had no effects on gating kinetics, preserving the hyperpolarization-dependent slow opening similar to Kir6.2[F168E] channels (Fig. 4-7A,B; Kir6.2[F168E][T297A] is provided as an example shown in Fig. 4-7A). However, numerous G-loop mutants (E288A, G289A, V290A, V291A, T294A, G295A, Q299A, and R301A) altered the gating kinetics of voltage-dependent channel opening (Fig. 4-7A,B; Kir6.2[F168E][T294A] is provided as an example shown in Fig. 4-7A). Five of these G-loop mutants (G289A, V290A, T294A, G295A, and R301A) also markedly diminished the ATP sensitivity, in conjunction with modifying the gating kinetics. Thus, although the faster gating kinetics caused by G-loop

mutants often occur together with weakened ATP sensitivity, these features are not absolutely correlated.

We have proposed that ATP sensitivity of Kir6.2 channels requires both an appropriate ATP binding site and an intact interface between the CTD and TMD. In Chapter III, we highlighted a unique ‘anchor residue’ D58 in the slide helix in Kir6.2 channels, which appears to be essential in functional expression and intimately involved in transmission of ligand binding in CTD to the channel gate. Mutations at D58 eliminated channel functional activity, abolished ATP inhibition, and markedly accelerated the slow gating kinetics imparted by the Kir6.2[F168E] mutation. Mutations at these five G-loop positions (G289, V290, T294, G295, and R301) mimicked D58 mutants, in the sense that they exhibited weakened ATP sensitivity together with accelerated gating kinetics. Overall, mutations with this phenotype appear to uncouple the TMD and CTD, such that ligand-mediated conformational changes of the CTD are no longer linked to the TMD. These five G-loop residues exhibit a very high degree of sequence conservation, and 3 of them (G289, T294, and R301) are absolutely conserved among all eukaryotic Kir channels (Fig. 4-1), suggesting their functional and/or structural necessity.

#### **4.2.5 Distinguishing functional roles of Kir6.2 interfacial residues**

The novel ‘forced gating’ rescue mechanism [F168E] to restore function in Kir6.2 loss-of-function mutant channels has enabled a systematic scan of interfacial residues. These experiments distinguish their contributions to formation of functional conductive channels, ligand sensing/communication between the CTD and TMD, and the relative overlap between these two functions. In this section, we have examined the data in more general terms to describe trends relating changes in channel kinetics and ATP sensitivity arising from mutations in the interfacial region. To do so, we have generated plots illustrating channel gating kinetics ( $1/\tau_{\text{step}}$ ),

together with the  $IC_{50}$  for ATP inhibition, for every mutation examined in the interfacial region (Figs. 3-2A, 4-2A, B, C) For ease of comparison, we have segregated these data in panels A and B in Figure 4-8, based on whether the mutation retains function (i.e. forms conductive channels, panel A), or whether the mutation causes moderate or complete loss of function (grey and black symbols, respectively, panel B). Lastly, we have highlighted the small subset of residues that exhibit functional rescue by F168E, but not C166S, in panel B with large red symbols. To mine through the data set, we hope to highlight several trends that we perceive to be important.

Firstly, all Kir6.2 interfacial mutants exhibiting robust functional activity (Fig. 4-8A) preserved relatively slow gating kinetics ( $1/\tau_{\text{step}} < 0.25 \text{ ms}^{-1}$ ). This is apparent when comparing panels A and B-kinetics among functional conductive channels cluster around slower rates (Fig. 4-8A), relative to loss-of-function channels (Fig. 4-8B). We interpret these data as consistent with a notion that a) the intact TMD-CTD coupling is crucial for the formation of conductive channels, and b) the kinetics of intrinsic gating (on the F168E background) reflects the ‘efficiency’ of coupling between the TMD and CTD. In Chapter III, we speculated that slide helix mutants that perturb the TMD-CTD interface tended to generate rapid gating kinetics, since weaker coupling enabled the gating conformational change in the TMD to occur without the influence of conformational changes in the cytoplasmic domain. Overall, the expanded interfacial screen seems consistent with this idea: residues that preserve coupling (i.e. slow kinetics) also preserve channel function. A notable subset involves mutations in the vicinity of the ATP binding site (i.e. I49A, R50A), which significantly diminish the ATP sensitivity, but preserve slow gating kinetics similar to the F168E background channel (Fig. 4-8A; clustered at the right bottom quarter). This is consistent with their overall phenotype: they preserve function

and slow gating (because they do not perturb the interface), but have very weak ATP sensitivity because they disrupt the ATP binding site.

Secondly, we draw attention to Kir6.2 interfacial mutants exhibiting reduced (Fig. 4-8B grey symbols) or complete loss-of-function (Fig. 4-8B black symbols). Most of these loss-of-function interfacial mutants disturbed [F168E]-mediated slow gating kinetics, consistent with notion that uncoupling between the CTD and TMD decreases the overall functional activity of Kir6.2 channels. The ATP sensitivity of many loss-of-function interfacial mutants is relatively weakly perturbed, implying that many interfacial residues have essential roles in generating functional conductive channels, but less significant effects on ligand sensitivity (i.e. a modulatory role, rather than an essential role in transduction of ligand binding).

Thirdly, we highlight a subset of interfacial loss-of-function mutants that caught our attention because paradoxically, they exhibit a complete loss-of-function (Po of zero), despite being essentially insensitive to ATP (Fig. 4-8B; clustered at the right top quarter). These residues, including residue D58 and T61 at the slide helix kink, five unique G-loop residues G289, V290, T294, G295 and R301 at the apex of CTD, one C-linker residue **R177**, and one  $\beta$ C- $\beta$ D residue **D204**, appear to be required for both the formation of conductive channels as well as appropriate communication of ligand binding.

Lastly, among these essential ‘coupling residues’, five residues (Fig. 4-8B red symbols) stood out even further, for their property of dichotomous responses to the C166S vs F168E rescue mechanisms. That is, loss-of-function mutants at these five positions are only rescued using the forced gating approach (Kir6.2[F168E]), but not the ‘allosteric rescue’ mechanism (Kir6.2[C166S]) (D58, T61, R177, D204, and T294) (Fig. 4-8B red symbols). We suspect that this feature implies a subset of essential interface ‘anchor residues’ that are required for TMD-

CTD coupling and appropriate ligand sensing. All five residues exhibit high degree of sequence conservation among all eukaryotic Kir channels (Fig. 4-1), emphasizing the functional significance across the entire Kir superfamily. Guided by the recent crystal structure of GIRK channel, the R177 equivalent side chain closely approaches residue D204, and the side chain of residue T294 is projected close to slide helix residues including F60, T61, and D65, raising possibilities for functionally relevant salt bridge and hydrogen bond interactions between multiple interfacial motifs.

Taken together, the TMD-CTD interface in Kir6.2 channels (comprising the slide helix, G-loop, C-linker, and  $\beta$ C– $\beta$ D loop) is particularly sensitive to perturbation by mutagenesis. A novel rescue mechanism is applied to restore function in Kir6.2 loss-of-function mutant channels and enabled distinction of specific interfacial residues with different functional roles in either formation of conductive channels, or communication of ligand binding, or both. From this large scan, we have highlighted five ‘anchor residues’ in the TMD-CTD interface that are required for both functional expression as well as ligand sensitivity.

### **4.3 Discussion:**

K<sub>ATP</sub> channels are essential for numerous physiological activities by modulating cellular membrane potential in response to metabolic state and signaling pathways (Ashcroft, 1988; Terzic et al., 1995; Tung and Kurachi, 1991). These physiological functions largely rely on inhibition by intracellular ATP molecules, which bind to the cytoplasmic domain of Kir6 channels and induce channel closure. Despite the essential role of slide helix on coupling CTD with TMD, multiple other motifs located at the TMD-CTD interface have been highlighted as potential required elements for functional channel expression and ligand-dependent channel

gating. This chapter has exploited our development of a novel rescue mechanism to further characterize this TMD-CTD domain interface.

#### **4.3.1 Non-equivalence of loss-of-function interfacial mutations**

Our findings indicate that the TMD-CTD interface (comprising the slide helix, G-loop, C-linker, and  $\beta$ C- $\beta$ D loop) in Kir6.2 channels is particularly sensitive to mutations, and would be impossible to characterize without functional rescue approaches. Out of 38 mutations we have introduced at various interfacial motifs in Kir6.2 channels, 23 mutations exhibited modest or complete loss of functional activity, reinforcing the functional and structural significance of integrity of the entire interfacial domain. Due to the loss-of-function phenotype of most interfacial mutants, we adopted a ‘forced gating’ approach (Kir6.2[F168E]) to evaluate the functional role of residues in multiple motifs at the TMD-CTD interface. This approach has allowed us to distinguish functional differences between loss-of-function mutations at the TMD-CTD interface. Our experiments highlight residues (D58, T61, T294, R177, and D204) that appear to be essential for both generation of conductive channels, and intimately involved in transduction of ATP binding in CTD to TMD. These contrast with other positions that are also essential for functional channel formation, but make smaller contributions to interdomain coupling and ligand communication.

#### **4.3.2 Ineffectiveness of ‘allosteric approach’ [C166S]**

As described in Chapter III, before our development of a ‘forced gating’ approach, a common rescue approach for Kir6.2 loss-of-function channel mutants was the ‘allosteric rescue’ approach with C166 mutant backgrounds with high intrinsic open probability (Ribalet et al., 2006; Shyng et al., 2000; Enkvetchakul et al., 2001). In our study, we also attempted to apply this high  $P_o$  allosteric rescue approach to functionally recover Kir6.2 loss-of-function interfacial

mutants. Surprisingly, we identified five interfacial positions, including G-loop mutant T294A, C-linker mutant R177A, slide helix mutants D58A and T61A, and  $\beta$ C– $\beta$ D loop mutant D204A, which were unrecoverable by the C166S mutation. Therefore, our ‘forced gating’ approach seems to be more ‘powerful’ and general since all the loss-of-function mutations we introduced at the TMD-CTD interface can be functionally rescued using forced gating approach (so long as the mutant is appropriately trafficked to the cell surface).

We do not have a definitive answer as to why these five loss-of-function interfacial mutants cannot be functionally rescued using C166S background. However, we speculate that this is related to an essential role for these residues in creating a functional TMD-CTD interface. The general logic behind applying C166 mutations as a rescue mechanism is that channels with intrinsically low open state stability might exhibit greater activity due to allosteric interactions with the C166 mutations. However, if a mutation severely perturbs the TMD-CTD coupling/interface, we speculate that the C166S rescue approach would be completely ineffective, because these channels would be unable to form a stable open state.

#### **4.3.3 Comparison of ‘forced gating’ vs ‘allosteric rescue’ approaches**

Our findings reinforce the advantage of the ‘forced gating’ approach in the context of studying mechanisms of ATP inhibition in Kir 6.2 channels. The most important feature of the F168E background, in this context, is that it does not significantly perturb ATP sensitivity. Reflecting this, most G-loop mutations on the [F168E] background maintained a strong sensitivity to ATP inhibition. In contrast, an inherent drawback of the allosteric high Po rescue approach (Kir6.2[C166S]) is that it significantly alters ATP sensitivity. Therefore, in our experiments, most G-loop mutants on Kir6.2[C166S] background exhibited strong insensitivity to ATP inhibition, making it difficult to resolve any functional contributions of these residues to



channel inhibition by ATP. Highlighting this difference, we observed a significant number of G-loop mutants (E288A, V291A, E292A, T293A, T297A, T298A, and Q299A) that preserved strong sensitivity to ATP inhibition on Kir6.2[F168E] background, but exhibited profound insensitivity to ATP on Kir6.2[C166S] background.

Overall, these findings highlight that the ‘allosteric rescue’ approach Kir6.2[C166S] likely confounds comparisons of ATP sensitivity between G-loop mutants or other important interfacial mutants based on its intrinsic high open probability. In contrast, our ‘forced gating’ rescue approach Kir6.2[F168E] retains a robust mechanism for ATP inhibition.

#### **4.3.4 Functional significance of G-loop on TMD-CTD coupling**

The cytoplasmic pore-facing G-loop located at TMD-CTD junction are anchored by two highly conserved glycine residues on the backbone of Kir channels, potentially allowing flexibility underlying conformational changes during ligand-dependent channel activation (Lopes et al., 2002). The crystal structure of KirBac3.1-Kir3.1 chimera suggests the intrinsically flexible cytoplasmic G-loop has two conformations- dilated or constricted (Nishida et al., 2007). In the constricted conformation, the I296 equivalent residue (M308) occludes the cytoplasmic pore, preventing ion permeation.

Our findings highlight five Kir6.2 G-loop mutations that profoundly weakened ATP sensitivity and dramatically altered the gating kinetics of voltage-dependent channel opening. These five G-loop residues (G289, V290, T294, G295, and R301) mimicked similar effects generated by D58 mutants on the slide helix in Kir6.2 channels, suggesting a similar functional significance on generation of conductive channels and appropriate communication of ligand binding in the CTD to the gating domain in the TMD. Three of these five G-loop residues (G289, T294, and R301) are absolutely conserved among all eukaryotic Kir channels. Our rescue and

functional screening highlights that many of the neonatal diabetes-causing mutations identified in the G-loop positions (E292, T293, I296) (Shimomura et al., 2009; Proks et al., 2005b; Girard et al., 2006) are not especially severe perturbations of interdomain communication relative to mutations of these five unique G-loop residues (Figs 4-2A, 4-6C).

Our findings suggest that various G-loop residues are required for both functional expression and strong sensitivity to ATP inhibition in Kir6.2 channels. Consistent with their essential roles in channel function and ligand-dependent channel gating, previous studies have demonstrated numerous Andersen's syndrome-associated G-loop mutations (G300V, V302M and E303K in Kir2.1, equivalent to G289, V291, and E292 in Kir6.2) abolished channel function and disrupted channel gating (Lopes et al., 2002; Bendahhou et al., 2003; Tristani-Firouzi et al., 2002). Among these five highlighted G-loop residues, loss-of-function mutations at residues T294 and R301 have been previously identified in patients with congenital hyperinsulinism (Shimomura et al., 2009; Lin et al., 2003). Residue R301 is suggested to be involved in inter-subunit interactions between adjacent Kir6.2 channel subunit, with disruption of inter-subunit interactions accounting for the decreased channel function and significantly perturbed channel gating (Lin et al., 2008). Mutations at T294 reduced intrinsic channel open probability, stabilizing the mutant channels in the closed conformation (Shimomura et al., 2009). Our findings reinforce the functional relevance of G-loop on ligand-regulated Kir channel gating.

#### **4.3.5 Paradoxical effects of G-loop mutations**

It is noteworthy that similar to D58 mutants, these five G-loop mutations (G289A, V290A, T294A, G295A, and R301A) exhibit paradoxical loss-of-function (Po closed to zero), together with remarkable ATP insensitivity. As described before, the underlying mechanism remains unknown, but this paradoxical phenotype is suggested to be unique for essential

interfacial residues on functional channel expression and ligand sensitivity. Mutations of this small subset of residues at the TMD-CTD interface likely uncouple the ligand sensing domain from channel gating domain, resulting in non-functional channels and ligand insensitivity.

#### **4.4 Conclusion**

K<sub>ATP</sub> channels couple cellular metabolism to membrane potential and electrical excitability by sensing changes in ATP concentrations. Mutations that alter the sensitivity of K<sub>ATP</sub> channels to intracellular ATP/ADP lead to impaired channel function and severe physiological consequences. Our study demonstrates the utility of a ‘forced gating’ approach to probe highly mutation-sensitive interfacial motifs in Kir6.2 channels, and identified five unique G-loop residues (including G289, V290, T294, G295, and R301) as essential coupling components for ATP-dependent channel gating. Furthermore, as compared to an allosteric high Po rescue background [C166S] with significantly disturbed ATP sensitivity, our ‘forced gating’ approach enables rescue of all loss-of-function mutation we have tested without inherently perturbing ATP sensitivity. Lastly, our observations highlight a set of ‘anchor residues’ at the Kir6.2 TMD-CTD interface that are required for both formation of conductive channels, and appropriate communication of ligand binding. Disruption of these residues uncouples the TMD and CTD, causing loss of function combined with profound ligand insensitivity.

## 4.5 Figures

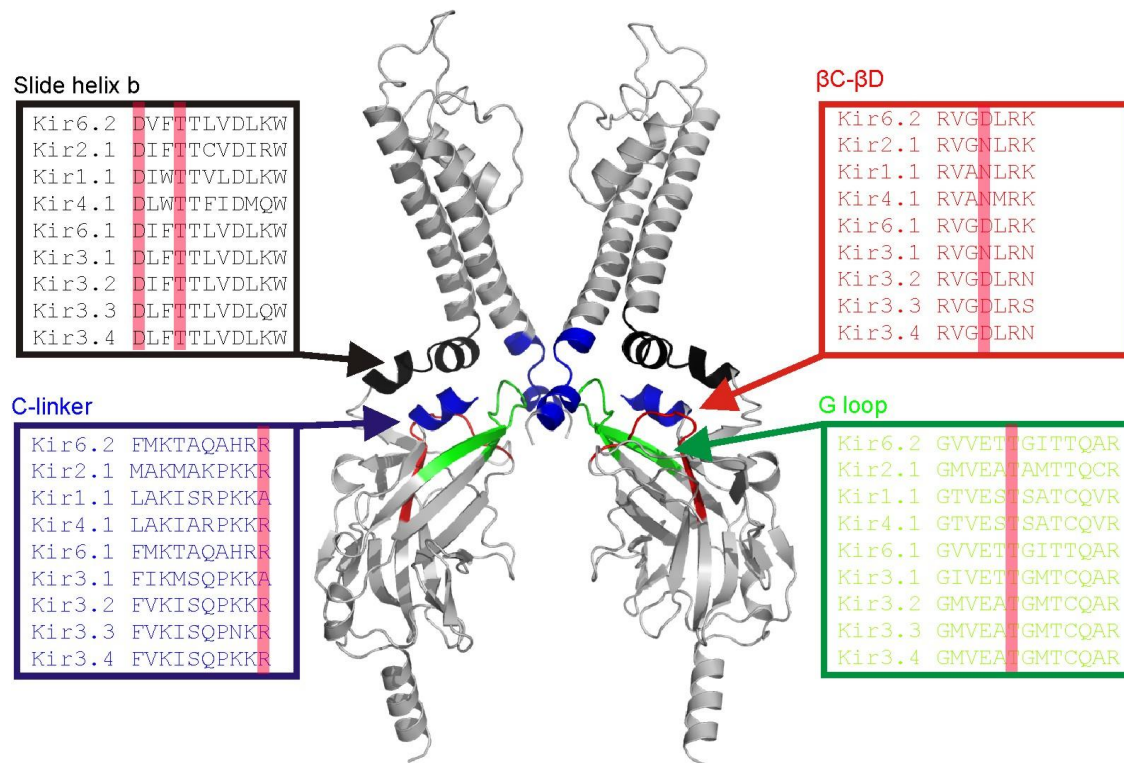


**Figure 4-1 Domain interface of Kir channels.**

(A) Kir channel structure (Kir3.2+PIP2, pdb: 3SPI) highlighting the interface domain between transmembrane domain (TMD) and cytoplasmic domain (CTD), with the interfacial 'slide' helix highlighted in black, C-terminal extension ('C-linker') of the TM2 helix highlighted in blue, cytoplasmic pore-facing G-loop highlighted in green, and cytoplasmic βC-βD loop highlighted in red. (B) Alignment of multiple Kir channel interfacial motifs, including the slide helix segment b, C-linker, G-loop and βC-βD loop. The highlighted positions correspond to residue D58 at the 'kink' between helices Sa and Sb, residue R177 on C-linker involved in PIP2 binding, residue T294 on the cytoplasmic G-loop projecting toward the slide helix, and residue D204 on the βC-βD loop positioning toward C-linker.

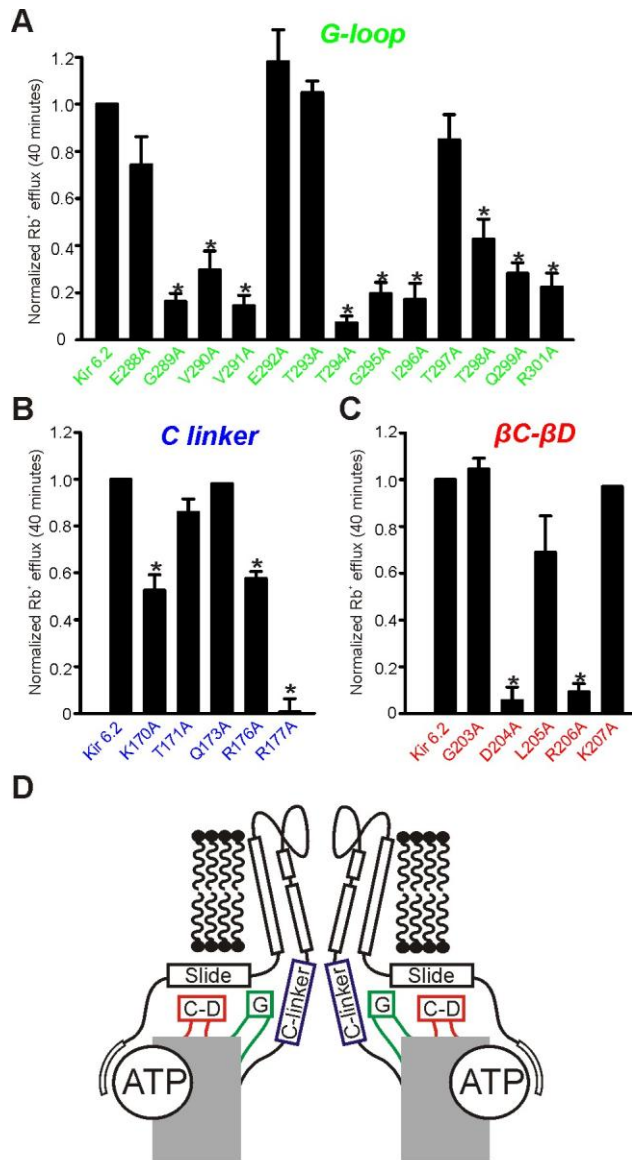


**Figure 4-2 Systemic functional scan in Kir6.2 G-loop, C-linker, and βC-βD loop mutants.**

(A-C) A non-radioactive rubidium efflux assay was used to determine channel activity of Kir6.2 G-loop mutants (A), C-linker mutants (B) and βC-βD mutants (C) (co-expressed with SUR1, in CosM6 cells). Rubidium efflux from pre-loaded cells was measured by atomic absorption spectrometry to determine the percentage of loaded Rb<sup>+</sup> released during a 40-minute incubation. For presentation, data has been normalized to Rb<sup>+</sup> efflux from cells expressing WT Kir6.2 + SUR1 (n=6 per construct), in the presence of metabolic inhibitors. One-way ANOVA followed by post-hoc Dunnett's test between WT Kir6.2 and each mutant was carried out in each condition (\* indicates p<0.05 relative to WT Kir6.2 for comparisons in metabolic inhibition). Note that statistical tests were carried out using the raw data (% efflux) – normalized data is presented for clarity of comparisons. (D) Schematic model illustrating multiple motifs at the TMD-CTD interface in Kir6.2 channels, with G-loop colored in green, C-linker in blue, and βC-βD loop in red and slide helix in black.

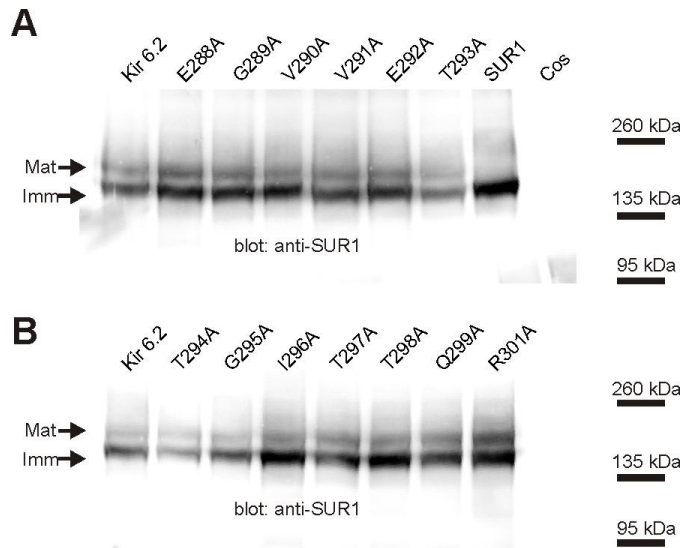


**Figure 4-3 Surface expression in Kir6.2 G-loop mutants.**

(A,B) Western blots to probe trafficking of the Kir6.2 G-loop mutants. Total cell lysates from CosM6 cells transfected with SUR1 alone or with WT Kir6.2 were probed with a monoclonal anti-SUR1 antibody (NeuroMAb), along with untransfected cells (Cos). CosM6 cells transfected with SUR1 only produce only a lower molecular weight band (immature core-glycosylated 'Imm') band. Co-transfection of SUR1 and all indicated Kir6.2 G-loop mutations generate a higher molecular weight band (mature glycosylated, 'Mat').

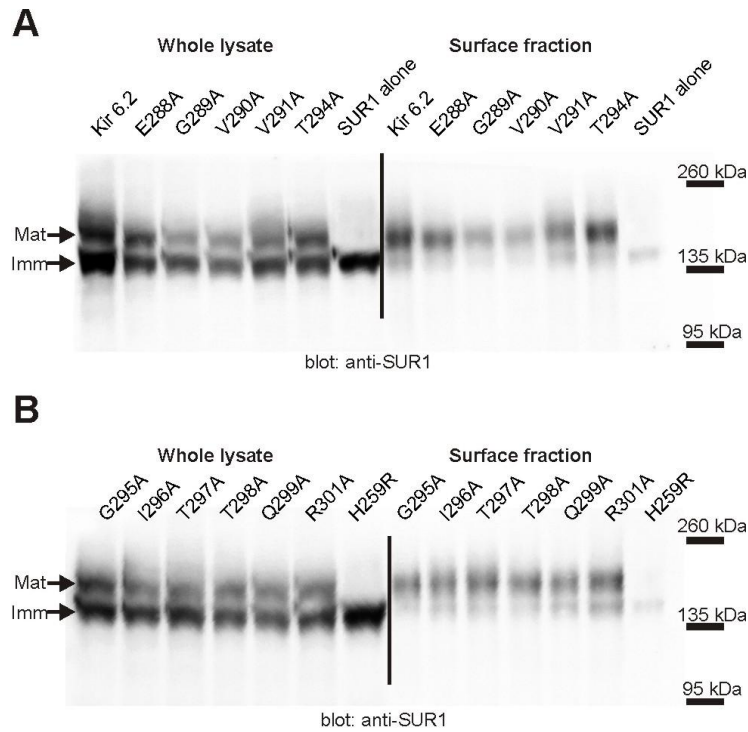


**Figure 4-4 Cell surface expression of loss-of-function G-loop mutant channels.**

(A,B) CosM6 cells were cotransfected with SUR1 and various indicated Kir6.2 G-loop mutants that result in loss-of-function in  $Rb^{+}$  efflux assays (Fig. 4-2A). In addition, the Kir6.2[H259R] (co-expressed with WT SUR1), previously reported to disrupt trafficking of  $K_{ATP}$  channels, were tested. Labeling of surface exposed protein was done using sulfo-NHS-SS-biotin, followed by isolation of biotinylated protein using streptavidin coated beads. Proteins in the cell lysate, or the purified surface fraction were separated by SDS-PAGE and detected with a monoclonal anti-SUR1 antibody (NeuroMAb). Similar data were obtained in three separate experiments.

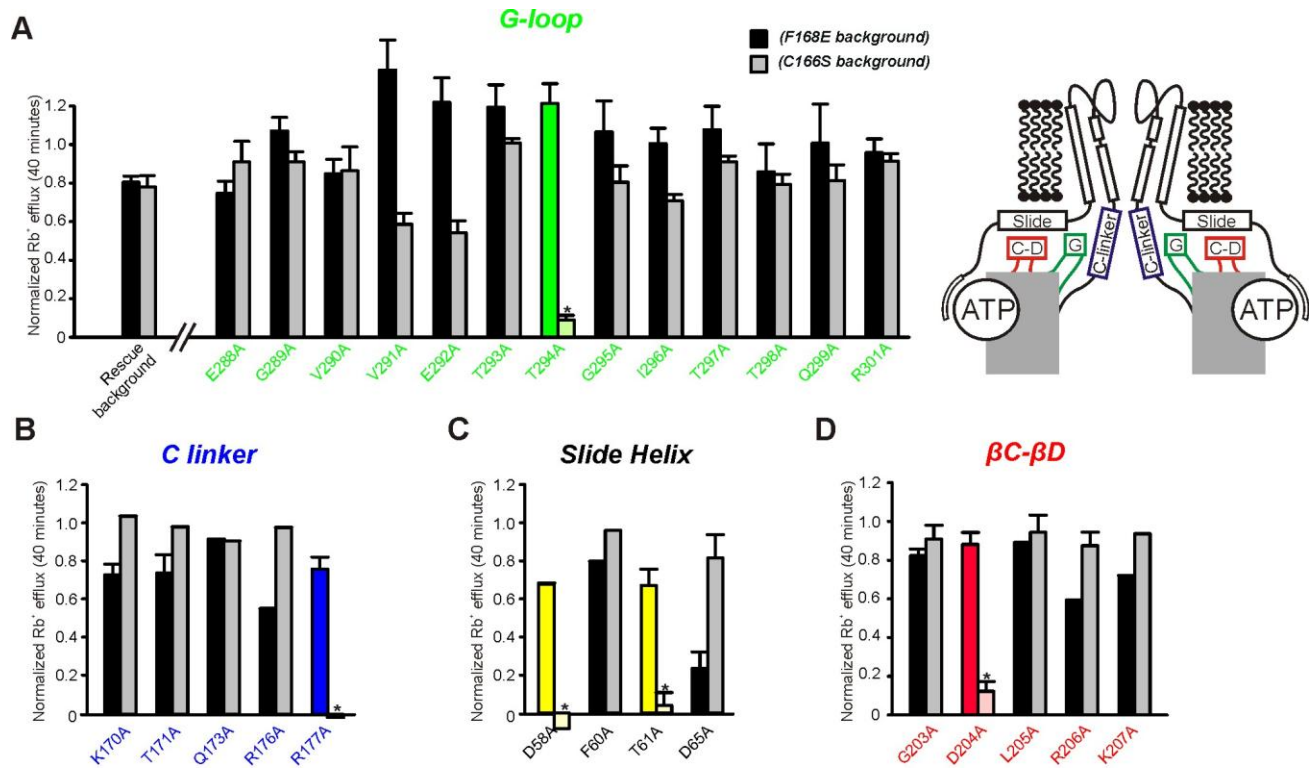


**Figure 4-5 Systemic functional scan in Kir6.2 loss-of-function interfacial mutant channels on two rescue background [F168E] and [C166S].**

(A-D) A non-radioactive rubidium efflux assay was used to determine channel activity of Kir6.2 interfacial domain mutants, (A) G-loop mutants; (B) C- linker mutants; (C) Slide helix b segment loss-of-function mutants; (D) βC-βD loop mutants, on two different rescue background [F168E] (colored in black) and [C166S] (colored in grey) (co-expressed with SUR1, in CosM6 cells). Rubidium efflux from pre-loaded cells was measured by atomic absorption spectrometry to determine the percentage of loaded Rb<sup>+</sup> released during a 40-minute incubation. For presentation, data has been normalized to Rb<sup>+</sup> efflux from cells expressing WT Kir6.2 + SUR1 (n=6 per construct), in the presence of metabolic inhibitors. The highlighted residues correspond to T294 in G-loop (green), R177 in C-linker (blue), D58A and T61A in slide helix b (yellow), and D204A in βC-βD loop (red), which exhibit extremely low Rb<sup>+</sup> efflux on [C166S] rescue background, but robust Rb<sup>+</sup> efflux on [F168E] rescue background. One-way ANOVA followed by post-hoc Dunnett's test between Kir6.2 interfacial mutants on [C166S] background for comparisons to the corresponding mutants on Kir6.2[F168E] background was used, with \* indicating p<0.05 relative to the Rb<sup>+</sup> efflux of interfacial mutants on Kir6.2[F168E] background.



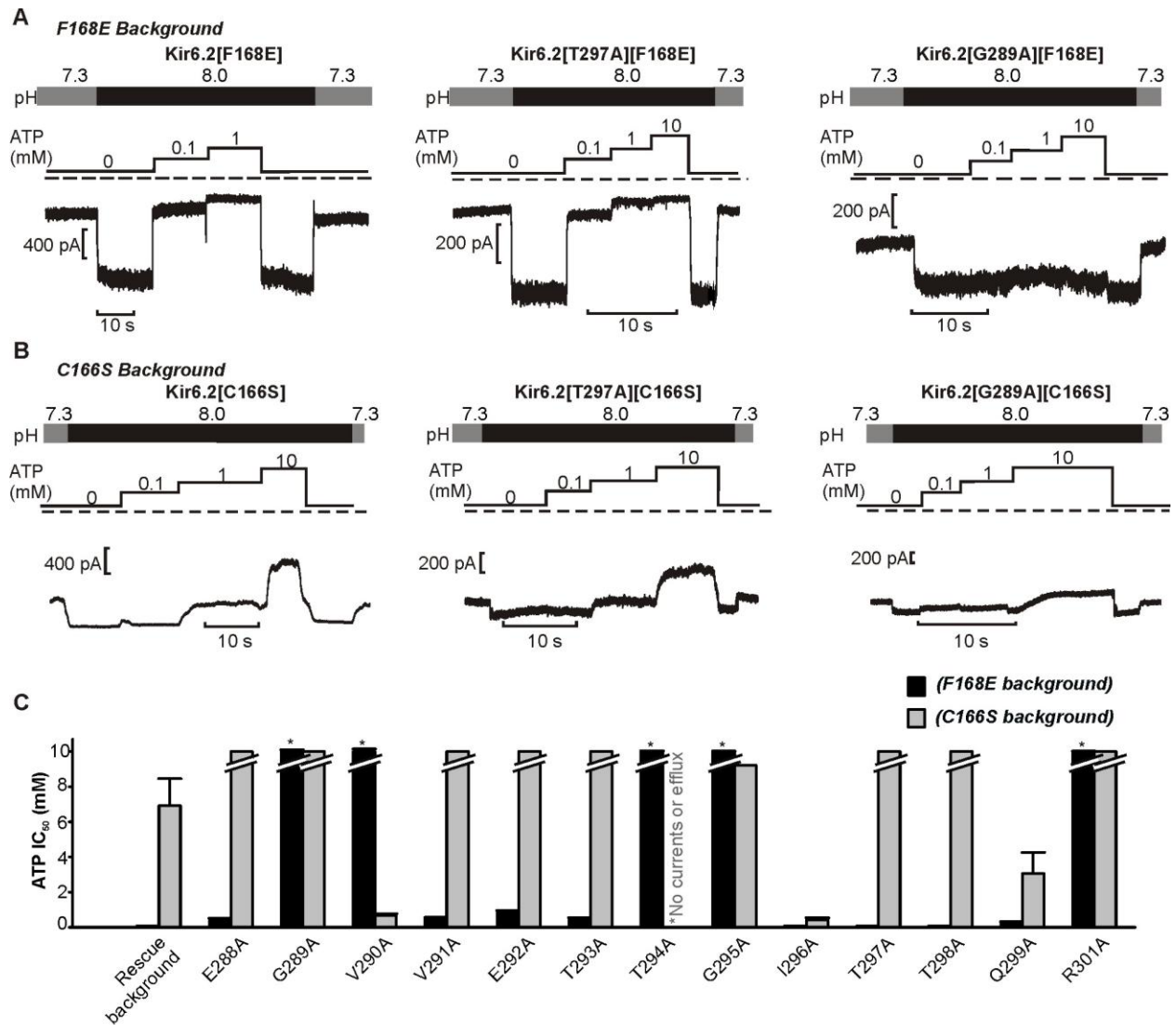


**Figure 4-6 ATP-sensitivity of Kir6.2 G-loop mutant channels on two rescue backgrounds [F168E] and [C166S].**

(A,B) Continuous inside-out patch clamp recordings at -50mV for CosM6 cells expressing (A) Kir6.2[F168E] and exemplar Kir6.2[F168E] G-loop mutants, and (B) Kir6.2[C166S] and exemplar Kir6.2[C166S] G-loop mutants (all co-expressed with SUR1). Dashed line represents reversal potential current at 0 mV. Internal pH and ATP concentrations were switched as indicated, with a rapid solution exchange device. (C) IC<sub>50</sub> for ATP-inhibition of G-loop mutants on the Kir6.2[F168E] (colored in black) and Kir6.2[C166S] (colored in grey) background. ATP inhibition was recorded at internal pH 8.0 (n=6-10 per construct). The broken bars for G289A, T294A, G295A, and R301A on Kir6.2[F168E] background and E288A, G289A, V291A, E292A, T293A, T297A, T298A, and R301A on Kir6.2[C166S] indicate IC<sub>50</sub> concentrations considerably higher than the largest ATP concentration (10 mM) tested. One-way ANOVA followed by a post-hoc Dunnett's test for comparisons to the Kir6.2[F168E] control was used, with \* indicating p<0.05 relative to Kir6.2[F168E].

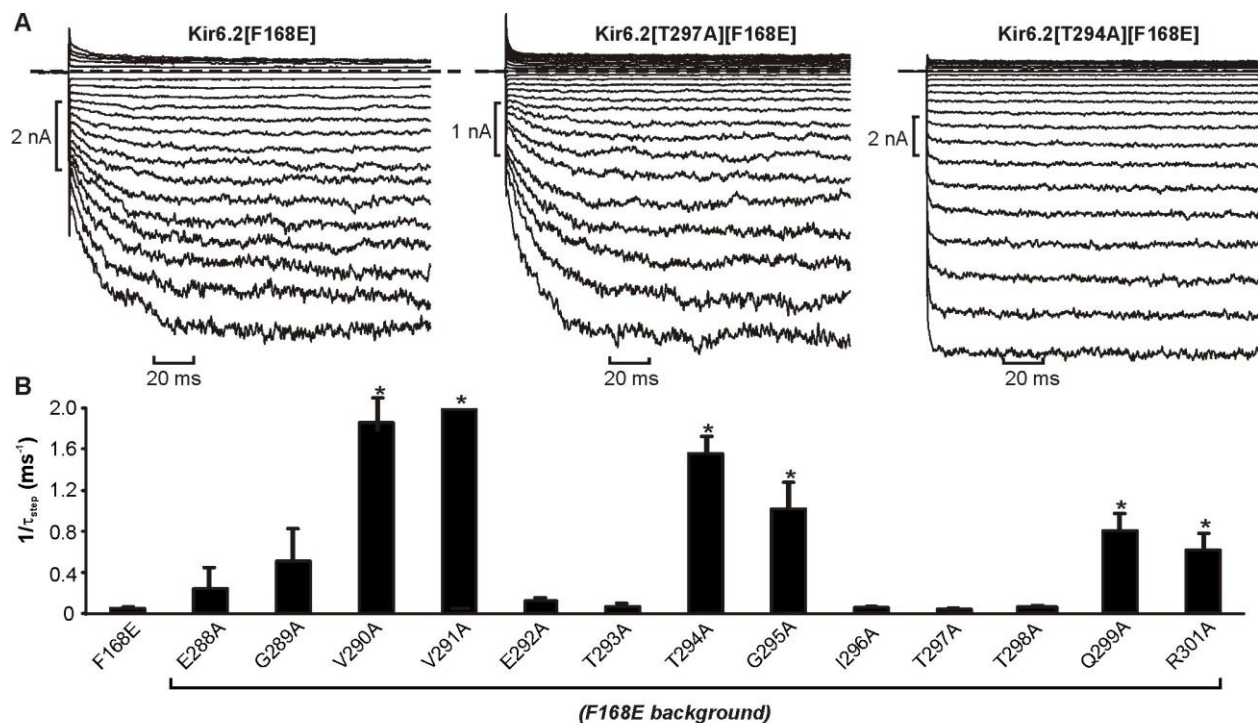


**Figure 4-7 Effects of G-loop mutations on the unique kinetic features of Kir6.2[F168E] channels.**

(A) Inside-out patch recordings from CosM6 cells expressing Kir6.2[F168E] and various exemplar Kir6.2[F168E] G-loop mutants (all co-expressed with SUR1). Patches were pulsed between -150 mV and +50 mV (0 mV holding potential), in 10 mV steps. Dashed line represents the reversal potential current at 0 mV. (B) Activating components of current after voltage steps to -150 mV were fit with a single exponential equation to extract the time constant  $\tau_{\text{step}}$  at pH 8.0 ( $n=6-10$  per construct). One-way ANOVA followed by a post-hoc Dunnet's test for comparisons to the Kir6.2[F168E] control was used, with \* indicating  $p<0.05$  relative to Kir6.2[F168E].

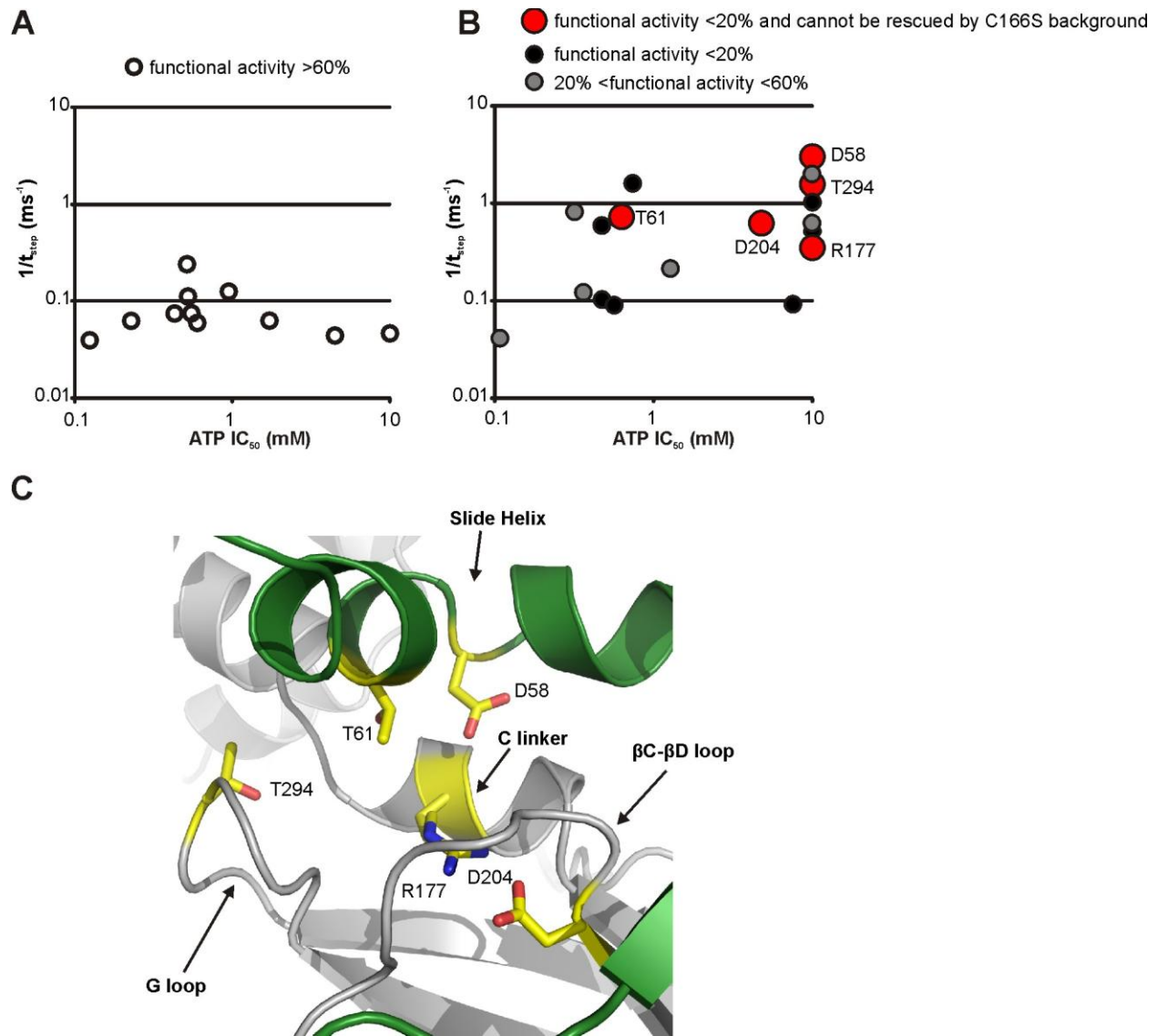


**Figure 4-8 Distinguished functional roles of Kir6.2 interfacial mutant channels.**

(A,B) The relationship of ATP  $IC_{50}$  and channel gating kinetics ( $1/\tau_{step}$ ) for all Kir6.2 interfacial mutants (expressed on Kir6.2[F168E] background). (A) Kir6.2 interfacial mutants exhibiting robust functional activity (white symbols). Most interfacial residues preserve relatively slow gating and strong ATP sensitivity. Notably, mutations in the vicinity of the ATP binding site (i.e. I49A, R50A) significantly diminish the ATP sensitivity with preserved slow gating kinetics (clustered at the right bottom quarter). (B) Kir6.2 interfacial mutants exhibiting moderate (grey symbols) or complete (black symbols) loss of function. Most of these loss-of-function interfacial mutants disturbed [F168E]-mediated slow gating kinetics. A small subset of ‘anchor residues’ are highlighted that exhibit functional rescue by F168E, but not C166S (red symbols). (C) Structural model of the TMD-CTD interacting surface in Kir6.2 channels. The five ‘anchor residues’ in close proximity are highlighted.

## Chapter 5: Conclusion

Appropriate regulation of Kir channel activity is essential for various physiological processes, such as modulation of cellular membrane excitability, cardiac action potential repolarization, and control on hormone secretion. Among all potassium channels, ATP-sensitive Kir (Kir6.2/K<sub>ATP</sub>) channels are uniquely regulated by cytoplasmic nucleotides and specific pharmacological agents. Particularly, ATP inhibition of Kir6.2 channels is essential for glucose-dependent insulin secretion in pancreatic  $\beta$ -cells and disruption of ATP sensing mechanism in Kir6.2 channels leads to genetically inherited defects in pancreatic insulin release, resulting in severe neonatal diabetes. Crystallization of various Kir channel domains illustrates the overall structural arrangement of K<sub>ATP</sub> channels. However, the dynamic changes that govern ligand-dependent channel gating remain mostly unclear. The overarching theme of this thesis is to characterize the molecular mechanism underlying the communication/sensing of ligand binding in the cytoplasmic domain to gating domain in Kir6.2 channels, by ‘deconstructing’ the interface between these channel domains. Due to the strong sequence conservation and homology in pore architecture of Kir channels, a better understanding of ligand-regulated channel gating in Kir6.2 channels may permit elucidation of important features of channel gating that are relevant to other Kir channels. Additionally, a deeper understanding of the transduction mechanism of ligand-dependent channel function will aid us in developing an improved conception in Kir channel physiology and associated diseases, with the potential to develop novel therapeutic treatments in various disorders.

The general architecture of Kir channels reveals a non-covalent interface between the ‘ligand-sensing’ cytoplasmic domain and the canonical pore-forming ‘gating domain’. In Chapter III, we identified potential molecular components that play fundamental roles on

transducing the ATP-binding signal to the closing of the bundle-crossing gate in Kir6.2 channels by systematically scanning the functional effects of mutations in the slide helix. A significant barrier we overcame was that many functionally important channel motifs are highly sensitive to mutagenesis, resulting in a loss-of-function phenotype. We adopted a novel ‘forced gating’ approach to functionally rescue electrically silent channel mutants by substituting a protonable glutamate in the hydrophobic Kir channel bundle-crossing (F168E mutation in Kir6.2), generating channels that are pH-sensitive and can be forced open by alkalization on the intracellular side (Khurana et al., 2011). Without exception, expression of electrically silent interfacial mutants on the Kir6.2[F168E] background rescues all loss-of-function, enabling characterization of essential channel motifs that are otherwise electrically silent. We highlighted an essential ‘anchor residue’ D58 on the slide helix in functional expression and intimately involved in transmission of ligand binding in CTD to the channel gate. Further, we hypothesized that this ‘aspartate anchor’ D58 interacts with various nearby positively charged residues in the CTD, coupling the conformational changes in the CTD to channel gating in the TMD.

We demonstrated that neutralization of R206 (and/or its neighbour K207) has little effect on ATP sensitivity, whereas neutralization of R177 has the most significant effect on ATP sensitivity of all the charged CTD residues tested. Recent GIRK channel structure suggests an additional interaction between R177 and a nearby aspartate residue D204 in the  $\beta$ C- $\beta$ D loop. Our results highlight that R177 seems to interact with D204 in a channel state-dependent way since the double cysteine mutant Kir6.2[R177C][D204C] (on [F168E] background) exhibits relatively strong ATP sensitivity comparable to WT Kir6.2 channels. In Kir channels, R177 side chain is “sandwiched” between the slide helix and  $\beta$ C- $\beta$ D loop, raising the possibility that R177 side chain might dynamically ‘flip’ between these channel motifs.

In Chapter IV, we expanded our systematic structure-based mutagenic scan beyond the transverse ‘slide helix’ to include other motifs located in the TMD-CTD interface region. We highlighted a small subset of ‘anchor residues’ at the TMD-CTD interface in Kir6.2 channels (D58, T61, R177, D204, and T294) that appear to be essential both for generation of conductive channels, and appropriate communication of ligand binding to gating domains. Disruption of these residues uncouples the TMD and CTD, again causing a paradoxical loss-of-function phenotype coupled with profound ligand insensitivity and gating defects. Loss-of-function mutants at these five positions are only rescued using the ‘forced gating’ approach (Kir6.2[F168E]), but not the ‘allosteric rescue’ mechanism (Kir6.2[C166S]), suggesting a general application of ‘forced gating’ on rescue loss-of-function mutants in mutation-sensitive motifs in Kir6.2 channels.

Another advantage of the novel ‘forced gating’ approach (Kir6.2[F168E]) is that it does not significantly perturb ATP sensitivity in Kir6.2 channels. In contrast, the ‘allosteric rescue’ approach Kir6.2[C166S] mutation significantly alters ATP sensitivity of Kir6.2 channels (ATP  $IC_{50}$  ~5 mM) and likely confounds comparisons of ATP sensitivity between Kir6.2 interfacial mutants based on its intrinsic high open probability. However, Kir6.2[F168E] channels exhibit a unique intrinsic voltage-dependence, by a mechanism that remains unclear. Therefore, the functional interpretation of the hyperpolarization-stimulated slow opening imparted by Kir6.2[F168E] mutation (and its alteration by additional mutations) are less understood.

We observed two groups of interfacial residues play essential roles on ATP sensitivity of Kir6.2 channels. One group is clustered in the vicinity of the putative ATP binding site (i.e. I49, R50) and mutations at these residues most likely directly disrupt the ATP binding site and thus reduce channel ATP sensitivity. The other group lies far from the putative ATP binding site (i.e.

D58, T61, R177, D204, G289, V290, T294, G295, and R301) and thus it is unlikely that mutations at these positions directly perturb the ATP binding, but rather affect the ATP inhibition allosterically. These groups could be distinguished by their effects on F168E channel gating kinetics. Specifically, ATP binding site mutations (I49A, R50A) did not significantly alter the functional activity or the slow gating kinetics, but the other group of mutants significantly accelerated the gating kinetics. Therefore we have hypothesized that the second group of residues are components of the domain interface for generation of conductive channels and transduction of ligand binding. A shortcoming of these studies is that we are unable to probe the integrity of the ATP binding site and whether ATP molecules still bind to these Kir6.2 mutant channels. We have tested the ATP inhibition of Kir6.2 mutant channels using dye-labelled ATP molecules with patch clamp experiments. However, even WT Kir6.2 channels exhibited no sensitivity to tagged ATP, likely due to the large fluorophore moiety preventing ATP from accessing the ATP binding site (data not shown). In future studies, single channel inside-out recording could be carried out, which would provide additional complimentary information on distinguishing residues directly involved in ATP binding from the ones that are crucial for coupling TMD-CTD domains without making direct contacts with ATP.

As highlighted above, recent crystal Kir structures suggest numerous close contacts of charged side chains in the TMD-CTD interface. We identified two residues (R206 and R177) in the CTD of Kir6.2 channels that seem to interact with the essential ‘aspartate anchor’ D58 on the slide helix. We have attempted multiple approaches, including targeted disulfide bond formation, targeted metal bridges, and complimentary charge reversal mutations (between D58 and either R206 or R177) to further assess the hypothetical potential salt bridge. We attempted charge reversal double mutations (Kir6.2[D58R][R206D] and Kir6.2[D58R][R177D]) (expressed on

[F168E] background) to examine if the electrostatic attraction between the two nearby oppositely charged residues are sufficient for TMD-CTD coupling and ligand transduction. We have also attempted to modulate these potential electrostatic interactions by creating mutants such as Kir6.2[D58E][R206K] and Kir6.2[D58E][R177K] (expressed on [F168E] background), which preserve the charges while varying their spatial arrangement. However, none of these mutations regenerate WT channel function, highlighting the extreme stringency of position D58. All of them significantly abolished the ATP sensitivity and accelerated voltage-dependent slow gating kinetics (Appendix Fig.A-1). We have also attempted targeted disulfide bond formation by engineering site-specific double cysteine pairs Kir6.2[D58C][R206C] and Kir6.2[D58C][R177C] (expressed on [F168E] background). Moreover, we introduced site-specific double histidine pairs by substituting each residue pair with histidines (Kir6.2[D58H][R206H], Kir6.2[D58H][R177H], both on [F168E] background) to allow high affinity metal bridge formation upon exposure to  $\text{Zn}^{2+}$  solution (50  $\mu\text{M}$ ). In all cases, none of these conditions exhibit WT Kir6.2 channel function. As a result, alternative approaches will be required to investigate potential state-dependent contacts between residues in this region.

Our findings highlight the importance of residues R177 in C-linker and D204 in  $\beta\text{C}-\beta\text{D}$  for ATP inhibition. The double cysteine Kir6.2[F168E][D204C][R177C] mutant exhibited relatively strong ATP inhibition, with moderately accelerated channel gating kinetics. We repeated the targeted metal bridge formation between R177 and D204 to further investigate any functional relevant interactions. Once again, the F168E background was exploited to rescue electrically silent mutants. Our findings showed that high affinity metal bridges formed rapidly and reversibly at Kir6.2[F168E][D204H][R177H] upon exposure to  $\text{Zn}^{2+}$  solution.



However, several problems and uncertainties have arisen from these double histidine pairs regarding of the experimental design and data interpretation. Firstly, ATP is a significant chelating agent for  $\text{Zn}^{2+}$ . The free  $[\text{Zn}^{2+}]$  must be held constant in the absence and presence of ATP since the formation of metal bridges will be  $[\text{Zn}^{2+}]$  dependent. We tried to maintain the free  $[\text{Zn}^{2+}]$  constant by balancing  $[\text{Zn}^{2+}]$  with  $[\text{ATP}]$  according to the dissociation constant  $K_d$ . However, the exact free  $[\text{Zn}^{2+}]$  was not experimentally measured in our setting. Additionally,  $\text{Zn}^{2+}$  can also promote salt bridge formation between nearby cysteine residues. As a result, non-specific effects induced by  $\text{Zn}^{2+}$  could also potentially arise. Therefore, as emphasized previously, dynamic state-dependent interactions between densely charged side chains in the TMD-CTD interfacial domain are extremely difficult to convincingly demonstrate experimentally. Further investigation will be required to identify dynamic changes that underlie ligand-dependent channel gating in Kir channels.

How will research presented in my thesis affect our understanding of pathophysiology or potential therapeutic applications? Due to the abundant expression of  $\text{K}_{\text{ATP}}$  channels throughout human body,  $\text{K}_{\text{ATP}}$  channels defects and dysregulation are associated with multiple pathologies. My study has focused on the pancreatic  $\beta$ -cell  $\text{K}_{\text{ATP}}$  isoform, a keystone component for glucose stimulated insulin secretion. Mutations that perturb either the formation of functional channels or the coupling between cellular metabolism and  $\text{K}_{\text{ATP}}$  channel gating cause severe defects on insulin secretion, resulting in a spectrum of insulin secretory diseases, ranging from neonatal diabetes to congenial hyperinsulinism.

Due to their complex molecular architecture relative to other  $\text{K}^+$  channels (including large functionally coupled SUR subunits), elucidation of the molecular mechanisms underlying ligand-dependent channel gating will surely eventually require detailed  $\text{K}_{\text{ATP}}$  channel structures and

deep understanding of channel function. Progress described in this thesis will hopefully provide new tools to understand the complex function of these channels. Furthermore, due to strong homology among eukaryotic Kir channels, detailed understanding of ligand transduction mechanisms in  $K_{ATP}$  channels will hopefully provide general insights that translate to ligand-dependent gating mechanisms in other Kir families, such as  $G\beta\gamma$  regulation of GIRK channels, which are critically significant in diverse physiological processes, and expose therapeutic potentials toward related disorders (Schulze-Bahr, 2005;Plaster et al., 2001;Nichols, 2006;Gloyn et al., 2004;Choi et al., 2011;Pinney et al., 2008;Schulte et al., 1999).

The recognition that gain-of-function mutations in Kir6.2 channels are associated with neonatal diabetes has shifted clinical therapy for neonatal diabetics from insulin injection to sulfonylurea tablets, and this change emphasizes the significance of understanding the molecular basis underlying channelopathies. In contrast to the effectiveness of SUs on diabetic patients, most PHHI patients with loss-of-function mutations in  $K_{ATP}$  channels do not effectively respond to  $K^+$  channels openers such as diazoxide (most likely due to reduced channel expression) and require subtotal pancreatectomy to reduce insulin secretion (Hibino et al., 2010). Therefore, an effective novel therapeutic application is greatly in need. An ambitious application is to incorporate genetic therapy to replace the electrically silent  $K_{ATP}$  mutant channels with functional ones. My thesis reinforces and extends the understanding of structure and function of  $K_{ATP}$  channels and provides novel therapeutic potentials. However, due to the abundant expression of  $K_{ATP}$  channels, preventing undesired systemic side-effects might be a challenge.

## References

Abdulhadi-Atwan M, Bushman J, Tornovsky-Babaey S, Perry A, Abu-Libdeh A, Glaser B, Shyng S L and Zangen D H (2008) Novel De Novo Mutation in Sulfonylurea Receptor 1 Presenting As Hyperinsulinism in Infancy Followed by Overt Diabetes in Early Adolescence. *Diabetes* 57:1935-1940.

Accili EA, Kiehn J, Wible B A and Brown A M (1997) Interactions Among Inactivating and Noninactivating Kvbeta Subunits, and Kvalpha1.2, Produce Potassium Currents With Intermediate Inactivation. *J Biol Chem* 272:28232-28236.

Aguilar-Bryan L, Clement J P, Gonzalez G, Kunjilwar K, Babenko A and Bryan J (1998) Toward Understanding the Assembly and Structure of KATP Channels. *Physiol Rev* 78:227-245.

Aguilar-Bryan L, Nichols C G, Wechsler S W, Clement J P, Boyd A E, III, Gonzalez G, Herrera-Sosa H, Nguy K, Bryan J and Nelson D A (1995) Cloning of the Beta Cell High-Affinity Sulfonylurea Receptor: a Regulator of Insulin Secretion. *Science* 268:423-426.

Aittoniemi J, Fotinou C, Craig T J, de W H, Proks P and Ashcroft F M (2009) Review. SUR1: a Unique ATP-Binding Cassette Protein That Functions As an Ion Channel Regulator. *Philos Trans R Soc Lond B Biol Sci* 364:257-267.

Antcliff JF, Haider S, Proks P, Sansom M S and Ashcroft F M (2005) Functional Analysis of a Structural Model of the ATP-Binding Site of the KATP Channel Kir6.2 Subunit. *EMBO J* 24:229-239.

Ashcroft FM (1988) Adenosine 5'-Triphosphate-Sensitive Potassium Channels. *Annu Rev Neurosci* 11:97-118.

Ashcroft FM (2005) ATP-Sensitive Potassium Channelopathies: Focus on Insulin Secretion. *J Clin Invest* 115:2047-2058.

Ashcroft FM (2006) K(ATP) Channels and Insulin Secretion: a Key Role in Health and Disease. *Biochem Soc Trans* 34:243-246.

Ashcroft FM and Kakei M (1989) ATP-Sensitive K<sup>+</sup> Channels in Rat Pancreatic Beta-Cells: Modulation by ATP and Mg<sup>2+</sup> Ions. *J Physiol* 416:349-367.

Ashcroft FM and Rorsman P (1989) Electrophysiology of the Pancreatic Beta-Cell. *Prog Biophys Mol Biol* 54:87-143.

Ashfield R, Gribble F M, Ashcroft S J and Ashcroft F M (1999) Identification of the High-Affinity Tolbutamide Site on the SUR1 Subunit of the K(ATP) Channel. *Diabetes* 48:1341-1347.

Ashford ML, Boden P R and Treherne J M (1990a) Glucose-Induced Excitation of Hypothalamic Neurones Is Mediated by ATP-Sensitive K<sup>+</sup> Channels. *Pflugers Arch* 415:479-483.

Ashford ML, Boden P R and Treherne J M (1990b) Tolbutamide Excites Rat Glucoreceptive Ventromedial Hypothalamic Neurones by Indirect Inhibition of ATP-K<sup>+</sup> Channels. *Br J Pharmacol* 101:531-540.

Ashford ML, Sturgess N C, Trout N J, Gardner N J and Hales C N (1988) Adenosine-5'-Triphosphate-Sensitive Ion Channels in Neonatal Rat Cultured Central Neurones. *Pflugers Arch* 412:297-304.

Babenko AP and Bryan J (2002) SUR-Dependent Modulation of KATP Channels by an N-Terminal KIR6.2 Peptide. Defining Intersubunit Gating Interactions. *J Biol Chem* 277:43997-44004.

Babenko AP and Bryan J (2003) Sur Domains That Associate With and Gate KATP Pores Define a Novel Gatekeeper. *J Biol Chem* 278:41577-41580.

Babenko AP, Gonzalez G and Bryan J (2000) Pharmacology-Topology of Sulfonylurea Receptors. Separate Domains of the Regulatory Subunits of K(ATP) Channel Isoforms Are Required for Selective Interaction With K(+) Channel Openers. *J Biol Chem* 275:717-720.

Barrett-Jolley R and Davies N W (1997) Kinetic Analysis of the Inhibitory Effect of Glibenclamide on KATP Channels of Mammalian Skeletal Muscle. *J Membr Biol* 155:257-262.

Batulan Z, Haddad G A and Blunck R (2010) An Intersubunit Interaction Between S4-S5 Linker and S6 Is Responsible for the Slow Off-Gating Component in Shaker K<sup>+</sup> Channels. *J Biol Chem* 285:14005-14019.

**Baukrowitz T, Schulte U, Oliver D, Herlitze S, Krauter T, Tucker S J, Ruppersberg J P and Fakler B (1998) PIP<sub>2</sub> and PIP<sub>3</sub> As Determinants for ATP Inhibition of KATP Channels. *Science* 282:1141-1144.**

**Bavro VN, De Z R, Schmidt M R, Muniz J R, Zubcevic L, Sansom M S, Venien-Bryan C and Tucker S J (2012) Structure of a KirBac Potassium Channel With an Open Bundle Crossing Indicates a Mechanism of Channel Gating. *Nat Struct Mol Biol*.**

**Beech DJ, Zhang H, Nakao K and Bolton T B (1993) K Channel Activation by Nucleotide Diphosphates and Its Inhibition by Glibenclamide in Vascular Smooth Muscle Cells. *Br J Pharmacol* 110:573-582.**

**Bendahhou S, Donaldson M R, Plaster N M, Tristani-Firouzi M, Fu Y H and Ptacek L J (2003) Defective Potassium Channel Kir2.1 Trafficking Underlies Andersen-Tawil Syndrome. *J Biol Chem* 278:51779-51785.**

**Bernardi H, Fosset M and Lazdunski M (1988) Characterization, Purification, and Affinity Labeling of the Brain [3H]Glibenclamide-Binding Protein, a Putative Neuronal ATP-Regulated K<sup>+</sup> Channel. *Proc Natl Acad Sci U S A* 85:9816-9820.**

**Bienengraeber M, Alekseev A E, Abraham M R, Carrasco A J, Moreau C, Vivaudou M, Dzeja P P and Terzic A (2000) ATPase Activity of the Sulfonylurea Receptor: a Catalytic Function for the KATP Channel Complex. *FASEB J* 14:1943-1952.**

**Cartier EA, Conti L R, Vandenberg C A and Shyng S L (2001) Defective Trafficking and Function of KATP Channels Caused by a Sulfonylurea Receptor 1 Mutation Associated With Persistent Hyperinsulinemic Hypoglycemia of Infancy. *Proc Natl Acad Sci U S A* 98:2882-2887.**

**Cheng WW, Tong A, Flagg T P and Nichols C G (2008) Random Assembly of SUR Subunits in K(ATP) Channel Complexes. *Channels (Austin)* 2:34-38.**

**Choi M, Scholl U I, Yue P, Bjorklund P, Zhao B, Nelson-Williams C, Ji W, Cho Y, Patel A, Men C J, Lolis E, Wisgerhof M V, Geller D S, Mane S, Hellman P, Westin G, Akerstrom G, Wang W, Carling T and Lifton R P (2011) K<sup>+</sup> Channel Mutations in Adrenal Aldosterone-Producing Adenomas and Hereditary Hypertension. *Science* 331:768-772.**

**Clarke OB, Caputo A T, Hill A P, Vandenberg J I, Smith B J and Gulbis J M (2010) Domain Reorientation and Rotation of an Intracellular Assembly Regulate Conduction in Kir Potassium Channels. *Cell* 141:1018-1029.**

**Claydon TW, Makary S Y, Dibb K M and Boyett M R (2003) The Selectivity Filter May Act As the Agonist-Activated Gate in the G Protein-Activated Kir3.1/Kir3.4 K<sup>+</sup> Channel. *J Biol Chem* 278:50654-50663.**

**Craig TJ, Ashcroft F M and Proks P (2008) How ATP Inhibits the Open K(ATP) Channel. *J Gen Physiol* 132:131-144.**

**Cukras CA, Jeliaskova I and Nichols C G (2002) The Role of NH<sub>2</sub>-Terminal Positive Charges in the Activity of Inward Rectifier KATP Channels. *J Gen Physiol* 120:437-446.**

**de Wet H, Proks P, Lafond M, Aittoniemi J, Sansom M S, Flanagan S E, Pearson E R, Hattersley A T and Ashcroft F M (2008) A Mutation (R826W) in Nucleotide-Binding Domain 1 of ABCC8 Reduces ATPase Activity and Causes Transient Neonatal Diabetes. *EMBO Rep* 9:648-654.**

**de WH, Rees M G, Shimomura K, Aittoniemi J, Patch A M, Flanagan S E, Ellard S, Hattersley A T, Sansom M S and Ashcroft F M (2007) Increased ATPase Activity Produced by Mutations at Arginine-1380 in Nucleotide-Binding Domain 2 of ABCC8 Causes Neonatal Diabetes. *Proc Natl Acad Sci U S A* 104:18988-18992.**

**Dirnagl U, Iadecola C and Moskowitz M A (1999) Pathobiology of Ischaemic Stroke: an Integrated View. *Trends Neurosci* 22:391-397.**

**Doyle DA, Morais C J, Pfuetzner R A, Kuo A, Gulbis J M, Cohen S L, Chait B T and MacKinnon R (1998) The Structure of the Potassium Channel: Molecular Basis of K<sup>+</sup> Conduction and Selectivity. *Science* 280:69-77.**

**Doyle ME and Egan J M (2003) Pharmacological Agents That Directly Modulate Insulin Secretion. *Pharmacol Rev* 55:105-131.**

**Dunne MJ, Cosgrove K E, Shepherd R M, Aynsley-Green A and Lindley K J (2004) Hyperinsulinism in Infancy: From Basic Science to Clinical Disease. *Physiol Rev* 84:239-275.**

**Edghill EL, Gloyn A L, Gillespie K M, Lambert A P, Raymond N T, Swift P G, Ellard S, Gale E A and Hattersley A T (2004) Activating Mutations in the KCNJ11 Gene Encoding the ATP-Sensitive K<sup>+</sup> Channel Subunit Kir6.2 Are Rare in Clinically Defined Type 1 Diabetes Diagnosed Before 2 Years. *Diabetes* 53:2998-3001.**

**Edwards G and Weston A H (1990) Potassium Channel Openers and Vascular Smooth Muscle Relaxation. *Pharmacol Ther* 48:237-258.**

**Edwards G and Weston A H (1993) The Pharmacology of ATP-Sensitive Potassium Channels. *Annu Rev Pharmacol Toxicol* 33:597-637.**

**Enkvetchakul D, Loussouarn G, Makhina E and Nichols C G (2001) ATP Interaction With the Open State of the K(ATP) Channel. *Biophys J* 80:719-728.**

**Enkvetchakul D, Loussouarn G, Makhina E, Shyng S L and Nichols C G (2000) The Kinetic and Physical Basis of K(ATP) Channel Gating: Toward a Unified Molecular Understanding. *Biophys J* 78:2334-2348.**

**Enkvetchakul D and Nichols C G (2003) Gating Mechanism of KATP Channels: Function Fits Form. *J Gen Physiol* 122:471-480.**

**Fan Z and Makielski J C (1997) Anionic Phospholipids Activate ATP-Sensitive Potassium Channels. *J Biol Chem* 272:5388-5395.**

**Fang K, Csanady L and Chan K W (2006) The N-Terminal Transmembrane Domain (TMD0) and a Cytosolic Linker (L0) of Sulphonylurea Receptor Define the Unique Intrinsic Gating of KATP Channels. *J Physiol* 576:379-389.**

**Flagg TP, Kurata H T, Masia R, Caputa G, Magnuson M A, Lefer D J, Coetzee W A and Nichols C G (2008) Differential Structure of Atrial and Ventricular K-ATP Atrial K-ATP Channels Require SUR1. *Circulation Research* 103:1458-U228.**

**Gillis KD, Gee W M, Hammoud A, McDaniel M L, Falke L C and Misler S (1989) Effects of Sulfonamides on a Metabolite-Regulated ATPi-Sensitive K<sup>+</sup> Channel in Rat Pancreatic B-Cells. *Am J Physiol* 257:C1119-C1127.**

**Girard CA, Shimomura K, Proks P, Absalom N, Castano L, Perez de N G and Ashcroft F M (2006) Functional Analysis of Six Kir6.2 (KCNJ11) Mutations Causing Neonatal Diabetes. *Pflugers Arch* 453:323-332.**

**Gloyn AL, Pearson E R, Antcliff J F, Proks P, Bruining G J, Slingerland A S, Howard N, Srinivasan S, Silva J M, Molnes J, Edghill E L, Frayling T M, Temple I K, Mackay D, Shield J P, Sumnik Z, van Rhijn A, Wales J K, Clark P, Gorman S, Aisenberg J, Ellard S, Njolstad P R, Ashcroft F M and Hattersley A T (2004) Activating Mutations in the Gene Encoding the ATP-Sensitive Potassium-Channel Subunit Kir6.2 and Permanent Neonatal Diabetes. *N Engl J Med* 350:1838-1849.**

**Gloyn AL, Reimann F, Girard C, Edghill E L, Proks P, Pearson E R, Temple I K, Mackay D J, Shield J P, Freedenberg D, Noyes K, Ellard S, Ashcroft F M, Gribble F M and Hattersley A T (2005) Relapsing Diabetes Can Result From Moderately Activating Mutations in KCNJ11. *Hum Mol Genet* 14:925-934.**

**Grafe P, Quasthoff S, Strupp M and Lehmann-Horn F (1990) Enhancement of K<sup>+</sup> Conductance Improves in Vitro the Contraction Force of Skeletal Muscle in Hypokalemic Periodic Paralysis. *Muscle Nerve* 13:451-457.**

**Gribble FM, Tucker S J and Ashcroft F M (1997) The Essential Role of the Walker A Motifs of SUR1 in K-ATP Channel Activation by Mg-ADP and Diazoxide. *EMBO J* 16:1145-1152.**

**Gross GJ and Auchampach J A (1992) Blockade of ATP-Sensitive Potassium Channels Prevents Myocardial Preconditioning in Dogs. *Circ Res* 70:223-233.**

**Hansen SB, Tao X and MacKinnon R (2011) Structural Basis of PIP<sub>2</sub> Activation of the Classical Inward Rectifier K<sup>+</sup> Channel Kir2.2. *Nature* 477:495-498.**

**Hattersley AT and Ashcroft F M (2005) Activating Mutations in Kir6.2 and Neonatal Diabetes: New Clinical Syndromes, New Scientific Insights, and New Therapy. *Diabetes* 54:2503-2513.**

**Heginbotham L, Lu Z, Abramson T and MacKinnon R (1994) Mutations in the K<sup>+</sup> Channel Signature Sequence. *Biophys J* 66:1061-1067.**



Hibino H, Inanobe A, Furutani K, Murakami S, Findlay I and Kurachi Y (2010) Inwardly Rectifying Potassium Channels: Their Structure, Function, and Physiological Roles. *Physiol Rev* 90:291-366.

Hilgemann DW and Ball R (1996) Regulation of Cardiac Na<sup>+</sup>,Ca<sup>2+</sup> Exchange and KATP Potassium Channels by PIP<sub>2</sub>. *Science* 273:956-959.

Hollenstein K, Dawson R J and Locher K P (2007) Structure and Mechanism of ABC Transporter Proteins. *Curr Opin Struct Biol* 17:412-418.

Huang CL, Feng S and Hilgemann D W (1998) Direct Activation of Inward Rectifier Potassium Channels by PIP<sub>2</sub> and Its Stabilization by Gbetagamma. *Nature* 391:803-806.

Huang CL, Jan Y N and Jan L Y (1997) Binding of the G Protein Betagamma Subunit to Multiple Regions of G Protein-Gated Inward-Rectifying K<sup>+</sup> Channels. *FEBS Lett* 405:291-298.

Huang CW, Tsai J J, Ou H Y, Wang S T, Cheng J T, Wu S N and Huang C C (2008) Diabetic Hyperglycemia Is Associated With the Severity of Epileptic Seizures in Adults. *Epilepsy Res* 79:71-77.

Hunter M and Giebisch G (1988) Calcium-Activated K-Channels of Amphiuma Early Distal Tubule: Inhibition by ATP. *Pflugers Arch* 412:331-333.

Huopio H, Reimann F, Ashfield R, Komulainen J, Lenko H L, Rahier J, Vauhkonen I, Kere J, Laakso M, Ashcroft F and Otonkoski T (2000) Dominantly Inherited Hyperinsulinism Caused by a Mutation in the Sulfonylurea Receptor Type 1. *J Clin Invest* 106:897-906.

Inagaki N, Gonoi T, Clement J P, Namba N, Inazawa J, Gonzalez G, Aguilar-Bryan L, Seino S and Bryan J (1995) Reconstitution of IKATP: an Inward Rectifier Subunit Plus the Sulfonylurea Receptor. *Science* 270:1166-1170.

Inagaki N, Gonoi T, Clement J P, Wang C Z, Aguilar-Bryan L, Bryan J and Seino S (1996) A Family of Sulfonylurea Receptors Determines the Pharmacological Properties of ATP-Sensitive K<sup>+</sup> Channels. *Neuron* 16:1011-1017.

**Inanobe A, Matsuura T, Nakagawa A and Kurachi Y (2007) Structural Diversity in the Cytoplasmic Region of G Protein-Gated Inward Rectifier K<sup>+</sup> Channels. *Channels* 1.**

**Isomoto S, Kondo C, Yamada M, Matsumoto S, Higashiguchi O, Horio Y, Matsuzawa Y and Kurachi Y (1996) A Novel Sulfonylurea Receptor Forms With BIR (Kir6.2) a Smooth Muscle Type ATP-Sensitive K<sup>+</sup> Channel. *J Biol Chem* 271:24321-24324.**

**Jiang Y, Lee A, Chen J, Cadene M, Chait B T and MacKinnon R (2002) Crystal Structure and Mechanism of a Calcium-Gated Potassium Channel. *Nature* 417:515-522.**

**Jiang Y, Lee A, Chen J, Ruta V, Cadene M, Chait B T and MacKinnon R (2003) X-Ray Structure of a Voltage-Dependent K<sup>+</sup> Channel. *Nature* 423:33-41.**

**Jin T, Peng L, Mirshahi T, Rohacs T, Chan K W, Sanchez R and Logothetis D E (2002) The (Beta)Gamma Subunits of G Proteins Gate a K<sup>(+)</sup> Channel by Pivoted Bending of a Transmembrane Segment. *Mol Cell* 10:469-481.**

**John SA, Weiss J N and Ribalet B (2001) Regulation of Cloned ATP-Sensitive K Channels by Adenine Nucleotides and Sulfonylureas: Interactions Between SUR1 and Positively Charged Domains on Kir6.2. *J Gen Physiol* 118:391-405.**

**John SA, Weiss J N and Ribalet B (2005) ATP Sensitivity of ATP-Sensitive K<sup>+</sup> Channels: Role of the Gamma Phosphate Group of ATP and the R50 Residue of Mouse Kir6.2. *J Physiol* 568:931-940.**

**John SA, Weiss J N, Xie L H and Ribalet B (2003) Molecular Mechanism for ATP-Dependent Closure of the K<sup>+</sup> Channel Kir6.2. *J Physiol* 552:23-34.**

**Khurana A, Shao E S, Kim R Y, Vilin Y Y, Huang X, Yang R and Kurata H T (2011) Forced Gating Motions by a Substituted Titratable Side Chain at the Bundle Crossing of a Potassium Channel. *J Biol Chem* 286:36686-36693.**

**Kim D and Bang H (1999) Modulation of Rat Atrial G Protein-Coupled K<sup>+</sup> Channel Function by Phospholipids. *J Physiol* 517 ( Pt 1):59-74.**

**Koster JC, Kurata H T, Enkvetchakul D and Nichols C G (2008) DEND Mutation in Kir6.2 (KCNJ11) Reveals a Flexible N-Terminal Region Critical for ATP-Sensing of the K-ATP Channel. *Biophysical Journal* 95:4689-4697.**

**Koster JC, Marshall B A, Ensor N, Corbett J A and Nichols C G (2000) Targeted Overactivity of Beta Cell K(ATP) Channels Induces Profound Neonatal Diabetes. *Cell* 100:645-654.**

**Koster JC, Remedi M S, Dao C and Nichols C G (2005) ATP and Sulfonylurea Sensitivity of Mutant ATP-Sensitive K<sup>+</sup> Channels in Neonatal Diabetes: Implications for Pharmacogenomic Therapy. *Diabetes* 54:2645-2654.**

**Kuo A, Gulbis J M, Antcliff J F, Rahman T, Lowe E D, Zimmer J, Cuthbertson J, Ashcroft F M, Ezaki T and Doyle D A (2003) Crystal Structure of the Potassium Channel KirBac1.1 in the Closed State. *Science* 300:1922-1926.**

**Kurata HT, Cheng W W and Nichols C G (2011) Polyamine Block of Inwardly Rectifying Potassium Channels. *Methods Mol Biol* 720:113-126.**

**Kurata HT, Phillips L R, Rose T, Loussouarn G, Herlitze S, Fritzenschaft H, Enkvetchakul D, Nichols C G and Baukrowitz T (2004) Molecular Basis of Inward Rectification: Polyamine Interaction Sites Located by Combined Channel and Ligand Mutagenesis. *J Gen Physiol* 124:541-554.**

**Kurata HT, Rapedius M, Kleinman M J, Baukrowitz T and Nichols C G (2010) Voltage-Dependent Gating in a "Voltage Sensor-Less" Ion Channel. *PLoS Biol* 8:e1000315.**

**Li L, Wang J and Drain P (2000) The I182 Region of K(Ir)6.2 Is Closely Associated With Ligand Binding in K(ATP) Channel Inhibition by ATP. *Biophys J* 79:841-852.**

**Lin YW, Bushman J D, Yan F F, Haidar S, Macmullen C, Ganguly A, Stanley C A and Shyng S L (2008) Destabilization of ATP-Sensitive Potassium Channel Activity by Novel KCNJ11 Mutations Identified in Congenital Hyperinsulinism. *J Biol Chem* 283:9146-9156.**

**Lin YW, Jia T, Weinsoft A M and Shyng S L (2003) Stabilization of the Activity of ATP-Sensitive Potassium Channels by Ion Pairs Formed Between Adjacent Kir6.2 Subunits. *J Gen Physiol* 122:225-237.**

- Logothetis DE, Kurachi Y, Galper J, Neer E J and Clapham D E (1987) The Beta Gamma Subunits of GTP-Binding Proteins Activate the Muscarinic K<sup>+</sup> Channel in Heart. *Nature* 325:321-326.**
- Long SB, Campbell E B and MacKinnon R (2005) Crystal Structure of a Mammalian Voltage-Dependent Shaker Family K<sup>+</sup> Channel. *Science* 309:897-903.**
- Lopatin AN, Makhina E N and Nichols C G (1994) Potassium Channel Block by Cytoplasmic Polyamines As the Mechanism of Intrinsic Rectification. *Nature* 372:366-369.**
- Lopes CM, Zhang H, Rohacs T, Jin T, Yang J and Logothetis D E (2002) Alterations in Conserved Kir Channel-PIP2 Interactions Underlie Channelopathies. *Neuron* 34:933-944.**
- Loussouarn G, Makhina E N, Rose T and Nichols C G (2000) Structure and Dynamics of the Pore of Inwardly Rectifying K(ATP) Channels. *J Biol Chem* 275:1137-1144.**
- Loussouarn G, Phillips L R, Masia R, Rose T and Nichols C G (2001) Flexibility of the Kir6.2 Inward Rectifier K(+) Channel Pore. *Proc Natl Acad Sci U S A* 98:4227-4232.**
- Lu Z (2004) Mechanism of Rectification in Inward-Rectifier K<sup>+</sup> Channels. *Annu Rev Physiol* 66:103-129.**
- Lu Z, Klem A M and Ramu Y (2002) Coupling Between Voltage Sensors and Activation Gate in Voltage-Gated K<sup>+</sup> Channels. 2002/10/31:663-676.**
- Lu Z and MacKinnon R (1994) Electrostatic Tuning of Mg<sup>2+</sup> Affinity in an Inward-Rectifier K<sup>+</sup> Channel. *Nature* 371:243-246.**
- MacGregor GG, Dong K, Vanoye C G, Tang L, Giebisch G and Hebert S C (2002) Nucleotides and Phospholipids Compete for Binding to the C Terminus of KATP Channels. *Proc Natl Acad Sci U S A* 99:2726-2731.**
- Mannikko R, Jefferies C, Flanagan S E, Hattersley A, Ellard S and Ashcroft F M (2010) Interaction Between Mutations in the Slide Helix of Kir6.2 Associated With Neonatal Diabetes and Neurological Symptoms. *Hum Mol Genet* 19:963-972.**

**Mannikko R, Stansfeld P J, Ashcroft A S, Hattersley A T, Sansom M S, Ellard S and Ashcroft F M (2011) A Conserved Tryptophan at the Membrane-Water Interface Acts As a Gatekeeper for Kir6.2/SUR1 Channels and Causes Neonatal Diabetes When Mutated. *J Physiol* 589:3071-3083.**

**Marthinet E, Bloc A, Oka Y, Tanizawa Y, Wehrle-Haller B, Bancila V, Dubuis J M, Philippe J and Schwitzgebel V M (2005) Severe Congenital Hyperinsulinism Caused by a Mutation in the Kir6.2 Subunit of the Adenosine Triphosphate-Sensitive Potassium Channel Impairing Trafficking and Function. *J Clin Endocrinol Metab* 90:5401-5406.**

**Matsuo M, Tanabe K, Kioka N, Amachi T and Ueda K (2000) Different Binding Properties and Affinities for ATP and ADP Among Sulfonylurea Receptor Subtypes, SUR1, SUR2A, and SUR2B. *J Biol Chem* 275:28757-28763.**

**McTaggart JS, Clark R H and Ashcroft F M (2010) The Role of the KATP Channel in Glucose Homeostasis in Health and Disease: More Than Meets the Islet. *J Physiol* 588:3201-3209.**

**Mikhailov MV, Mikhailova E A and Ashcroft S J (2001) Molecular Structure of the Glibenclamide Binding Site of the Beta-Cell K(ATP) Channel. *FEBS Lett* 499:154-160.**

**Minor DL, Jr., Masseling S J, Jan Y N and Jan L Y (1999) Transmembrane Structure of an Inwardly Rectifying Potassium Channel. *Cell* 96:879-891.**

**Mizumura T, Nithipatikom K and Gross G J (1995) Bimakalim, an ATP-Sensitive Potassium Channel Opener, Mimics the Effects of Ischemic Preconditioning to Reduce Infarct Size, Adenosine Release, and Neutrophil Function in Dogs. *Circulation* 92:1236-1245.**

**Morais-Cabral JH, Zhou Y and MacKinnon R (2001) Energetic Optimization of Ion Conduction Rate by the K<sup>+</sup> Selectivity Filter. *Nature* 414:37-42.**

**Murry CE, Jennings R B and Reimer K A (1986) Preconditioning With Ischemia: a Delay of Lethal Cell Injury in Ischemic Myocardium. *Circulation* 74:1124-1136.**

**Nichols CG (2006) KATP Channels As Molecular Sensors of Cellular Metabolism. *Nature* 440:470-476.**

**Nichols CG and Lopatin A N (1997) Inward Rectifier Potassium Channels. *Annu Rev Physiol* 59:171-191.**

**Nichols CG, Shyng S L, Nestorowicz A, Glaser B, Clement J P, Gonzalez G, Aguilar-Bryan L, Permutt M A and Bryan J (1996) Adenosine Diphosphate As an Intracellular Regulator of Insulin Secretion. *Science* 272:1785-1787.**

**Nishida M, Cadene M, Chait B T and MacKinnon R (2007) Crystal Structure of a Kir3.1-Prokaryotic Kir Channel Chimera. *EMBO J* 26:4005-4015.**

**Nishida M and MacKinnon R (2002) Structural Basis of Inward Rectification: Cytoplasmic Pore of the G Protein-Gated Inward Rectifier GIRK1 at 1.8 Å Resolution. *Cell* 111:957-965.**

**Noma A (1983) ATP-Regulated K<sup>+</sup> Channels in Cardiac Muscle. *Nature* 305:147-148.**

**Ohno-Shosaku T and Yamamoto C (1992) Identification of an ATP-Sensitive K<sup>+</sup> Channel in Rat Cultured Cortical Neurons. *Pflugers Arch* 422:260-266.**

**Otonkoski T, Ammala C, Huopio H, Cote G J, Chapman J, Cosgrove K, Ashfield R, Huang E, Komulainen J, Ashcroft F M, Dunne M J, Kere J and Thomas P M (1999) A Point Mutation Inactivating the Sulfonylurea Receptor Causes the Severe Form of Persistent Hyperinsulinemic Hypoglycemia of Infancy in Finland. *Diabetes* 48:408-415.**

**Partridge CJ, Beech D J and Sivaprasadarao A (2001) Identification and Pharmacological Correction of a Membrane Trafficking Defect Associated With a Mutation in the Sulfonylurea Receptor Causing Familial Hyperinsulinism. *J Biol Chem* 276:35947-35952.**

**Paynter JJ, Andres-Enguix I, Fowler P W, Tottey S, Cheng W, Enkvetchakul D, Bavro V N, Kusakabe Y, Sansom M S, Robinson N J, Nichols C G and Tucker S J (2010) Functional Complementation and Genetic Deletion Studies of KirBac Channels: Activatory Mutations Highlight Gating-Sensitive Domains. *J Biol Chem* 285:40754-40761.**

**Pegan S, Arrabit C, Slesinger P A and Choe S (2006) Andersen's Syndrome Mutation Effects on the Structure and Assembly of the Cytoplasmic Domains of Kir2.1. *Biochemistry* 45:8599-8606.**

**Pegan S, Arrabit C, Zhou W, Kwiatkowski W, Collins A, Slesinger P A and Choe S (2005) Cytoplasmic Domain Structures of Kir2.1 and Kir3.1 Show Sites for Modulating Gating and Rectification. *Nat Neurosci* 8:279-287.**

**Perozo E, Cortes D M and Cuello L G (1999) Structural Rearrangements Underlying K<sup>+</sup>-Channel Activation Gating. 1999/07/03:73-78.**

**Phillips LR, Enkvetchakul D and Nichols C G (2003) Gating Dependence of Inner Pore Access in Inward Rectifier K(+) Channels. *Neuron* 37:953-962.**

**Phillips LR and Nichols C G (2003) Ligand-Induced Closure of Inward Rectifier Kir6.2 Channels Traps Spermine in the Pore. *J Gen Physiol* 122:795-804.**

**Pinney SE, Macmullen C, Becker S, Lin Y W, Hanna C, Thornton P, Ganguly A, Shyng S L and Stanley C A (2008) Clinical Characteristics and Biochemical Mechanisms of Congenital Hyperinsulinism Associated With Dominant KATP Channel Mutations. *J Clin Invest* 118:2877-2886.**

**Plaster NM, Tawil R, Tristani-Firouzi M, Canun S, Bendahhou S, Tsunoda A, Donaldson M R, Iannaccone S T, Brunt E, Barohn R, Clark J, Deymeer F, George A L, Jr., Fish F A, Hahn A, Nitu A, Ozdemir C, Serdaroglu P, Subramony S H, Wolfe G, Fu Y H and Ptacek L J (2001) Mutations in Kir2.1 Cause the Developmental and Episodic Electrical Phenotypes of Andersen's Syndrome. *Cell* 105:511-519.**

**Polak M and Shield J (2004) Neonatal and Very-Early-Onset Diabetes Mellitus. *Semin Neonatol* 9:59-65.**

**Proks P, Antcliff J F and Ashcroft F M (2003) The Ligand-Sensitive Gate of a Potassium Channel Lies Close to the Selectivity Filter. *EMBO Rep* 4:70-75.**

**Proks P, Antcliff J F, Lippiat J, Gloyn A L, Hattersley A T and Ashcroft F M (2004) Molecular Basis of Kir6.2 Mutations Associated With Neonatal Diabetes or Neonatal Diabetes Plus Neurological Features. *Proc Natl Acad Sci U S A* 101:17539-17544.**

**Proks P, Arnold A L, Bruining J, Girard C, Flanagan S E, Larkin B, Colclough K, Hattersley A T, Ashcroft F M and Ellard S (2006) A Heterozygous Activating Mutation in the Sulphonylurea Receptor SUR1 (ABCC8) Causes Neonatal Diabetes. *Hum Mol Genet.***

**Proks P, Girard C and Ashcroft F M (2005a) Functional Effects of KCNJ11 Mutations Causing Neonatal Diabetes: Enhanced Activation by MgATP. *Hum Mol Genet* 14:2717-2726.**

**Proks P, Girard C, Haider S, Gloyn A L, Hattersley A T, Sansom M S and Ashcroft F M (2005b) A Gating Mutation at the Internal Mouth of the Kir6.2 Pore Is Associated With DEND Syndrome. *EMBO Rep* 6:470-475.**

**Proks P, Gribble F M, Adhikari R, Tucker S J and Ashcroft F M (1999) Involvement of the N-Terminus of Kir6.2 in the Inhibition of the KATP Channel by ATP. *J Physiol* 514 ( Pt 1):19-25.**

**Proks P, Shimomura K, Craig T J, Girard C A and Ashcroft F M (2007) Mechanism of Action of a Sulphonylurea Receptor SUR1 Mutation (F132L) That Causes DEND Syndrome. *Hum Mol Genet* 16:2011-2019.**

**Quast U (1996) ATP-Sensitive K<sup>+</sup> Channels in the Kidney. *Naunyn Schmiedebergs Arch Pharmacol* 354:213-225.**

**Quayle JM, Nelson M T and Standen N B (1997) ATP-Sensitive and Inwardly Rectifying Potassium Channels in Smooth Muscle. *Physiol Rev* 77:1165-1232.**

**Rapedius M, Fowler P W, Shang L, Sansom M S, Tucker S J and Baukrowitz T (2007) H Bonding at the Helix-Bundle Crossing Controls Gating in Kir Potassium Channels. *Neuron* 55:602-614.**

**Reimann F, Huopio H, Dabrowski M, Proks P, Gribble F M, Laakso M, Otonkoski T and Ashcroft F M (2003) Characterisation of New KATP-Channel Mutations Associated With Congenital Hyperinsulinism in the Finnish Population. *Diabetologia* 46:241-249.**

**Reimann F, Ryder T J, Tucker S J and Ashcroft F M (1999) The Role of Lysine 185 in the Kir6.2 Subunit of the ATP-Sensitive Channel in Channel Inhibition by ATP. *J Physiol* 520 Pt 3:661-669.**

**Ribalet B, John S A, Xie L H and Weiss J N (2006) ATP-Sensitive K<sup>+</sup> Channels: Regulation of Bursting by the Sulphonylurea Receptor, PIP<sub>2</sub> and Regions of Kir6.2. *J Physiol* 571:303-317.**



**Rohacs T, Chen J, Prestwich G D and Logothetis D E (1999) Distinct Specificities of Inwardly Rectifying K(+) Channels for Phosphoinositides. *J Biol Chem* 274:36065-36072.**

**Rohacs T, Lopes C M, Jin T, Ramdya P P, Molnar Z and Logothetis D E (2003) Specificity of Activation by Phosphoinositides Determines Lipid Regulation of Kir Channels. *Proc Natl Acad Sci U S A* 100:745-750.**

**Roper J and Ashcroft F M (1995) Metabolic Inhibition and Low Internal ATP Activate K-ATP Channels in Rat Dopaminergic Substantia Nigra Neurones. *Pflugers Arch* 430:44-54.**

**Rytter L, Troelsen S and Beck-Nielsen H (1985) Prevalence and Mortality of Acute Myocardial Infarction in Patients With Diabetes. *Diabetes Care* 8:230-234.**

**Sadja R, Smadja K, Alagem N and Reuveny E (2001) Coupling Gbetagamma-Dependent Activation to Channel Opening Via Pore Elements in Inwardly Rectifying Potassium Channels. *Neuron* 29:669-680.**

**Sagen JV, Raeder H, Hathout E, Shehadeh N, Gudmundsson K, Baevre H, Abuelo D, Phornphutkul C, Molnes J, Bell G I, Gloyn A L, Hattersley A T, Molven A, Sovik O and Njolstad P R (2004) Permanent Neonatal Diabetes Due to Mutations in KCNJ11 Encoding Kir6.2: Patient Characteristics and Initial Response to Sulfonylurea Therapy. *Diabetes* 53:2713-2718.**

**Sakura H, Ammala C, Smith P A, Gribble F M and Ashcroft F M (1995) Cloning and Functional Expression of the cDNA Encoding a Novel ATP-Sensitive Potassium Channel Subunit Expressed in Pancreatic Beta-Cells, Brain, Heart and Skeletal Muscle. *FEBS Lett* 377:338-344.**

**Schmid-Antomarchi H, De W J, Fosset M and Lazdunski M (1987a) The Antidiabetic Sulfonylurea Glibenclamide Is a Potent Blocker of the ATP-Modulated K<sup>+</sup> Channel in Insulin Secreting Cells. *Biochem Biophys Res Commun* 146:21-25.**

**Schmid-Antomarchi H, De W J, Fosset M and Lazdunski M (1987b) The Receptor for Antidiabetic Sulfonylureas Controls the Activity of the ATP-Modulated K<sup>+</sup> Channel in Insulin-Secreting Cells. *J Biol Chem* 262:15840-15844.**

Schulte U, Hahn H, Konrad M, Jeck N, Derst C, Wild K, Weidemann S, Ruppersberg J P, Fakler B and Ludwig J (1999) PH Gating of ROMK (K(Ir)1.1) Channels: Control by an Arg-Lys-Arg Triad Disrupted in Antenatal Bartter Syndrome. *Proc Natl Acad Sci U S A* 96:15298-15303.

Schulz R, Rose J and Heusch G (1994) Involvement of Activation of ATP-Dependent Potassium Channels in Ischemic Preconditioning in Swine. *Am J Physiol* 267:H1341-H1352.

Schulze D, Krauter T, Fritzenschaft H, Soom M and Baukrowitz T (2003) Phosphatidylinositol 4,5-Bisphosphate (PIP<sub>2</sub>) Modulation of ATP and PH Sensitivity in Kir Channels. A Tale of an Active and a Silent PIP<sub>2</sub> Site in the N Terminus. *J Biol Chem* 278:10500-10505.

Schulze-Bahr E (2005) Short QT Syndrome or Andersen Syndrome: Yin and Yang of Kir2.1 Channel Dysfunction. *Circ Res* 96:703-704.

Schwappach B, Zerangue N, Jan Y N and Jan L Y (2000) Molecular Basis for K(ATP) Assembly: Transmembrane Interactions Mediate Association of a K<sup>+</sup> Channel With an ABC Transporter. *Neuron* 26:155-167.

Shang L and Tucker S J (2008) Non-Equivalent Role of TM2 Gating Hinges in Heteromeric Kir4.1/Kir5.1 Potassium Channels. *Eur Biophys J* 37:165-171.

Sharma N, Crane A, Gonzalez G, Bryan J and Aguilar-Bryan L (2000) Familial Hyperinsulinism and Pancreatic Beta-Cell ATP-Sensitive Potassium Channels. *Kidney Int* 57:803-808.

Shieh CC, Coghlan M, Sullivan J P and Gopalakrishnan M (2000) Potassium Channels: Molecular Defects, Diseases, and Therapeutic Opportunities. *Pharmacol Rev* 52:557-594.

Shimomura K, Flanagan S E, Zadek B, Lethby M, Zubcevic L, Girard C A, Petz O, Mannikko R, Kapoor R R, Hussain K, Skae M, Clayton P, Hattersley A, Ellard S and Ashcroft F M (2009) Adjacent Mutations in the Gating Loop of Kir6.2 Produce Neonatal Diabetes and Hyperinsulinism. *EMBO Mol Med* 1:166-177.

Shimomura K, Girard C A, Proks P, Nazim J, Lippiat J D, Cerutti F, Lorini R, Ellard S, Hattersley A T, Barbetti F and Ashcroft F M (2006) Mutations at

**the Same Residue (R50) of Kir6.2 (KCNJ11) That Cause Neonatal Diabetes Produce Different Functional Effects. *Diabetes* 55:1705-1712.**

**Shimomura K, Horster F, de W H, Flanagan S E, Ellard S, Hattersley A T, Wolf N I, Ashcroft F and Ebinger F (2007) A Novel Mutation Causing DEND Syndrome: a Treatable Channelopathy of Pancreas and Brain. *Neurology* 69:1342-1349.**

**Shyng S and Nichols C G (1997) Octameric Stoichiometry of the KATP Channel Complex. 110:655-664.**

**Shyng SL, Cukras C A, Harwood J and Nichols C G (2000) Structural Determinants of PIP(2) Regulation of Inward Rectifier K(ATP) Channels. *J Gen Physiol* 116:599-608.**

**Shyng SL and Nichols C G (1998) Membrane Phospholipid Control of Nucleotide Sensitivity of KATP Channels. *Science* 282:1138-1141.**

**Shyng SL, Sha Q, Ferrigni T, Lopatin A N and Nichols C G (1996) Depletion of Intracellular Polyamines Relieves Inward Rectification of Potassium Channels. *Proc Natl Acad Sci U S A* 93:12014-12019.**

**Slingerland AS, Nuboer R, Hadders-Algra M, Hattersley A T and Bruining G J (2006) Improved Motor Development and Good Long-Term Glycaemic Control With Sulfonylurea Treatment in a Patient With the Syndrome of Intermediate Developmental Delay, Early-Onset Generalised Epilepsy and Neonatal Diabetes Associated With the V59M Mutation in the KCNJ11 Gene. *Diabetologia* 49:2559-2563.**

**Soler NG, Pentecost B L, Bennett M A, Fitzgerald M G, Lamb P and Malins J M (1974) Coronary Care for Myocardial Infarction in Diabetics. *Lancet* 1:475-477.**

**Spruce AE, Standen N B and Stanfield P R (1987) Studies of the Unitary Properties of Adenosine-5'-Triphosphate-Regulated Potassium Channels of Frog Skeletal Muscle. *J Physiol* 382:213-236.**

**Spuler A, Lehmann-Horn F and Grafe P (1989) Cromakalim (BRL 34915) Restores in Vitro the Membrane Potential of Depolarized Human Skeletal Muscle Fibres. *Naunyn Schmiedebergs Arch Pharmacol* 339:327-331.**

**Stanfield PR, Nakajima S and Nakajima Y (2002) Constitutively Active and G-Protein Coupled Inward Rectifier K<sup>+</sup> Channels: Kir2.0 and Kir3.0. *Rev Physiol Biochem Pharmacol* 145:47-179.**

**Stanford IM and Lacey M G (1996) Electrophysiological Investigation of Adenosine Trisphosphate-Sensitive Potassium Channels in the Rat Substantia Nigra Pars Reticulata. *Neuroscience* 74:499-509.**

**Taschenberger G, Mougey A, Shen S, Lester L B, LaFranchi S and Shyng S L (2002) Identification of a Familial Hyperinsulinism-Causing Mutation in the Sulfonylurea Receptor 1 That Prevents Normal Trafficking and Function of KATP Channels. *J Biol Chem* 277:17139-17146.**

**Terzic A, Jahangir A and Kurachi Y (1995) Cardiac ATP-Sensitive K<sup>+</sup> Channels: Regulation by Intracellular Nucleotides and K<sup>+</sup> Channel-Opening Drugs. *Am J Physiol* 269:C525-C545.**

**Terzic A, Tung R T, Inanobe A, Katada T and Kurachi Y (1994) G Proteins Activate ATP-Sensitive K<sup>+</sup> Channels by Antagonizing ATP-Dependent Gating. *Neuron* 12:885-893.**

**Thomas P, Ye Y and Lightner E (1996) Mutation of the Pancreatic Islet Inward Rectifier Kir6.2 Also Leads to Familial Persistent Hyperinsulinemic Hypoglycemia of Infancy. *Hum Mol Genet* 5:1809-1812.**

**Thomas PM, Cote G J, Wohllk N, Haddad B, Mathew P M, Rabl W, Aguilar-Bryan L, Gagel R F and Bryan J (1995) Mutations in the Sulfonylurea Receptor Gene in Familial Persistent Hyperinsulinemic Hypoglycemia of Infancy. *Science* 268:426-429.**

**Trapp S, Haider S, Jones P, Sansom M S and Ashcroft F M (2003) Identification of Residues Contributing to the ATP Binding Site of Kir6.2. *EMBO J* 22:2903-2912.**

**Trapp S, Proks P, Tucker S J and Ashcroft F M (1998) Molecular Analysis of ATP-Sensitive K Channel Gating and Implications for Channel Inhibition by ATP. *J Gen Physiol* 112:333-349.**

**Tristani-Firouzi M, Jensen J L, Donaldson M R, Sansone V, Meola G, Hahn A, Bendahhou S, Kwiecinski H, Fidzianska A, Plaster N, Fu Y H, Ptacek L J and Tawil R (2002) Functional and Clinical Characterization of KCNJ2**

**Mutations Associated With LQT7 (Andersen Syndrome). *J Clin Invest* 110:381-388.**

**Trube G and Hescheler J (1984) Inward-Rectifying Channels in Isolated Patches of the Heart Cell Membrane: ATP-Dependence and Comparison With Cell-Attached Patches. *Pflugers Arch* 401:178-184.**

**Tsuboi T, Lippiat J D, Ashcroft F M and Rutter G A (2004) ATP-Dependent Interaction of the Cytosolic Domains of the Inwardly Rectifying K<sup>+</sup> Channel Kir6.2 Revealed by Fluorescence Resonance Energy Transfer. *Proc Natl Acad Sci U S A* 101:76-81.**

**Tucker SJ, Gribble F M, Proks P, Trapp S, Ryder T J, Haug T, Reimann F and Ashcroft F M (1998) Molecular Determinants of KATP Channel Inhibition by ATP. *EMBO J* 17:3290-3296.**

**Tucker SJ, Gribble F M, Zhao C, Trapp S and Ashcroft F M (1997) Truncation of Kir6.2 Produces ATP-Sensitive K<sup>+</sup> Channels in the Absence of the Sulphonylurea Receptor. *Nature* 387:179-183.**

**Tung RT and Kurachi Y (1991) On the Mechanism of Nucleotide Diphosphate Activation of the ATP-Sensitive K<sup>+</sup> Channel in Ventricular Cell of Guinea-Pig. *J Physiol* 437:239-256.**

**Ueda K, Inagaki N and Seino S (1997) MgADP Antagonism to Mg<sup>2+</sup>-Independent ATP Binding of the Sulfonylurea Receptor SUR1. *J Biol Chem* 272:22983-22986.**

**Ueda K, Komine J, Matsuo M, Seino S and Amachi T (1999) Cooperative Binding of ATP and MgADP in the Sulfonylurea Receptor Is Modulated by Glibenclamide. *Proc Natl Acad Sci U S A* 96:1268-1272.**

**Whorton MR and MacKinnon R (2011) Crystal Structure of the Mammalian GIRK2 K<sup>+</sup> Channel and Gating Regulation by G Proteins, PIP2, and Sodium. *Cell* 147:199-208.**

**Wible BA, Tagliatela M, Ficker E and Brown A M (1994) Gating of Inwardly Rectifying K<sup>+</sup> Channels Localized to a Single Negatively Charged Residue. *Nature* 371:246-249.**

**Wickenden A (2002) K(+) Channels As Therapeutic Drug Targets. *Pharmacol Ther* 94:157-182.**

**Wickman KD, Iniguez-Lluhl J A, Davenport P A, Taussig R, Krapivinsky G B, Linder M E, Gilman A G and Clapham D E (1994) Recombinant G-Protein Beta Gamma-Subunits Activate the Muscarinic-Gated Atrial Potassium Channel. *Nature* 368:255-257.**

**Xiao J, Zhen X G and Yang J (2003) Localization of PIP2 Activation Gate in Inward Rectifier K<sup>+</sup> Channels. *Nat Neurosci* 6:811-818.**

**Yamada M, Ishii M, Hibino H and Kurachi Y (2004) Mutation in Nucleotide-Binding Domains of Sulfonylurea Receptor 2 Evokes Na-ATP-Dependent Activation of ATP-Sensitive K<sup>+</sup> Channels: Implication for Dimerization of Nucleotide-Binding Domains to Induce Channel Opening. *Mol Pharmacol* 66:807-816.**

**Yamada M, Isomoto S, Matsumoto S, Kondo C, Shindo T, Horio Y and Kurachi Y (1997) Sulphonylurea Receptor 2B and Kir6.1 Form a Sulphonylurea-Sensitive but ATP-Insensitive K<sup>+</sup> Channel. *J Physiol* 499 ( Pt 3):715-720.**

**Yamada M and Kurachi Y (2004) The Nucleotide-Binding Domains of Sulfonylurea Receptor 2A and 2B Play Different Functional Roles in Nicorandil-Induced Activation of ATP-Sensitive K<sup>+</sup> Channels. *Mol Pharmacol* 65:1198-1207.**

**Yan F, Lin C W, Weisiger E, Cartier E A, Taschenberger G and Shyng S L (2004) Sulfonylureas Correct Trafficking Defects of ATP-Sensitive Potassium Channels Caused by Mutations in the Sulfonylurea Receptor. *J Biol Chem* 279:11096-11105.**

**Yan FF, Lin Y W, Macmullen C, Ganguly A, Stanley C A and Shyng S L (2007) Congenital Hyperinsulinism-Associated ABCC8 Mutations That Cause Defective Trafficking of ATP-Sensitive Potassium Channels: Identification and Rescue. *Diabetes*.**

**Yellen G (2008) Ketone Bodies, Glycolysis, and KATP Channels in the Mechanism of the Ketogenic Diet. *Epilepsia* 49 Suppl 8:80-82.**

**Yellon DM and Downey J M (2003) Preconditioning the Myocardium: From Cellular Physiology to Clinical Cardiology. *Physiol Rev* 83:1113-1151.**

**Yi BA, Lin Y F, Jan Y N and Jan L Y (2001a) Yeast Screen for Constitutively Active Mutant G Protein-Activated Potassium Channels. *Neuron* 29:657-667.**

**Yi BA, Minor D L, Jr., Lin Y F, Jan Y N and Jan L Y (2001b) Controlling Potassium Channel Activities: Interplay Between the Membrane and Intracellular Factors. *Proc Natl Acad Sci U S A* 98:11016-11023.**

**Zerangue N, Schwappach B, Jan Y N and Jan L Y (1999) A New ER Trafficking Signal Regulates the Subunit Stoichiometry of Plasma Membrane K(ATP) Channels. *Neuron* 22:537-548.**

**Zhou M and MacKinnon R (2004) A Mutant KcsA K(+) Channel With Altered Conduction Properties and Selectivity Filter Ion Distribution. *J Mol Biol* 338:839-846.**

**Zhou Y, Morais-Cabral J H, Kaufman A and MacKinnon R (2001) Chemistry of Ion Coordination and Hydration Revealed by a K<sup>+</sup> Channel-Fab Complex at 2.0 Å Resolution. *Nature* 414:43-48.**

**Zingman LV, Hodgson D M, Bienengraeber M, Karger A B, Kathmann E C, Alekseev A E and Terzic A (2002) Tandem Function of Nucleotide Binding Domains Confers Competence to Sulfonylurea Receptor in Gating ATP-Sensitive K<sup>+</sup> Channels. *J Biol Chem* 277:14206-14210.**

## Appendix

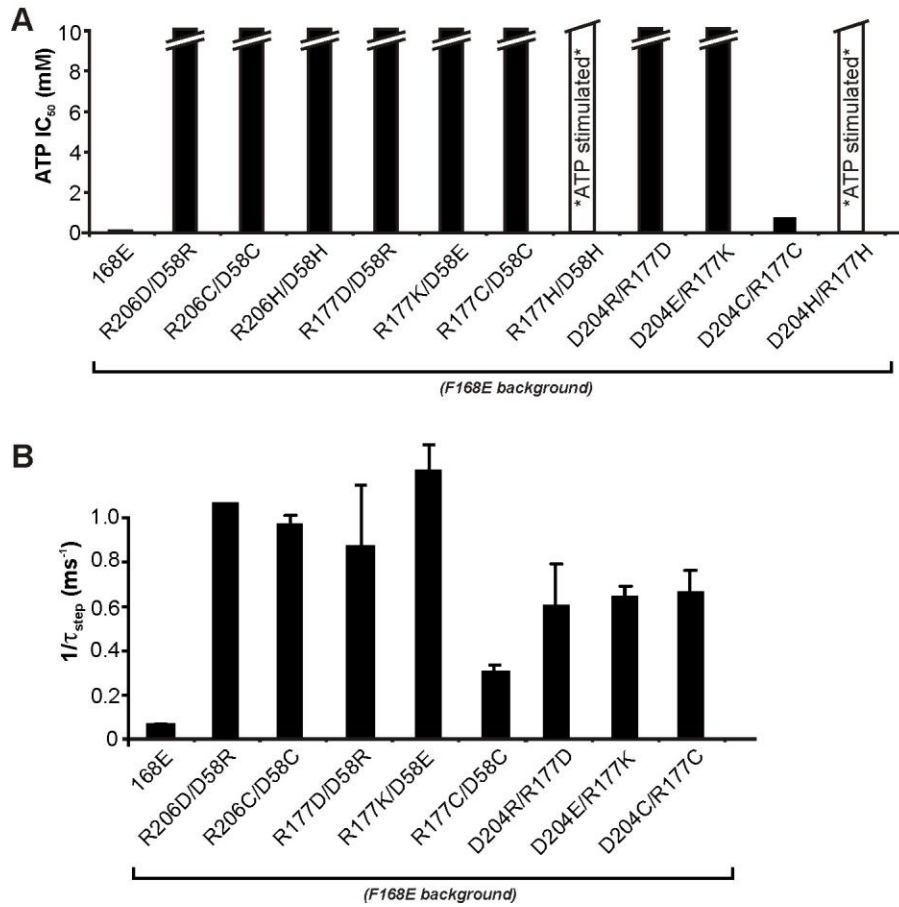


**Figure A-1 Functional assessment of multiple potential salt bridges between key interfacial residues in Kir6.2 channels.**

Various approaches, including targeted disulfide bond formation, targeted metal bridges, and complimentary charge reversal mutations between key residues at TMD-CTD interface in Kir6.2 channels were attempted to assess their hypothetical interactions. (A) IC<sub>50</sub> for ATP inhibition of site-specific mutant channels was determined on F168E background. Most of them exhibited strong ATP insensitivity with IC<sub>50</sub> exceeding 10mM. The double cysteine Kir6.2[F168E][D204C][R177C] mutant exhibited a relatively strong ATP inhibition. (B) Gating kinetics of multiple site-specific mutant channels expressed on the Kir6.2[F168E] background.